
Proximal TCR signaling in self tolerance

Inauguraldissertation

zur

Erlangung der Würde eines Doktors der Philosophie

vorgelegt der

Philosophisch-Naturwissenschaftlichen Fakultät

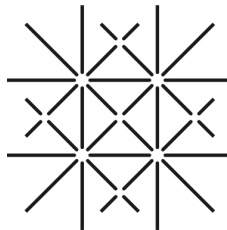
der Universität Basel

von

Michel Mallaun

aus Basel (Schweiz)

Basel, November 2008



UNI
BASEL

Genehmigt von der Philosophisch-Naturwissenschaftlichen Fakultät auf Antrag von

Prof. Dr. Ed Palmer

Prof. Dr. Antonius Rolink

Basel, den 9. Dezember 2008

Dekan

Prof. Dr. Eberhard Parlow

Life is pretty simple: You do some stuff.

Most fails. Some works.

You do more of what works.

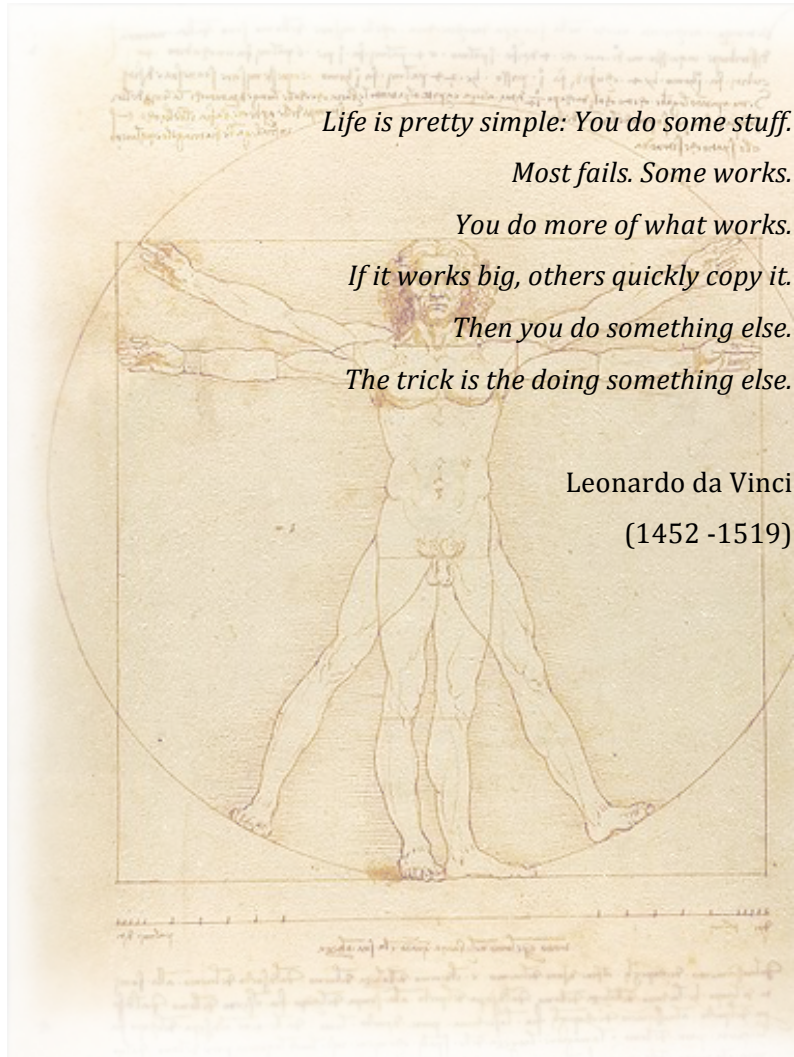
If it works big, others quickly copy it.

Then you do something else.

The trick is the doing something else.

Leonardo da Vinci

(1452 -1519)



to Anja

Acknowledgments

First of all, I would like to thank Ed Palmer. The strong support I received from Ed while I worked in his laboratory was based on three main aspects. First, Ed was always there to discuss scientific problems and helped me with his profound knowledge and enthusiasm. Second, Ed gave me the opportunity to broaden my experience through high-impact immunology meetings and by giving me the possibility to learn about FRET microscopy at the Scripps Institute in LaJolla, USA. Lastly, Ed let me develop my own ideas by giving me complete scientific freedom in my projects.

I want to thank all members of the Transplantation Immunology Lab, in particular Dieter Naehrer, Barbara Hausmann, Simona Rossi, Carolyn King, Ernst Wagner, Denise Biemann, Doris Lutz, Claudia Petit, Gideon Hönger, Nicolai Hodel, Virginie Galati and Martin Schaad. Their technical support, their experience in planning, conducting and analyzing experiments and their critical opinions on scientific issues were invaluable. Among the former members of the Lab 415, I would like to thank Emma Teixeira, Diana Gil Pages, Dominique Roubaty, Adam Schrum, and Mark Daniels for great discussions and for teaching me many molecular techniques.

The members of my thesis committee are Ed Palmer, my supervisor and ‘Fakultätsverantwortlicher’, Ton Rolink as co-referee and Oreste Acuto as specialist in TCR signaling. I want to thank Ton Rolink for the discussions and for his excellent seminars on immunology and Oreste Acuto for helpful inputs and his acceptance to travel from Oxford to Basel for the thesis defense. Furthermore, I would like to thank Peter Scheiffele for being my ‘Prüfungsvorsitzender’.

I am also grateful to Nick Gascoigne and Pia Yachi at Scripps for accepting me as a summer student and teaching me how to use, build and maintain a microscope in an expert way.

The DBM PhD Student Club has always been a place of decent presentations and lively discussions – and friendship. In particular, I would like to thank Célia Groeper, Dani Vonwil, Bea Bolinger, Hati Karaüzüm, Marco Cavallari, Gabi Zenhäusern, Cornelia Bigler, Corinne Lochmatter, Bojana Durovic, Federica Facciotti, Naja Jann, Mathias Schmalzer and Magda Filipowicz-Sarasin for sharing their time and spirit.

During my graduate studies I enjoyed the priceless support of my friends and my beloved family, making them the ones that should be appreciated most. The largest part of my affection goes to Anja: my partner, source of inspiration and future wife.

Table of contents

Acknowledgments	4
Summary	8
1. Introduction	10
1.1 T-cell development in the thymus	10
1.2 Positive and negative selection of thymocytes	11
1.3 CD4/CD8 lineage decision	12
1.4 The T-cell receptor complex	14
1.5 TCR co-receptor interactions	15
1.6 TCR-proximal signaling	17
1.6.1 The immunological synapse	20
1.6.2 Costimulation	21
1.6.3 Systematic signaling regulation	22
1.6.4 Ras/MAPK signaling.....	22
1.6.5 Negative feedback in TCR signaling	23
1.6.6 How TCR signaling distinguishes ligands	25
1.7 A closer look at ZAP-70	26
1.7.1 ZAP-70 discovery and relevance	26
1.7.2 ZAP-70 binding to TCR ITAMs and activation	26
1.7.3 ZAP-70 mutational analysis	27
1.7.4 ZAP-70 structure	28
1.7.5 ZAP-70 in development and disease.....	29
2. Materials and methods	31
2.1 Reagents	31
2.1.1 For molecular techniques	31
2.1.2 For cellular techniques.....	31
2.1.3 For biochemical techniques.....	32
2.1.4 Enzymes.....	32
2.1.5 Kits	32
2.2 Solutions and media	32
2.2.1 For molecular techniques	32
2.2.2 For biochemical techniques.....	33
2.2.3 For SDS-Page and Western blotting	33
2.2.4 For cellular techniques.....	34
2.2.5 Media used for cell culture	35

2.2.6 Instruments.....	36
2.2.7 Software.....	36
2.2.8 Antibodies.....	37
2.2.9 Peptides	38
2.2.10 Expression vectors	38
2.3 cDNA sequences.....	38
2.3.1 OT-I α -chain (wildtype).....	39
2.3.2 OT-I $\alpha\delta$ -chimera II.....	39
2.3.3 OT-I $\alpha\delta$ -chimera IV	39
2.3.4 OT-I β -chain (wildtype)	39
2.3.5 OT-I $\beta\gamma$ -chimera III.....	40
2.4 DNA constructs.....	40
2.5 Cell lines	41
2.6 Molecular techniques	41
2.6.1 Transformation of competent bacteria.....	41
2.6.2 Plasmid preparation.....	41
2.6.3 PCR.....	42
2.6.4 Restriction enzyme digestion of plasmid DNA	42
2.6.5 DNA ligation.....	42
2.6.6 DNA sequencing.....	42
2.7 Cellular techniques.....	42
2.7.1 Production of lentivirus.....	42
2.7.2 Production of retrovirus.....	43
2.7.3 Transduction of 58 hybridomas.....	43
2.7.4 Fluorescence activated cell sorting (FACS).....	44
2.7.5 RMA-S peptide loading.....	44
2.7.6 Conjugate formation assay	44
2.7.7 TCR endocytosis.....	44
2.7.8 IL-2 detection by ELISA	45
2.7.9 Stimulation of T-cell hybridomas for FRET microscopy	45
2.7.10 FRET microscopy	45
2.7.11 FRET analysis	45
2.7.12 Isolation of B-cells from spleen	46
2.7.13 Stimulation of thymocytes and immunostaining for fluorescence microscopy	46
2.7.14 Fetal thymic organ culture (FTOC)	47
2.8 Biochemical techniques	47
2.8.1 Fixation of APCs	47

2.8.2 Immunoprecipitation and Western blot.....	47
2.8.3 ZAP-70 <i>in vitro</i> kinase assay	48
3. Results	49
3.1 The T-cell receptor's α-chain connecting peptide motif promotes close approximation of the CD8 co-receptor allowing efficient signal initiation	49
3.2 A discrete affinity driven elevation of ZAP-70 activity distinguishes positive and negative selection.....	61
3.2.1 Summary	61
3.2.2 Introduction.....	62
3.2.3 Materials and Methods.....	65
3.2.4 Results.....	67
3.2.5 Discussion	72
3.2.6 Figures.....	75
3.2.7 Figure Legends	81
4. Discussion.....	87
4.1 A zipper model for TCR-CD8 interactions.....	87
4.2 ZAP-70 in positive and negative selection.....	89
5. References	92
6. Curriculum Vitae	102

Summary

This thesis investigates the molecular mechanisms involved in T-cell receptor (TCR) signaling during thymocyte selection. The T-cell receptor of developing T-cells interacts with antigen-presenting cells (APCs) that display peptide-MHC ligands (p-MHC) of different nature on their surface. The TCR interacts with these ligands and translates the binding affinity for different p-MHC (characterized by the dissociation constant, K_D) into a quantitative readout, thereby providing the basis for downstream signaling. How the TCR distinguishes between high affinity ligands that induce apoptosis of individual thymocytes (negative selection) and low affinity ligands that induce differentiation of thymocytes into single-positive immature T-cells (positive selection) has fascinated immunologists and biochemists for many years. This mechanism is critical to establish a self-MHC restricted, self-tolerant T-cell repertoire (central tolerance).

The first part of this thesis investigates the molecular interaction between the TCR and the CD8 co-receptor in thymic selection. By tagging both molecules with variants of the green fluorescent protein (GFP) and assessing their molecular approximation in the immunological synapse by FRET microscopy (developed by P. Yachi and N. Gascoigne at the Scripps Institute, LaJolla, USA), we found that negative-selecting p-MHC ligands induced strong and sustained TCR/CD8 association. In contrast, positive-selecting ligands induce weak and delayed TCR/CD8 association in the synapse of T-cell hybridomas with antigen-presenting cells (APCs). We found that the TCR/CD8 interaction in response to positive- or negative-selecting ligands was reflected in the phosphorylation of the ζ -chain. Therefore, the ability of the TCR to tightly associate with the co-receptor is the critical parameter that determines whether a p-MHC ligand mediates strong intracellular tyrosine phosphorylation and subsequently induces negative selection signaling. The α -chain connecting peptide motif (α -CPM) is a region of 8 conserved amino acids in the membrane-proximal part of the constant region of the TCR α -chain. Mutating the α -CPM did not affect ligand binding since α -CPM mutant TCRs had similar p-MHC affinities like wild-type TCRs. However, TCR/CD8 interaction as measured by FRET microscopy, changed substantially in α -CPM mutant TCRs. In response to negative-selecting ligands, TCR/CD8 association was reduced in α -CPM mutant cells, which was also reflected in decreased ζ phosphorylation. Remarkably, in response to positive-selecting ligands, α -CPM mutant cells displayed no detectable TCR/CD8 interactions and failed to induce ζ phosphorylation. Therefore, the α -CPM is responsible for the molecular approximation of the CD8 co-receptor to the TCR complex, allowing efficient signaling initiation. We hypothesize that the TCR and the co-receptor may act like a molecular zipper. By binding to the same p-MHC molecule the zippering mechanism allows the two molecules to become tightly associated via the α -CPM towards

the plasma membrane. Inside the cell, the co-receptor carries the Src kinase, Lck and shuffles it efficiently to the CD3 complex once the zipper is fully closed. Only the zippered configuration allows efficient signaling initiation, emphasizing the importance of the α -CPM to functionally link the TCR and CD8.

In the second part of this thesis we investigated TCR proximal signaling downstream of the TCR complex. The ζ -chain associated protein of 70 kDa (ZAP-70) plays a central role in transmitting the TCR-generated signal to downstream signaling molecules. ZAP-70 binds to phosphorylated immunoreceptor tyrosine activation motifs (ITAMs) located on the ζ or CD3 molecules of the TCR complex. The tyrosine kinase activity of ZAP-70 is triggered if the molecule binds to doubly phosphorylated ITAMs via its tandem SH2-domain and subsequently becomes phosphorylated at several tyrosine residues. We wondered whether ZAP-70 would function as molecular switch in TCR signaling, converting varying TCR inputs (by binding p-MHC ligands of different binding affinity) into discrete signaling responses by generating distinct levels of ZAP-70 kinase activity. In response to negative-selecting ligands, ZAP-70 was efficiently recruited to the immunological synapse. In the synapse, ZAP-70 became phosphorylated at critical tyrosine residues, which induced its kinase activity. *In vitro* kinase assays revealed a discrete 2-fold increase in ZAP-70 kinase activity precisely at the negative selection threshold. In contrast, ZAP-70 recruitment to the synapse and its kinase activity remained low in response to positive-selecting ligands. Therefore, we speculate that a discrete elevation of ZAP-70 activity occurs at the threshold of positive and negative selection. Further evidence for such a mechanism came from fetal thymic organ cultures (FTOCs), where negative selection was converted into partial positive selection by reducing ZAP-70 kinase activity with a specific inhibitor. We also asked whether the increased ZAP-70 kinase activity in negative selection is generated by an increase in the ratio of ZAP-70 / TCR in the synapse. This idea seemed reasonable since multiple ITAMs and therefore potential ZAP-70 binding sites exist among the CD3 molecules. However, we did not detect an increase in the ZAP-70 / TCR ratio. Relative to positive selecting ligands, negative selectors induced a 2-fold increase in the amount of TCR and ZAP-70 recruited to the immunological synapse. However, the ZAP-70 / TCR ratio was similar in both forms of selection and therefore, the number of TCR molecules recruited to the synapse determines the selection outcome. We postulate a model of TCR-proximal signaling, where TCR-associated ZAP-70 is recruited into the synapse proportionally to the TCR's ability to bind p-MHC ligands and recruit the co-receptor. According to the zipper model, only negative-selecting ligands mediate efficient co-receptor association and therefore, increased ζ phosphorylation. ZAP-70 becomes phosphorylated accordingly, which initiates a 2-fold increase in its kinase activity in response to p-MHC ligands above the negative selection threshold. This step-wise increase in ZAP-70 kinase activity is sufficient to mediate higher levels of LAT phosphorylation, which assembles a negative selection signaling complex.

1. Introduction

1.1 T-cell development in the thymus

T-cells develop in the thymus from bone marrow progenitor cells. Within the thymus, T-cell precursors progress through a sequence of phenotypically distinct stages. Early CD4⁻ CD8⁻ double-negative (DN) precursors are further subdivided based on their CD44 (hyaluronic acid binding adhesion molecule) and CD25 (the α -chain of the IL-2 receptor) expression. The earliest T-cell precursors in the thymus comprise the CD44⁺ CD25⁻ DN1 subset. They advance through the cKit⁺ (stem cell factor receptor) CD44⁺ CD25⁻ DN2 stage to become cKit⁻ CD44⁻ CD25⁺ DN3 cells. Genes encoding β , γ and δ chains of the TCR rearrange in the DN2 and DN3 subsets and if they are productive express either the pre-TCR (together with the pre-TCR invariant α -chain) or the $\gamma\delta$ TCR on the surface. For pre-TCR-expressing cells, this transition is called β -selection. Cells within the DN3 population that have not yet succeeded in TCR gene rearrangement and surface expression do not proliferate further. However, TCR-expressing cells downmodulate CD25 and advance to the CD44⁻ CD25⁻ DN4 stage. Thymocytes committed to the $\alpha\beta$ lineage become CD4⁺ CD8⁺ double-positive (DP) in contrast to $\gamma\delta$ cells that do not progress through the DP stage. Cells committed to the $\alpha\beta$ lineage are silencing γ -chain expression, deleting the δ locus and start to rearrange the α -chain, eventually leading to expression of the $\alpha\beta$ TCR on the cell surface. Some plasticity in lineage commitment remains inherent to a DN3 stage thymocyte, since a TCR $\gamma\delta$ ⁺ cell can still give rise to both $\alpha\beta$ and $\gamma\delta$ lineage. One hypothesis suggests that rather than the type of TCR, the strength of TCR signaling determines the lineage outcome, with strong signaling favoring $\gamma\delta$ and weak signaling $\alpha\beta$ lineage development (1). Conversely, another theory suggests that commitment to $\gamma\delta$ or $\alpha\beta$ lineages occurs before TCR expression at the DN2 stage and TCR signaling has rather a confirmatory role in commitment (2).

Developmental stages of thymocytes take place in separated locations within the thymus. Progenitor cells from the bone marrow enter the thymus through high endothelial venules at the cortico-medullary junction. First, they migrate to the subcapsular region of the cortex, where they undergo vigorous expansion, which is driven by the pre-TCR. As maturation proceeds and TCR rearrangement is completed, DP cells migrate deeper into the cortex. Interaction with cortical epithelial cells that express both MHC class I and class II molecules, is the foundation of positive selection (chapter 1.2). Immature DP thymocytes then migrate towards the cortico-medullary junction and into the medulla, where they interact with dendritic cells, macrophages and medullary epithelial cells. Compared to the cortex, there are substantially less cells in the medulla. Before maturation is completed, developing thymocytes are subjected to negative selection (chapter 1.2) to remove self-reactive cells.

The time between the entry of a T-cell progenitor cell into the thymus and its export as immature T-cell is estimated to take about 3 weeks in a mouse. Once maturation is completed, CD8⁺ or CD4⁺ SP cells leave the thymus either returning to the bloodstream directly via venules or via the lymphatic system.

1.2 Positive and negative selection of thymocytes

DP thymocytes undergo one of the following cell fates: they either fail to recognize peptide-MHC ligands and die 'by neglect' or they are positively or negatively selected. Death by neglect comprises the vast majority of developing thymocytes (~90-95%) and involves autoinduced cell death due to the $\alpha\beta$ TCR's failure to engage peptide-MHC ligands, thereby not providing a survival signal to the cell. Positive selection and differentiation into SP T-cells is based on restriction to the own set of MHC molecules and combinatorial recognition of the presented peptide with moderate TCR binding affinity. The nature of the selecting peptide has been controversial, but some of them have been identified by different strategies. In several TCR transgenic systems it turned out that among putative self-peptides (based on their homology to an original positive selecting peptide) only a minority of candidates was able to promote selection, suggesting that the number of functionally relevant self-peptide ligands is low. Therefore, relatively rare, low-affinity self-peptides promote positive selection, giving rise to mature T-cells with potentially high affinity for foreign peptides in the periphery (referred to as foreign, agonist or antigenic peptides). Ligand-dependent signaling is a prerequisite for selection, whereas β -selection is thought to result from ligand-independent signaling. The role of the CD3 molecules, the scaffold proteins of TCR signaling, is difficult to study since deletion of the genes encoding for either CD3 γ , CD3 ϵ and ζ results in an early block of thymocyte development, before the DP stage. Interestingly, CD3 δ deficiency does not impair the generation of DP cells but abrogated positive selection. A plausible explanation for this apparent contradiction comes from a specific motif in the TCR α -chain connecting peptide (α -CPM; chapter 1.5) which is required for positive selection (3) and pMHC-induced TCR/co-receptor interaction (4), and which is important for retaining CD3 δ in the TCR complex. This suggests that CD3 δ deficient thymocytes, even though they develop past the ligand-independent β -selection step, do not undergo positive selection because the trimeric TCR-pMHC-co-receptor interaction is disrupted. CD3 δ has also been implied in transmitting a conformational change of the TCR upon ligand binding, further supporting its role in maintaining the integrity of the TCR/CD3 complex at developmental stages where TCR-mediated signaling is required.

By providing a three-dimensional microenvironment, cortical epithelial cells are quintessential for productive positive selection. Successful epithelial cell differentiation requires thymocytes and efficient thymocyte development requires epithelial cells. Recombination-deficient mice (that have no B- and T-cells) are disorganized and lack the normal three-dimensional epithelial network,

emphasizing this 'crosstalk' situation. By the use of two-photon laser scanning microscopy, the vigorous movement of single thymocytes around their environment can be visualized. Thymocytes that sample signals from the epithelial cells halt their migration upon encounter of a positive selecting peptide and then adhere to epithelial cells for several hours.

The principle of negative selection is to cause deletion of thymocytes that would respond to 'self' ligands in the periphery. The elimination of self-reactivity in the thymus is extremely sensitive and based on recognition of self-ligands predominantly presented by medullary epithelial cells. The transcription factor AIRE induces an array of peripheral-tissue antigens in these cells and its deletion results in multiorgan inflammatory infiltrates and generation of autoantibodies (5, 6).

Taken together, thymic selection establishes a diverse, self-MHC restricted, self-tolerant T-cell repertoire (referred to as central tolerance). Recently the principle of thymic selection became more precisely defined (7). Several different MHC class I-restricted TCRs use the same apparent affinity threshold of TCR-pMHC-CD8 interaction to discriminate between positive and negative selecting ligands. Therefore, for class I restricted T-cells, this threshold is likely to be universal and consequently defines the basis of self tolerance and T-cell specificity. Inside the cell, the signaling machinery ensures that the threshold is precisely translated into diverging cellular responses (8).

1.3 CD4/CD8 lineage decision

During thymic selection, the CD4 and CD8 co-receptors are central in determining whether a developing DP thymocyte becomes a CD4⁺ or a CD8⁺ single positive (SP) T-cell (Figure 1). DP thymocytes expressing MHC class II restricted TCRs differentiate into CD4⁺ SP T-cells, whereas DP thymocytes expressing MHC class I restricted TCRs differentiate into CD8⁺ SP T-cells. Therefore, the CD4/CD8-lineage choice is determined by the MHC-restriction specificity of the $\alpha\beta$ TCR. Given that the TCR's specificity is randomly generated by somatic recombination, it's formally possible that non-MHC ligands may bind to the TCR. A possible explanation comes from Lck, a critical tyrosine kinase for the initiation of TCR signaling (chapter 1.6) that is associated with the co-receptor. Since there is little 'free' Lck in DP thymocytes, only co-engagement of pMHC with the TCR and the co-receptor results in successful signaling initiation.

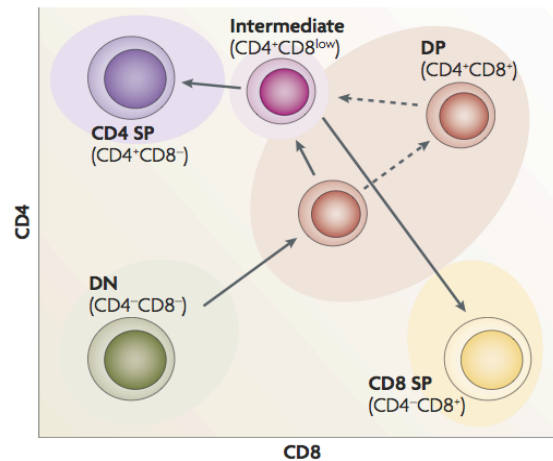


Figure 1. T-cell development in the thymus. CD4⁻ CD8⁻ double-negative (DN) cells differentiate into CD4⁺ CD8⁺ double-positive (DP) cells, which are the first cells to express a functional $\alpha\beta$ TCR. DP thymocytes with potentially useful TCR specificities undergo positive selection and become intermediate CD4⁺ CD8^{low} cells, which are still lineage-uncommitted cells. Subsequently these cells differentiate into either CD4⁺ or CD8⁺ single-positive (SP) cells.

DP thymocytes depend solely on signals that are downstream of TCR engagement and are virtually unresponsive to other survival signals (as for example, DP thymocytes do not respond to the pro-survival cytokine IL-7, for which they do not express the receptor). DP thymocytes express SOCS-1 (suppressor of cytokine signaling 1), a potent inhibitor of intracellular cytokine signal transduction. Since DP thymocytes are expressing both co-receptors, they are able to receive signals from both MHC class I and MHC class II restricted TCRs, thereby enabling all potentially useful TCRs to initiate positive selection.

The stochastic model of CD4/CD8 lineage choice postulates that positive-selecting TCR signals randomly terminate the expression of either CD4 or CD8. This leads to short-lived intermediate CD4⁺CD8^{low} cells that would undergo apoptosis unless they were rescued by a second, TCR-mediated signal, which is co-receptor-matched. However, this model seems unlikely since 50% of positively selected cells would fail to survive in absence of the appropriate co-receptor. Another model defines the strength of the TCR signal as decisive parameter of CD4/CD8 lineage commitment. Weak TCR signals (as generated by TCR-MHC-CD8) would terminate *cd4* transcription, whereas strong TCR signals (as generated by TCR-MHC-CD4) would terminate *cd8* transcription. The strength-of-signal model was challenged by reducing the number of ITAMs (chapter 1.6) in the TCR complex. The decreased TCR signal resulted in fewer SP T-cells but did not alter CD4/CD8 lineage choice, thereby disproving the model.

The duration of the TCR signal is the basis for the third model, which postulates that short and/or weak TCR signals terminate *cd4* transcription, whereas long and/or strong TCR signals terminate *cd8* transcription. Both of the latter models are based on the hypothesis that MHC class I-restricted and MHC class II-restricted TCR signals differ in duration and intensity (although their TCR binding

affinities are presumably similar). A higher percentage of CD4 co-receptors are associated with Lck than CD8 and since the total amount of Lck in a thymocyte is limiting, this may contribute to a stronger overall signal. The duration-of-signal model provided the basis for the most recent model of CD4/CD8 lineage commitment, called the kinetic signaling model (9). Positively selecting TCR signals induce DP thymocytes to terminate *cd8* gene expression and to convert into CD4⁺ CD8^{low} intermediates, in which the lineage choice is made. Persistence of TCR signaling in CD4⁺ CD8^{low} intermediate thymocytes blocks IL-7 mediated signaling and induces differentiation into CD4⁺ SP cells. Cessation of TCR signaling allows IL-7 mediated signaling leads to co-receptor reversal in CD4⁺ CD8^{low} intermediate thymocytes and differentiation into CD8⁺ SP cells.

1.4 The T-cell receptor complex

The $\alpha\beta$ TCR recognizes antigen by a specifically binding to a short peptide bound to an MHC molecule on the surface of an APC (10, 11). Besides critical residues on the peptide, the TCR recognizes a substantial portion of the MHC molecule, which is the basis of self-MHC restriction. The $\alpha\beta$ TCR complex consists of the rearranged α - and the β -chain and 3 dimeric CD3 chains, $\delta\epsilon$, $\gamma\epsilon$ and $\zeta\zeta$. The transmembrane regions of the CD3 molecules contain acidic residues and the TCR α - and β -chain contain basic residues, thereby providing electrostatic attraction among the different components of the TCR/CD3 complex. The CD3 chains contain a total of ten immunoreceptor tyrosine-based activation motifs (ITAMs) in their cytoplasmic tails, one in each molecule of the $\delta\epsilon$ and $\gamma\epsilon$ heterodimers and three in each ζ -chain of the homodimer. These motifs are important signaling modules and provide the scaffold for TCR signaling (Figure 2).

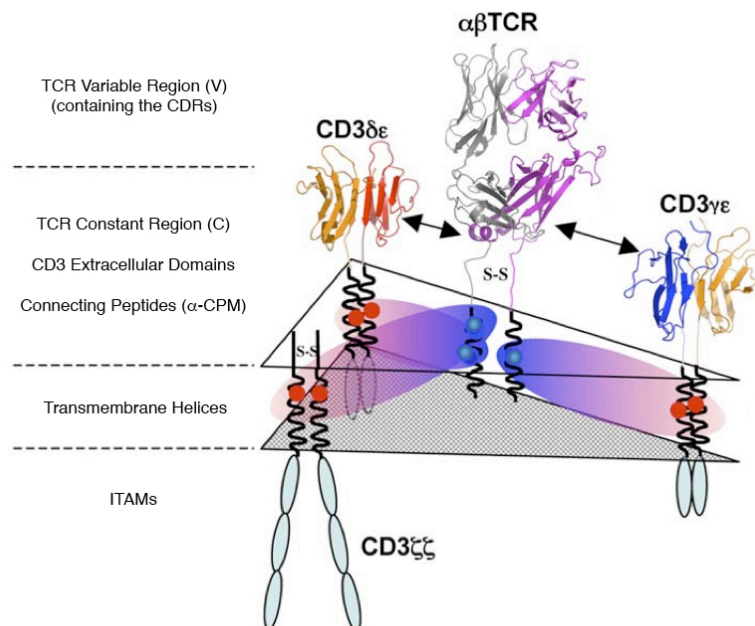


Figure 2. Composition of the TCR/CD3 complex (adapted from (12)). Extracellular, transmembrane and intracellular regions are shown. The CD3 $\delta\epsilon$ heterodimer is located on the α -chain side of the TCR, whereas the CD3 $\gamma\epsilon$ heterodimer is positioned next to the TCR β -chain. Acidic residues in the transmembrane regions of the CD3 molecules are depicted in red and the basic TCR transmembrane residues are colored in blue. The two acidic-one basic electrostatic interactions are depicted in the red to blue ovals. The intracellular ITAMs are shown as grey ovals.

TCRs bind pMHC via their complementarity-determining region (CDR) loops, namely germ line encoded CDR1 (α/β), CDR2 (α/β) and (partially) somatically rearranged CDR3 (α/β) of the $V\alpha$ and $V\beta$ chains, respectively. The engaged TCR lies diagonally above the pMHC surface, which is made from 2 α -helices that define a groove where the peptide is attached to the MHC. The six CDR loops of the TCR contact this surface to varying degrees. Usually, CDR1 β and CDR2 β interact with the α 1 helix of MHC class I or the α helix of MHC class II, whereas CDR1 α and CDR2 α bind to the α 2 helix of MHC class I or the β helix of MHC class II. The interactions of CDR3 α and CDR3 β usually focus on amino acids of the peptide. The angle and pitch with which TCRs settle onto MHC varies because of differences in peptide and CDR3 sequences.

Recent studies indicate that the TCR V regions have emerged through evolution to react with MHC, which prevents the majority of thymocytes to undergo negative selection or death by neglect (13). Thus, CDR1s and CDR2s of most $V\alpha/V\beta$ combinations can produce inherently MHC-reactive TCRs and CDR3s sterically interfere differently with this reactivity. This is the principle to produce a repertoire of TCRs with a wide range of affinities for MHC.

1.5 TCR co-receptor interactions

The CD8 and CD4 co-receptors participate in antigen recognition by binding to structurally similar α 3 helices of MHC class I and class II molecules, respectively (14-17). The co-receptor binding sites are separated from the MHC's peptide-binding groove and therefore don't interfere with antigen recognition. Therefore, CD8-pMHC interaction is independent of the peptide potency (18). By binding to the same pMHC molecule as the TCR (19), one of the co-receptor's functions is to stabilize this trimeric interaction (20-22). In the absence of CD8 binding to pMHC, primary CD8 T-cells fail to form conjugates with APCs, even in the presence of high concentrations of antigenic peptide (23). While high-affinity TCR-pMHC interactions ($K_D < 6\mu\text{M}$) exhibit a certain independency of CD8 coengagement, low-affinity interactions ($K_D \geq 6\mu\text{M}$) require CD8 to enhance sensitivity (24). Thereby, the CD8 $\alpha\beta$ co-receptor, but not the CD8 $\alpha\alpha$ co-receptor significantly increases the affinity of TCR-pMHC binding (referred to as apparent affinity), as measured by binding to soluble monomeric pMHC (25). The same study suggests that CD8 β not only facilitates TCR signal induction by increasing the apparent affinity of TCR-pMHC binding, but also by docking TCR/CD3 to

glycolipid-enriched microdomains (GEMs). Another important function of the CD8 and CD4 co-receptors is their association with the Src tyrosine kinase Lck (26), which is critically involved in the initiation of TCR signaling and thymocyte development (27-29). Lck is a major kinase to phosphorylate the ITAMs of the CD3 molecules of the TCR/CD3 complex (30). The tyrosine phosphorylation pattern of an agonist ligand can be converted into a partial agonist pattern by blocking the recruitment of CD4 to the TCR, attributing the effect to the amount of co-receptor-associated Lck (31).

An important role of the molecular interaction between CD8 and the TCR was assigned to a sequence in the constant region of the TCR α -chain termed α -chain connecting peptide motif (α -CPM) (3, 32). It was observed that α -CPM deficient T-cell hybridomas exhibit a substantial defect in engaging CD8 for pMHC binding that could not be attributed to a TCR-intrinsic defect in pMHC binding (4). Mutations in this conserved motif of 8 amino acids (FETDxNLN) were initially described to promote unresponsiveness to TCR crosslinking or superantigens and later to promote defective positive selection, whereas negative selection was unaffected (3, 33). The presence of the α -CPM promotes positive selection by specifically activating the extracellular-regulated signal kinase (ERK) in a weak but sustained manner (34). Investigating the molecular composition of the TCR/CD3 complex revealed that α -CPM negative thymocytes and T-cells exhibit reduced association with the CD3 δ subunit (3). Another study described that CD8 $\alpha\beta$, but not CD8 $\alpha\alpha$, is associated with the TCR via CD3 δ (35). Similar to α -CPM negative thymocytes, CD3 δ -deficiency is also reflected in defective positive selection, underlining the functional link between these two molecules since both fail to cooperate with the co-receptor.

Time-lapse movies of T-cells hybridomas interacting with APCs showed that recruitment of the CD4 co-receptor to the immunological synapse (chapter 1.6.1) was almost instantaneous, with concentrations of CD4 detectable within 10 seconds of contact (36). Recruitment of CD4, but not CD3 ζ was found when the T-cell interacted with APCs that were not loaded with antigen, although CD4 recruitment to the immunological synapse in the absence of antigenic stimulation was slower than that seen when antigen was present. This shows that recognition of antigen increases the rate of CD4 translocation to the immunological synapse. CD4 recruitment occurred only if mature dendritic cells or a subset of a B-cell tumor was used as APCs, but not with immature dendritic cells nor with macrophages or MHC class II-transfected fibroblasts. Similar experiments were performed with MHC class I-restricted cells expressing CD3 ζ -CFP and CD8 β -YFP (37). Also in this case, the CD8 co-receptor was recruited rapidly to the immunological synapse, although there was no difference between the presence or absence of antigen. In both CD4⁺ and CD8⁺ cells, co-receptor concentration in the contact area with the APC was much more evident than TCR concentration. The amount of CD8 recruited to the synapse correlates with the number of class I molecules on the surface of the APC, as shown with Tap-deficient RMA-S cells that only stabilize class I molecules on their surface

upon addition of exogenous peptide. This clearly shows that CD8 recruitment is caused by the non-cognate interaction between CD8 and MHC class I (37).

1.6 TCR-proximal signaling

Engagement of the $\alpha\beta$ TCR with antigenic pMHC induces phosphorylation of the ITAMs in the cytoplasmic tails of the CD3 subunits. Although the precise mechanism of ITAM phosphorylation remains partly unresolved, the Src-family leukocyte-specific protein tyrosine kinase (Lck) plays an important role. The extent of ITAM phosphorylation and correlates with the half-life of TCR-pMHC binding and the availability of activated Lck (=Lck that has been phosphorylated on tyrosine 394) (38). The regulation of Lck involves a complex interplay between activating/inactivating components. One portion of the cellular pool of Lck is thought to be constitutively active (Figure 3), raising the hypothesis that phosphorylation of the CD3 ITAMs might be initiated by bringing the TCR into proximity with pre-activated Lck. Both co-receptors CD4 and CD8 are associated with Lck and therefore deliver active Lck to pMHC-engaged TCRs (4, 39). Alternatively, especially since CD4 and CD8 are partially dispensable for TCR signaling in response to strong agonists, the (transient) co-localization of Lck and CD3 ITAMs may occur in glycolipid enriched microdomains (GEMs). Indeed, Lck carries a palmitoyl lipid anchor at two N-terminal cysteines that tethers the protein to GEMs of the plasma membrane. Positive and negative regulation of Lck is controlled by the transmembrane protein tyrosine phosphatase CD45. CD45 is removing the inhibitory phosphate from Lck tyrosine 505, thereby unfolding the enzyme to “prime” it for further activation. On the other hand, CD45 is also able to dephosphorylate tyrosine 394, which inactivates the kinase. Upon TCR engagement, CD45 is excluded from TCR microclusters in the synapse, confirming this (indirect) activation of Lck by the separation from its inactivating phosphatase.

Agonist ligands induce positive feedback regulation upon binding to the TCR. This feedback loop involves extensive activation of the extracellular signal-regulated serine/threonine kinase (Erk) that in turn positively regulates Lck by phosphorylating it at Serine 59 (40) (Figure 3). This mechanism prevents recruitment of the phosphatase SH2-domain containing protein tyrosine phosphatase 1 (SHP-1) and ensures the persistence of the signal. In contrast, weak ligands predominantly induce a negative feedback loop that involves the efficient recruitment of SHP-1, which inactivates Lck.

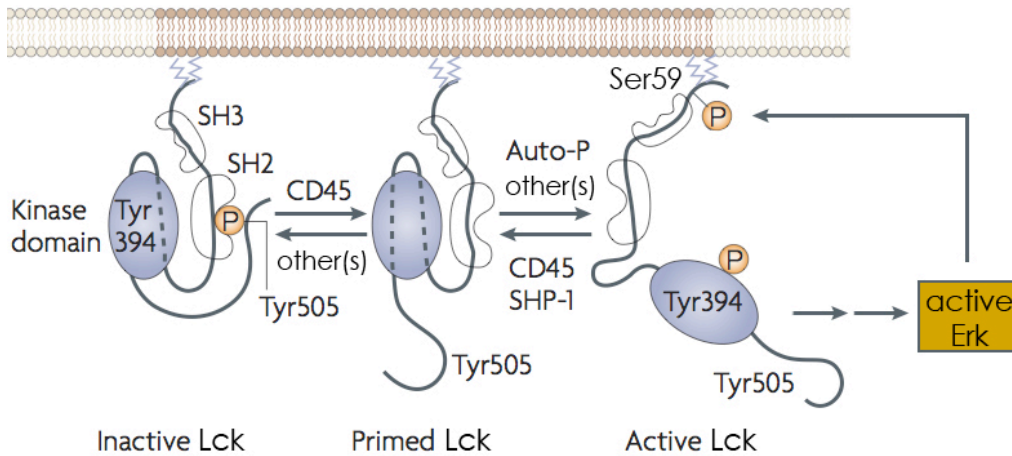


Figure 3. Regulation of Lck (adapted from (41)). The dynamic equilibrium between inactive and active Lck (left panel) is influenced by various factors such as the tyrosine phosphatase CD45 (not shown). Negative feedback by SHP-1 inhibits the enzyme (middle panel), whereas positive feedback by Erk overcomes SHP-1 inhibition and therefore activates the enzyme (right panel).

In naïve T-cells, CD3 ITAMs are to some degree phosphorylated (the CD3 ζ p21 species can be detected in resting cells (42)) by activated Src-family PTKs. The rate of ITAM dephosphorylation by phosphatases such as SHP-1 or CD45 ensures that the basal phosphorylation is not exceeded in resting cells, suggesting that this dynamic equilibrium does only favor phosphorylation upon TCR triggering.

Once both tyrosines within an ITAM of CD3 ζ or ϵ are phosphorylated, the ζ -chain associated protein of 70kDa (ZAP-70), a PTK, can bind to the ITAM via its tandem Src-homology 2 (SH2) domain. Since ZAP-70 is of particular interest for the work presented in this thesis, it is discussed in greater detail in chapter 1.7. ZAP-70 binding to phospho-ITAMs prolongs the transient TCR-pMHC interaction, thereby generating a more sustained intracellular signal. ZAP-70 applies its kinase activity on multiple downstream signaling and adaptor molecules. An important target of ZAP-70 mediated tyrosine phosphorylation is the linker for activation of T-cells (LAT), a GEM-associated adaptor protein. Upon phosphorylation at several tyrosine residues, LAT recruits various signaling and other adaptor molecules in order to diversify and regulate downstream signaling. Among the nine conserved tyrosines, the last four LAT tyrosines at position 132, 171, 191, and 226 (136, 175, 195 and 235 in mouse) are known to be important for LAT function. Besides ZAP-70, Itk, and Lck have been identified as *in vivo* LAT kinases. When phosphorylated, these four conserved LAT tyrosines serve as docking sites for SH2 domain-containing proteins, including phospholipase C- γ 1 (PLC- γ 1), Grb2, Gads and the p85 subunit of phosphoinositide 3-kinase (PI3K) (43). In turn, these molecules recruit SH3 domain ligands including Src homology 2 domain-containing leukocyte protein of 76kDa (SLP-76), son of sevenless (SOS), and c-Cbl. Functional studies have shown that

PLC- γ 1 binds to LAT Y132, thereby inducing its own tyrosine phosphorylation (44). Similarly, Grb2, in association with its SH3 domain ligands SOS and c-Cbl, associates with LAT Y171, Y191, and Y226, whereas Gads and its SH3 domain ligand SLP-76 interact with LAT Y171 and Y191. Therefore, the recruitment of signaling molecules to LAT results in the formation of multiprotein complexes that bind to specific tyrosines on LAT through a combination of affinity preferences and cooperative interactions (45).

The phosphorylation of three critical tyrosines of SLP-76 in a ZAP-70/LAT-dependent manner is functionally activating SLP-76. These tyrosines serve as binding sites for SH2 domain-containing proteins including an apparent trimolecular complex among SLP-76, Vav and Itk, a member of the Tec family of tyrosine kinases. The trimolecular complex appears to be important for the localization of Itk to the LAT complex. Interestingly, both the tyrosine phosphorylation and lipase activity of PLC- γ 1 is dependent on LAT, SLP-76, and Itk, since T-cells deficient in these molecules have reduced PLC- γ 1 phosphorylation and Ca²⁺ influx. Therefore, LAT and SLP-76 may localize Itk to the LAT complex, leading to the phosphorylation of PLC- γ 1 by Itk.

Removing the signaling units from the CD3 ζ chain (six out of ten ITAMs in the CD3 complex are located on the ζ -chain; see chapter 1.X) surprisingly does not lead to substantially reduced numbers of positively selected thymocytes (46). However, such cells have a very limited TCR repertoire. On the other hand, several Src and Syk family tyrosine kinases involved in proximal TCR signaling are critical in positive selection and their deletion strongly impairs thymic selection. On the other hand, deletion of negative regulators of TCR signaling (chapter 1.6.5) that would normally oppose the involved kinases, leads to increased numbers of positively selected thymocytes. In terms of signaling, positive selection can also be abrogated by cyclosporine A or FK506, which are potent inhibitors of Ca²⁺-dependent calcineurin signaling. PLC γ -1, which is central in generating a Ca²⁺ flux severely affects β -selection and positive selection when missing, as shown by a mutant form of the adapter protein LAT that cannot recruit PLC γ -1. Also, deletion of LAT itself completely blocks thymocyte development already at the DN3 stage.

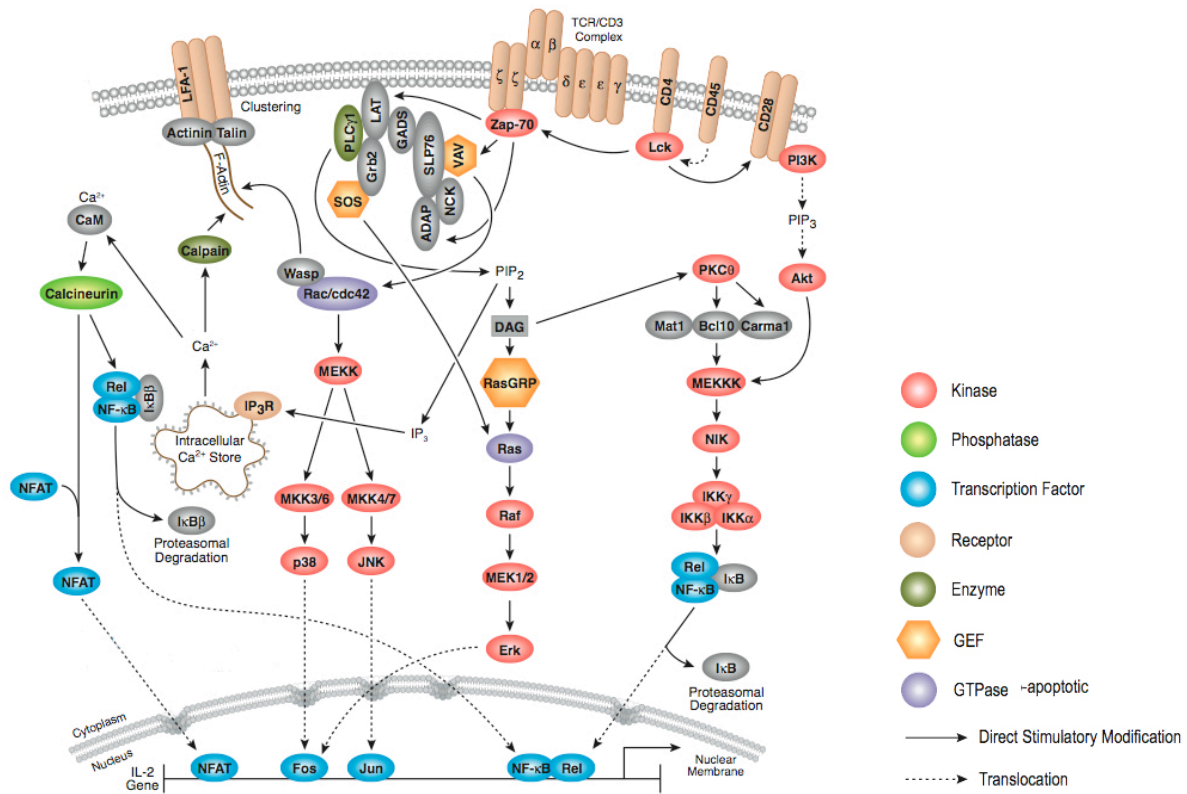


Figure 4. Activatory steps in T-cell signaling (adapted from Cell Signaling Technologies). Some of the major effectors in TCR-, CD28 and LFA-1-mediated signaling are depicted schematically. Proteins are color coded according to their function (table on the right). Some relevant transcription factors induced by these signaling pathways are shown in light blue although they are not covered by the manuscript.

1.6.1 The immunological synapse

Antigen recognition and signal initiation takes place at the interface between a T-cell and an antigen presenting cell (APC), which is called the immunological synapse. The immunological synapse consists of a central zone, the central supramolecular activation cluster (c-SMAC), which contains the TCR and surface accessory molecules such as the co-receptor, CD2 and CD28 (47, 48). Surrounding the central zone is another zone, the peripheral supramolecular activation cluster (p-SMAC), which is enriched in adhesion molecules such as integrins and LFA-1. Although the function of the immunological synapse has not been entirely elucidated, it is the area of adhesion and sustained TCR-pMHC interaction (37, 49). Microscopy provided insight into the first signaling steps of T-cells. In a MHC class II restricted system, peripheral CD4 T-cells were transduced with signaling constructs attached to fluorescent proteins. When these cells were stimulated by the presentation of agonist peptide-MHC anchored in a lipid bilayer on a slide, spatio-temporal behaviour of these constructs could be observed by total internal reflection microscopy (TIRFM) (50). TCR microclusters of about 11-17 TCRs in size, were first generated in the c-SMAC after very short time of contact (~5s) and then generated in the p-SMAC that served to sustain the signal. Analysis of the

signaling molecules ZAP-70 and SLP-76 revealed strong co-localization with freshly generated TCR microclusters in the p-SMAC. However, ZAP-70 only partially moved towards the c-SMAC together with the TCR (and the fraction that did, was not phosphorylated) and SLP-76 disappeared completely from central microclusters. In a further study, microcluster formation was found to be dependent on actin cytoskeleton remodeling, probably mediated by integrins (51). pMHC engagement forms F-actin dependent microclusters that exclude the phosphatase CD45 and are the site of signal initiation. This may per se allow increased phosphorylation by tyrosine kinases in the cluster. Additionally, Lck diffuses into the clusters from surrounding CD45-rich domains (52). Migration of the microclusters to the c-SMAC intermixes CD45 again and signaling stops. The c-SMAC is not involved in sustained Ca^{2+} signaling. Moreover, LBPA (a lipid that is generated at the site of multivesicular body formation and targets membrane proteins for degradation) accumulates in the c-SMAC, sorting ubiquitinated TCR for degradation, suggesting that the c-SMAC is predominantly a site of signal termination and endocytosis of the TCR.

1.6.2 Costimulation

Complete T-cell activation also requires the engagement of costimulatory receptors, in particular CD28, inducible T-cell costimulator (ICOS) and CD7, by their corresponding APC ligands. On the other hand, corepressors such as cytotoxic T lymphocyte antigen 4 (CTLA-4) and programmed cell death protein 1 (PD-1) have important inhibitory functions. Both coreceptor-driven signals are necessary to establish a productive immune response, which leads to cytokine production, increased survival and clonal expansion of naïve T-cells. In contrast, TCR engagement in absence of costimulation induces unresponsiveness and thereby promotes T-cell tolerance. CD28 is expressed by activated and naïve T-cells, underlining its importance for the induction of primary immune responses. In contrast, ICOS and CTLA-4 are only expressed on activated and memory T-cells. They co-regulate $\text{T}_\text{H}2$ responses and the termination of T-cell activation. Different coreceptors can be engaged by overlapping ligands, as it is the case for CD28 and CTLA-4, which are competing for association of B7-1 (CD80) or B7-2 (CD86), although CTLA-4 binds B7 molecules 20 times more avidly. B7 molecules are found exclusively on the surfaces of cells that stimulate T-cell proliferation and in their absence or blocking clonal expansion is prevented. CD28 binds B7 molecules during the activatory and expansion phase of a T-cell response, which upregulates CTLA-4 in order to limit antigen responsiveness and cytokine production. CTLA-4 deficiency leads to a massive overgrowth of activated lymphocytes, underlining its essential role in terminating the proliferative response of activated T-cells to antigen and B7. Other coreceptors are triggered by distinct ligands, for example, B7H for ICOS, PD-1L for PD-1 and K12 for CD7. Once a naïve T-cell is activated, it expresses proteins that modify the costimulatory signal such as the CD40 ligand (CD154). Binding of CD40 on the surface of APCs transmits activating signals to the T-cell and also activates the APC to express B7

molecules, thus stimulating further T-cell proliferation. Mice lacking CD40 ligand show a shortened clonal expansion of responding T-cells upon immunization.

1.6.3 Systematic signaling regulation

The stochastic expression of signaling molecules provides another approach to explain the variability (and with a closer look also the robustness) of cellular responses. For example, variable T-cell responses to antigenic stimulation within a clonal population are necessary to allow for the development of both effector and memory T-cell subsets from that population. In a population of uniform, agonist-stimulated T-cells, the Lck-associated CD8 co-receptor was identified as positive analog regulator (CD8 expression correlates with the EC_{50} of activated cells as measured by ppERK) (53). In contrast, SHP-1 functions as negative switch-like regulator (SHP-1 expression negatively correlates with the strength of activation but the EC_{50} remains constant). Although this theoretically leads to substantial variability in the responsiveness of a single T-cell in a clonal population of T-cells (based solely on the stochastic expression of signaling molecules), most antigen responses are highly uniform. To ensure this robustness, expression levels of CD8 and SHP-1 appear to be co-regulated, thereby reducing the response variation (53). In the bigger context of an immune response, co-regulation decreases the number of hyperresponsive cells and potentially limits the risk of self-responsiveness of T-cells.

1.6.4 Ras/MAPK signaling

Ras is a member of the large superfamily of small GTPases. Signal-induced conversion of the inactive (GDP-bound) form to the active (GTP-bound) form allows downstream signaling elements to be engaged. The GDP to GTP exchange is mediated by guanine nucleotide-exchange factors (GEFs). Due to its GTPase activity, Ras is a self-limiting, rather poor enzyme. However, the catalytic activity of Ras can be substantially improved by GEFs.

In T-cell signaling, N-Ras is of particular importance. Lymphoid malignancies linked to Ras mutations are almost always in the *nras* gene (54). N-Ras deficient mice exhibit defective T-cell function and are extremely sensitive to viral infections. Ras is required for thymocyte development, T-cell proliferation and IL-2 production (55). Positive selection is severely affected in mice expressing a dominant negative form of Ras (56). In contrast, negative selection remains intact.

Ras proteins are associated to the plasma membrane but do not themselves have signal sequences or hydrophobic membrane-spanning domains. Rather they are modified posttranscriptionally (including prenylation, palmitoylation and carboxyl-methylation) and targeted to cellular membranes, which is believed to be required for biological activity. As for example, N-Ras and H-Ras undergo a palmitoylation/depalmitoylation cycle, which regulates their trafficking from the plasma

membrane to the Golgi and back again (57). This bidirectional traffic may have a regulatory role in signaling.

The best characterized Ras-regulated signaling pathway is the mitogen-activated protein kinase (MAPK) pathway that proceeds through the MAP kinases Erk1 and Erk2 (extracellular signal-regulated kinases). The adapter protein Grb2 connects TCR signals to the Ras pathway, since Grb2 is constitutively associated with SOS (son of sevenless) through its SH3 domain. SOS is a GEF for Ras proteins. Therefore, TCR engagement leads to the recruitment of SOS to the plasma membrane, where it encounters Ras. Once Ras is activated, it recruits Raf-1, a serine/threonine kinase whose complex regulation is poorly understood. Raf-1 phosphorylates and activates MEK (MAPK/Erk kinase), a dual specificity tyrosine/threonine kinase that in turn phosphorylates and activates Erk1 and Erk2. Erk proteins are serine/threonine kinases that have numerous targets, including cytosolic proteins. However, phospho-Erk also forms dimers that can be transported into the nucleus in order to activate several transcription factors.

The GEF Ras guanine nucleotide-releasing protein 1 (RasGRP-1) disrupts thymic selection indicating that Ras/MAPK-mediated signaling downstream of the TCR is essential for thymocyte development and further experiments confirmed that RasGRP-1 is required for ideal TCR mediated Ras-Erk activation (58). In T-cells, RasGRP1 can translocate to the Golgi, leading to Ras activation in this organelle. Along the same lines, there is no Ras activity in PLC- γ 1 deficient T-cells (which by its enzymatic activity produces the secondary messenger DAG that directly binds to RasGRP-1 and activates it). Nevertheless, Ras can be activated at the plasma membrane by signaling via Grb2/SOS in response to strong, but not to weak stimuli (59). In accordance with this, thymocyte leads to compartmentalization of Ras/MAP kinase signaling (8). In response to high-affinity, negative-selecting pMHC ligands, RasGRP1, Ras and Raf-1 are recruited to the plasma membrane whereas with low-affinity, positive-selecting ligands these molecules are targeted to the Golgi. Phosphorylated Erk is also targeted to the membrane in response to strong stimuli in contrast to Jun amino terminal kinase (Jnk), which remains distributed throughout the cell independent of the TCR input. Therefore, positive and negative selection are characterized by the cellular localization of the MAPK signaling molecules.

1.6.5 Negative feedback in TCR signaling

Besides the activating mechanisms there are several inhibitory and negatively regulating mechanisms that control the outcome of TCR induced signaling. Negative feedback can further be distinguished by their mechanism and kinetics of induction. Regulatory mechanisms that are activated by inhibitory membrane-bound receptors include CD28, CD5, cytotoxic T-lymphocyte antigen 4 (CTLA-4), programmed cell death 1 (PD-1) and those that control degradation of signaling components, mainly by ubiquitylation. Inhibitory receptors like CD5, PD-1 and CTLA-4 are

recruiting protein tyrosine phosphatases to the membrane, thereby promoting negative feedback lasting for several hours after TCR stimulation. They modulate TCR signaling in effector and memory T-cells, as well as their differentiation. CTLA-4 targets downstream signaling molecules of phosphatidylinositol 3-kinase (PI3K) by activating the serine/threonine phosphatase PP2A. In contrast, PD-1 prevents the intracellular accumulation of 3-phosphorylated phosphatidylinositol lipids (by antagonizing PI3K directly), which are important second-messenger molecules. However, both inhibitory pathways converge at the serine/threonine kinase Akt (also known as PKB) (60).

More proximal negative feedback mechanisms are rapidly activated simultaneously to the activation of the TCR signalosome. These mechanisms act mainly in thymocytes and naïve T-cells and are induced by the TCR itself. Mice deficient in SHP-1 show enhanced positive and negative selection and T-cell activation. Eventually, these mice develop autoimmunity. Remarkably, low-affinity antagonist pMHC ligands (which do not activate mature T-cells), promote SHP-1 membrane recruitment and activation whereas high-affinity agonist ligands elicit delayed and lower SHP-1 recruitment (40, 61). Consequently, lowering SHP-1 activity converts antagonists into partial agonists that could induce calcium signaling. SHP-1 binds via its two SH2-domains to immunoreceptor tyrosine-based inhibitory motifs (ITIMs), thereby evolving its phosphatase activity. Besides binding to the ITIMs in the cytoplasmic tails of inhibitory receptors, there is evidence that SHP-1, upon TCR-antagonist binding, associates with Lck, becomes phosphorylated and in turn downregulates Lck kinase activity (40, 61). Other tyrosine phosphatases like PTPN22, SHP-2 or DUSP-5/6 strongly enhance TCR sensitivity when they are collectively silenced by expression of the micro-RNA miR-181a (61). However, it's not entirely understood whether the miR-181a controlled phosphatases are activated as negative feedback loop following TCR engagement or whether they act constitutively. TCR mediated antigen recognition is more sensitive in thymocytes. This allows positive selection by accumulation of low-affinity TCR-pMHC interactions that would not lead to stimulation of a peripheral T-cell. Along these lines, *shp-1 mRNA* levels are lower in DP thymocytes than in mature T-cells and miR-181a is highly expressed in DP thymocytes and decreased in positively selected SP thymocytes. This regulatory mechanism may provide the basis to explain the different TCR signaling sensitivity according to the developmental stage.

Another negative feedback mechanism involves the cytoplasmic adaptor proteins DOK1 and DOK2 (downstream of kinase 1). These adaptors become tyrosine phosphorylated and interact with LAT as a multi-protein complex, which also involves SHIP-1, an inositol phosphatase. The protein complex interferes with the generation of secondary signaling messengers and the membrane recruitment of Akt. Since these effects correlate with enhanced ZAP-70 and LAT phosphorylation and ERK activation, this pathway represents another feedback loop that is acting on TCR-proximal signaling components. DOK1/2 negative mice exhibit increased TCR-induced cytokine production and proliferation, show increased T-cell mediated antibody responses and develop a lupus-like disease.

How is a specific signal generated following the engagement of a TCR? The TCR-pMHC interaction is characterized by the half-life of binding, which is the average residual time of a pMHC ligand on the TCR. Once the 'binding input' is translated across the plasma membrane, tyrosine phosphorylations of the CD3 ITAMs provide the scaffold for the activation of intracellular signaling pathways (which in the case of the TCR can be fundamentally different, giving rise to proliferation/differentiation of a thymocyte or a T-cell but can also induce their apoptosis). The effectors of these cascades are kinases and phosphatases (as far as our current understanding of signaling goes, transfer or withdrawal of phosphate groups to tyrosine, serine or threonine residues are the predominant means to regulate signal propagation). Feedback loops (positive and negative) modify the rate of particular effector-catalyzed reactions, thereby establishing new steady states. This can be achieved in several ways: targeting of proteins into multi-protein complexes or into specific locations (such as membrane GEMs) provides the basis of functional cooperativity. Cooperativity converts a graded response into a switch-like response (eg. if a substrate that is activated by an enzyme induces further increase of the enzyme). Biophysically, the response curve of a graded reaction is linear for low substrate concentrations and plateaus with increasing substrate concentrations, being limited by the maximal catalytic rate of a particular enzyme. In contrast, the response curve of a switch-like reaction has a sigmoid shape and a threshold can be defined (such as the half-maximal catalytic rate). The degree of cooperativity determines how sharp the threshold is, with a high degree of cooperativity enhancing the switch-like character of a response. This principle ensures the bivalency of an enzymatic response and 'prevents' intermediate responses. Mechanistically this means that subtle changes in the TCR-pMHC half-life are translated into switch-like responses by the TCR-proximal phosphorylation and dephosphorylation events, thereby establishing a signaling threshold of activation.

1.6.6 How TCR signaling distinguishes ligands

'Steady state' signaling in thymocytes and T-cells is controlled by positive and negative regulatory mechanisms that can be shifted by TCR-pMHC engagement. High-affinity TCR-pMHC interactions, as characterized by an extended half-life of TCR-pMHC binding, strongly activate the receptor-proximal kinases. At the same time, phosphatases that downmodulate the kinase activity are induced, which results in an overall strong but transient tyrosine phosphorylation cascade (34). Negative selection is characterized by relatively coreceptor-independent extensive CD3 ITAM phosphorylation and hence full LAT phosphorylation. This leads to recruitment of Grb2/SOS1, and transient activation of Ras and ERK at the plasma membrane. One prerequisite of negative selection is the switch-like activation of Erk in the periphery in response to negative-selecting ligands (8). In contrast, the integration of many signals of low apparent affinity leads to moderate but sustained kinase activity that partially overcomes negative regulation (62). Positive selection involves

coreceptor-dependent signal transmission via the TCR's α -CPM/CD3 δ and leads to intermediate CD3 ITAM phosphorylation (4). Partial LAT phosphorylation recruits PLC γ -1 and Gads/Slp76/Itk, resulting in activation of PLC γ -1 and production of diacylglycerol (DAG) and calcium signals. The Ras activator RasGRP-1 is activated by DAG binding and stimulates sustained, low-level ERK activation while moderate calcium signaling may be sufficient to induce gene transcription.

Taken together, TCR-mediated signaling distinguishes negative- from positive-selecting ligands by inducing positive and negative effectors with different kinetics and as well by the separation of signaling components to either intracellular organelles or maintaining them in the periphery.

1.7 A closer look at ZAP-70

1.7.1 ZAP-70 discovery and relevance

ZAP-70 was first described as protein tyrosine kinase (PTK) that is associated with CD3z and undergoes tyrosine phosphorylation following TCR engagement (63). ZAP-70 deficient mice have neither CD4⁺ nor CD8⁺ single-positive (SP) T-cells (64). Due to this defect in positive selection, thymocytes are arrested in their double-positive (DP) state of development. Negative selection is also impaired since these cells are unresponsive to pMHC ligands. Human ZAP-70 reconstitutes both CD4⁺ and CD8⁺ SP populations, underlining the central role of this tyrosine kinase in T-cell development.

1.7.2 ZAP-70 binding to TCR ITAMs and activation

In cell-free assays, fully phosphorylated dimeric CD3 ζ is sufficient to promote ZAP-70 autophosphorylation and catalysis of a substrate (65). In contrast, monomeric CD3 ζ does not activate ZAP-70, independent of its phosphorylation state. Murine thymocytes exhibit constitutive association of ZAP-70 with partially phosphorylated (dimeric) CD3 ζ , yet ZAP-70 is not activated (66, 67). The discrepancy between these *in vitro* and *in vivo* findings may originate from dephosphorylation mechanisms of CD3 ITAMs, which do not occur in the described cell-free assay. This regulation prevents full CD3 ζ phosphorylation in resting thymocytes and therefore doesn't activate ZAP-70. Indeed, the tyrosine phosphatase SHP-1 binds to ZAP-70, resulting in increased SHP-1 phosphatase activity and decreased ZAP-70 kinase activity (68, 69). Thus, SHP-1 is as negative regulator of ZAP-70 and therefore TCR-mediated signaling.

ZAP-70 binds to tyrosine-phosphorylated ITAMs of CD3 ζ and CD3 ϵ . The biophysical parameters for ZAP-70 binding to these TCR subunits were determined by binding assays. The isolated N-terminal SH2-domain of ZAP-70 binds with 100-fold reduced affinity to the phosphorylated cytoplasmic portion of CD3 ζ compared to the complete tandem SH2-domain (70). No binding was observed if

the isolated C-terminal SH2-domain was used, which indicates positive binding cooperativity of the tandem SH2-domains and thereby ensures high affinity for the doubly phosphorylated ITAM. The binding affinity of the ZAP-70 tandem SH2-domain to peptides containing individual CD3 ζ ITAMs as well as the CD3 ϵ ITAM was measured and the hierarchy described as $\text{ITAM}(\zeta_1) \geq \text{ITAM}(\zeta_2) > \text{ITAM}(\text{CD3}\epsilon) \geq \text{ITAM}(\zeta_3)$ (index numbers denote the N- to C-terminal direction of CD3 ζ ITAMs) (71). Affinity differences of as much as 30-fold between the individual phospho-ITAMs suggests that ZAP-70 binds to ITAMs sequentially, provided that they are phosphorylated. Indeed, CD3 ζ ITAM phosphorylation is sequential and appears to be ordered (72). A basally phosphorylated form of CD3 ζ can be detected in resting cells (p21 form), whereas fully phosphorylated CD3 ζ (p23 form) is induced only upon stimulation with agonist pMHC ligands presented by APCs and involves phosphorylation of all 6 tyrosines within the 3 CD3 ζ ITAMs. Antagonist pMHC ligands promote intermediate CD3 ζ phosphorylation, which does not detectably activate ZAP-70. In mice with transgenic TCRs either restricted for MHC class I or class II, the percentage of positively selected CD8⁺ or CD4⁺ SP cells, respectively, decreases when going from 3 intact CD3 ζ ITAMs (wildtype) to 1 ITAM and to no ITAMs (73). This change of CD3 ζ ITAM multiplicity alters the efficiency of thymic selection since ZAP-70 binding is reduced and downstream signaling diminished. Along the same lines, T-cell clones stimulated with altered peptide ligands (APLs) induce only partial CD3 ζ ITAM phosphorylation, which greatly reduces ZAP-70 activation and PLC- γ 1 mediated phospholipid hydrolysis (74).

Besides Src family kinases such as Lck, ZAP-70 itself is also involved in CD3 ITAM phosphorylation (75). In DP thymocytes with limiting coreceptor-associated Lck, ZAP-70 is required for ITAM phosphorylation independent of its kinase activity (76). Rather than just protecting the ITAMs from dephosphorylation, ZAP-70 promotes ITAM phosphorylation by recruiting Lck via SH2-domain mediated interactions. Upon positive selection, the requirement for ZAP-70 decreases as the amount of Lck available to the TCR quantitatively increases. In accordance with this, mice with a spontaneous mutation in the ZAP-70 kinase domain failed to fully phosphorylate ζ , similar to ZAP-70^{-/-} mice (77), further supporting the idea that TCR-associated ZAP-70 functions as adaptor for coreceptor-associated Lck in DP thymocytes.

1.7.3 ZAP-70 mutational analysis

Substitution of tyrosine 319 with structurally similar phenylalanine (Y319F) in the interdomain B leads to dominant negative ZAP-70 behavior (78). Y319F prevents phosphorylation of further ZAP-70 regulatory residues such as Y493, therefore inhibits the kinase activity and antigen-induced IL-2 expression. Evidence is provided that Y319 is a binding site for Lck (SH2-domain mediated binding), which in turn positively regulates ZAP-70 (79). Therefore, a ZAP-70 mutant carrying the optimal

binding site for the SH2-domain of Lck (Y³¹⁹E EI instead of wildtype Y³¹⁹SDP) displays a gain-of-function phenotype, exhibited by increased tyrosine phosphorylation and catalytic activity. Tyrosine phosphorylation at residue 493 in the kinase domain of ZAP-70 is another positive regulatory step (80, 81). Substitution of Y493 with phenylalanine (Y493F) prevents ZAP-70 activation even if Y493F is co-expressed with constitutively active Lck.

Another study suggests that Y315 and Y319 are not substrate recruiting residues in the first place. Rather, they function as autoinhibitory switch, thereby regulating ZAP-70's kinase activity (82). By phosphorylating Y319 (and possibly Y315), Lck or other kinases activate ZAP-70, similar to the juxtamembrane region of several RTKs. These findings were supported by the crystallographic structure of ZAP-70 where phosphorylation at Y319 in the interdomain B promotes the separation between the tandem-SH2 domain and the kinase domain by electrostatic repulsion, which is necessary to activate the kinase (83). In contrast to the Y319F mutant, the Y315/319A mutant leads to Y493 phosphorylation, probably via an intermolecular *trans*-phosphorylation mechanism, arguing for an open conformation of the Y315/319A mutant and therefore a release from autoinhibition, similar to the tyrosine-phosphorylated wildtype ZAP-70 (82). Along the same lines, Lck is not very efficient in phosphorylating Y493 in a kinase-inactive ZAP-70 mutant (K369A), even when Y319 was phosphorylated and available for Lck-binding. This suggests that phosphorylation of interdomain B Y315 and Y319 is the only phosphorylation step depending on kinases other than ZAP-70 itself. However, these findings were contradictory to the observation that the K369A kinase-inactive mutant was hyperphosphorylated at both Y319 and Y493 in Cos or 293 cells. Therefore, although not very efficient, Lck participates in phosphorylating Y493 (79). Hypothetically, Lck may be responsible for the initial but rather inefficient phosphorylation of Y493 on several ZAP-70 molecules that *trans*-autophosphorylate other ZAP-70 molecules with which they are dimerized by paired ITAMs of the CD3 subunits.

1.7.4 ZAP-70 structure

Only recently the structure of full-length, inactive ZAP-70 has been resolved (83). In this model, the hinge region of the kinase domain forms a network of hydrogen bonds between the tandem-SH2 domain and the kinase domain. The hydrogen bonds are broken in the active conformation allowing more flexibility, which is required for catalysis (therefore, inactive ZAP-70 is considered 'autoinhibited'). Upon SH2-mediated, specific binding to doubly phosphorylated ITAMs, the side chain of Trp133 is moved away from Tyr315 and Tyr319, thereby disrupting the aromatic-aromatic interaction, which is normally stabilizing the linker-kinase interface (=interdomain B). This facilitates the access to phosphorylation sites Tyr315 and Tyr319 by Lck or potentially other PTKs (Figure 5). Therefore autoinhibition is released upon phosphorylation of these tyrosines residues.

Phosphorylation of tyrosines Tyr492 and Tyr493 in the activation loop is likely to promote its active extended conformation by preventing it from collapsing into the active ATP-binding site.

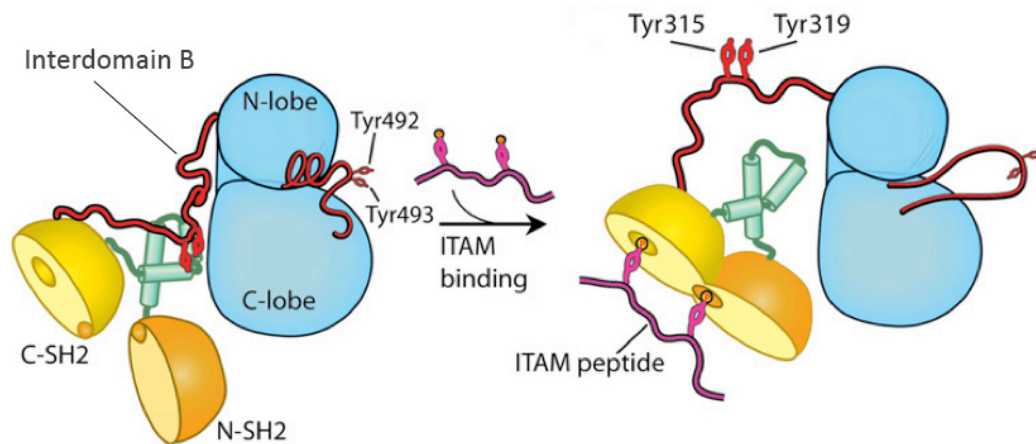


Figure 5. ZAP-70 ITAM binding (adapted from (83)). The conformational change of ZAP-70 is shown upon binding to a doubly phosphorylated ITAM peptide. Phospho-ITAM-bound ZAP-70 is susceptible to further phosphorylation steps at Y315/Y319 in the interdomain B and Y492/Y493 in the activation loop of the kinase domain. N-SH2: N-terminal SH2-domain, C-SH2: C-terminal SH2-domain, N-lobe and C-lobe: subdomains of the ZAP-70 kinase domain.

1.7.5 ZAP-70 in development and disease

A spontaneous occurring single amino acid substitution in the second SH2-domain (W163C) alters TCR-mediated signaling, the outcome of thymic selection and causes joint inflammation and infiltration of CD4⁺ T-cells in these animals, which is strongly reminiscent of rheumatoid arthritis in humans (84). If those mice are crossed with HY TCR-transgenic mice, male-specific thymocytes that are positively selected in non-transgenic female animals, fail to become CD8⁺ SP T-cells. In contrast, thymocytes that would be negatively selected in male animals develop to some degree into CD8⁺ SP T-cells, which points towards an altered threshold of thymic selection. Since the described point mutation affects the SH2 domain and therefore binding to phosphorylated ITAMs, one explanation for the altered thymocyte selection may be that high-affinity TCR signals would be weakened due to reduced ZAP-70 recruitment to activated TCR complexes. On the other hand, low-affinity TCR signals would be reduced to non-selecting levels due to inefficient recruitment and subsequent activation of ZAP-70.

In patients with selective T-cell deficiency (STD), who are characterized by persistent infections reminiscent of severe combined immunodeficiency, a DNA point mutation leads to alternative splicing of the *zap-70* gene (85). This results in a three amino acid insertion in the kinase that has no detectable enzymatic activity. T-cells from three patients, homozygous for the *zap-70* gene mutation, exhibit markedly reduced tyrosine phosphorylation. However, some Ca²⁺ mobilization

remains in activated peripheral T-cells, likely due to Fyn kinase that has more redundant ZAP-70 functions in humans than in mice. In contrast, ZAP-70 activity is indispensable for the positive selection of CD8⁺ SP thymocytes. These observations underline the essential role of ZAP-70 in thymic selection, whereas peripheral T-cells exhibit some independency of ZAP-70 in TCR-mediated signaling.

Another study demonstrates that a spontaneously occurring point mutation in the DLAARN motif (R464C) of ZAP-70's kinase domain (in fact DLAARN is conserved among all PTKs), results in defective TCR signaling and a complete arrest of thymocyte development at the CD4⁺ CD8⁺ DP stage (77). These mice express a catalytically inactive form of ZAP-70, again demonstrating the requirement for ZAP-70 activity in thymocyte development.

In healthy individuals, ZAP-70 expression is restricted to T-cells and NK cells. However, ZAP-70 is expressed in peripheral B-cells of the majority of poorer prognosis chronic lymphocytic leukemia (CLL) patients (with unmutated *IgVH* genes, showing 98 – 100% homology to the germline sequence), but absent in most cases with mutated *IgVH* genes (reviewed in (86)). This overexpression has functional consequences in CLL, although it is not clear whether this reflects the ongoing of transforming events or whether ZAP-70 expression is a consequence of a more activated B-cell type (there is some evidence that ZAP-70 expression is induced in B-cell progenitors and activated B-cells).

2. Materials and methods

2.1 Reagents

2.1.1 For molecular techniques

XL-1blue competent bacteria	Stratagene
Ampicillin	Sigma
Primers	Microsynth

2.1.2 For cellular techniques

β -mercaptoethanol (β -me)	Gibco
RPMI	Gibco
DMEM	Gibco
Fetal calf serum (FCS)	Amimed
Non-essential amino acids (100x)	Gibco
Sodium pyruvate (100x)	Gibco
Penicillin-streptavidin (100x)	Gibco
L-glutamine (100x)	Gibco
Polybrene	Sigma
Hygromycin B	Calbiochem
Geneticin (G418)	Sigma
Puromycin	Sigma
L-histidinol	Sigma
β -2 microglubulin (β 2m)	Calbiochem
PolyFect transfection reagent	Qiagen
Cy5 mono-reactive dye	GE Healthcare (Amersham)
Streptavidin-HRP	Zymed
0-phenylenediamine dihydrochloride	Sigma
Glutaraldehyde, 25%	Sigma
Formaldehyde, 16%	Polysciences Inc.
Anti-FITC MACS microbeads	Miltenyi Biotec
(3-Aminopropyl)triethoxy-silane (Tespä)	Sigma
Triton X-100	Bio-Rad
FlourSave Reagent	Calbiochem

2.1.3 For biochemical techniques

Protease inhibitor cocktail (+EDTA)	Sigma
Protein G sepharose	GE Healthcare
Trans-Blot nitrocellulose membrane	Bio-Rad
Dual color protein standard	Bio-Rad
Acrylamide/Bis 30:1 solution	Bio-Rad
Amonium persulfate (APS)	Bio-Rad
N,N,N',N'-Tetramethylethylenediamine (TEMED)	Bio-Rad
Ponceau red	Sigma
Skim milk powder	Bio-Rad
ECL Western blotting detection reagents	GE Healthcare (Amersham Biosciences)
Hyperfilm ECL	GE Healthcare (Amersham Biosciences)
LAT, recombinant protein	Millipore
ATP	Sigma

2.1.4 Enzymes

AccuPrime DNA polymerase	Invitrogen
Restriction Enzymes and buffers	New England Biolabs
Shrimp alkaline phosphatase	Roche

2.1.5 Kits

DNA Maxi Prep kit	Qiagen
DNA Mini Prep kit	Qiagen
Gel extraction kit	Qiagen
T4 DNA ligase kit (Ready To Go)	Amersham Biosciences
ABI Prism DNA sequencing kit	Applied Biosystems
Slowfade anti-fade kit	Invitrogen

2.2 Solutions and media

2.2.1 For molecular techniques

TAE	40mM	Tris-acetate pH 8.0
	1mM	EDTA

DNA loading buffer (5x)		H ₂ O
		30% glycerol
	0.25%	Bromphenol blue
	0.25%	Xylene cyanol

TE	10mM	Tris pH 8.0
	1mM	EDTA

2.2.2 For biochemical techniques

Lysis Buffer		H ₂ O
	1%	Brij 58 or Nonidet P-40
	50mM	Tris pH 7.5
	15mM	NaCl
	1mM	PMSF
	1mM	Sodium orthovanadate, activated
	1mM	NaF
	1mM	β -glycerophosphate
	1x	Protease inhibitor cocktail (+EDTA)

IP wash buffer	\pm 0.5%	Brij 58 or Nonidet P-40
	50mM	Tris pH 7.5
	15mM	NaCl

Kinase assay buffer	50mM	Tris pH 7.5
	30mM	NaCl
	5mM	MgCl ₂
	10mM	ATP

2.2.3 For SDS-Page and Western blotting

Separating gel		H ₂ O
	10% - 12%	30% Acrylamide/Bis 30:1 solution
	375 mM	Tris pH 8.8

	0.1%	SDS
	0.1%	APS
	0.01%	TEMED
Stacking gel		H ₂ O
	5%	30% Acrylamide/Bis 30:1 solution
	250 mM	Tris pH 6.8
	0.1%	SDS
	0.1%	APS
	0.01%	TEMED
SDS running buffer	25mM	Tris pH 8.0
	250mM	Glycine
	0.1%	SDS
SDS loading buffer (5x)	50mM	Tris pH 6.8
	20%	Glycerol
	2%	SDS
	5%	β-me
Transfer buffer	25mM	Tris pH 8.0
	250mM	Glycine
	20%	Methanol
TBS	50mM	Tris pH 7.6
	0.9%	NaCl
TBS-T		TBS
	0.1%	Tween 20
Blocking buffer		TBS-T
	5%	Skim milk powder
	0.02%	NaN ₃

2.2.4 For cellular techniques

PBS	137mM	NaCl
-----	-------	------

	2.7mM	KCl
	8.0mM	Na ₂ HPO ₄
	1.5mM	KH ₂ PO ₄
FACS buffer		PBS
	1%	FCS
	0.2%	NaN ₃
LB medium	1%	Bacto-tryptone
	0.5%	Bacto-yeast extract
	90mM	NaCl
LB freezing medium		LB medium
	15%	glycerol
LB agar plates		LB medium
	1.5%	Agar
		autoclaved, selective drug added if required

2.2.5 Media used for cell culture

Basic medium		RPMI or DMEM
	100U/ml	Penicillin
	100µg/ml	Streptomycin
	2mM	L-glutamine
	1mM	Non-essential amino acids
	1mM	Sodium pyruvate
	5mM	β-me
58 hybridoma medium		RPMI basic medium
	4%	FCS
APC medium		RPMI or DMEM basic medium
	8%	FCS
T-cell medium		DMEM basic medium
	10%	FCS

FTOC medium		DMEM basic medium
	10%	FCS
	5mg/ml	β 2m

2.2.6 Instruments

Biometra Thermocycler T3	Chatel-St. Denis, Switzerland
ABI Prism 310 Genetic Analyzer	Applied Biosystems Inc., USA
Ultracentrifuge Optima L-90K	Beckman Coulter Inc., USA
High-Speed Centrifuge Avanti J-25	Beckman Coulter Inc., USA
Table Top Centrifuge 5417R	Eppendorf AG, Germany
Multifuge 3 S-R	Heraeus Holding GmbH, Germany
Spectrophotometer SpectraMAX 250	MDS Analytical Technologies Inc., USA
Thermomixer 5436	Eppendorf AG, Germany
Water bath TW12	Julabo Labortechnik GmbH, Germany
Flow cytometer Cyan II	Dako Denmark S/A, Denmark
inFlux cell sorter	Cytopeia Inc, USA
Magnetic cell sorter AutoMACS	Miltenyi Biotech, Germany
Olympus IX-81 fluorescence microscope	Olympus AG, Switzerland
MT-20 Illumination unit	Olympus AG, Switzerland
Film Developer Curix 60	Agfa-Gevaert AG, Switzerland
Densitometer Gel Doc 2000	Bio-Rad Laboratories Inc., USA

2.2.7 Software

Program	Application	Provider
MacVector	DNA alignments	Accelrys Inc., USA
Summit	FACS acquisition	Dako Denmark S/A, Denmark
FlowJo	FACS analysis	Tree Star Inc., USA
SoftMax Pro	Spectro-photometry	GraphPad Software Inc., USA
Prism	Graphs, calculations	GraphPad Software Inc., USA
CellR	Image acquisition	Olympus AG, Switzerland
ImageJ	Image analysis, FRET	NIH, USA
Quantity One	Densitometry	Bio-Rad Laboratories Inc., USA
Illustrator	Graphics, Layout	Adobe Systems Inc., USA

Photoshop	Images	Adobe Systems Inc., USA
InDesign	Document Preparation, Layout	Adobe Systems Inc., USA
Keynote	Presentations	Apple Computer Inc., USA

2.2.8 Antibodies

Antigen	Clone	Reference	Provider
α -mouse CD3 ϵ	(145-2C11)	(87, 88)	BD Biosciences
α -mouse CD3 ζ	(H146-968)	(89)	BD Biosciences
α -mouse TCR-C β	(H57-597)	(88)	BD Biosciences
α -mouse TCR V α 2	(B20.1)		BD Biosciences
α -mouse TCR V β 5	(MR9-4)		BD Biosciences
α -mouse CD4	(RM4-5)		BD Biosciences
α -mouse CD8 α	(53-6.7)		BD Biosciences
α -mouse CD8 β	(53-5.8)		BD Biosciences
α -mouse ZAP-70	(99F2)	(78)	Cell Signaling
α -mouse ZAP-70	(clone 29)	(79)	BD Biosciences
α -mouse ZAP-70 pTyr319	(65E4)	(78)	Cell Signaling
α -mouse ZAP-70 pTyr493	(2704)	(78)	Cell Signaling
α -mouse LAT	(rabbit polycl.)	(43, 90)	Upstate
α -mouse IL-2 (capture)	(JES6-IAI2)		eBioscience
α -mouse IL-2 (detect)	(JES6-5H4)		eBioscience
α -mouse CD69	(H1.2F3)		BD Biosciences
α -mouse NK1.1	(PK136)		BD Biosciences
α -mouse CD19	(1D3)		BD Biosciences
α -mouse H-2K ^b	(AF6-88.5)	(37)	BD Biosciences
α -Phospho tyrosine	(4G10)		Upstate
α -GFP (rabbit monocl.)	(E385)		Epitomics
α -GFP (mouse monocl.)	(B-2)		Santa Cruz Biotech.

2.2.9 Peptides

OVA variant peptides were synthesized and purified as described (91) (92) and had the following affinity hierarchy for the OT-I TCR: OVA > Q4 > Q4R7 > T4 > Q4H7 > G4 > E1 >> VSV (8).

Sequence	Abbreviation	Selection in OT-I wt FTOC
SIINFEKL	OVA	neg.
SIIQFEKL	Q4	neg.
SIIQFERL	Q4R7	neg.
SIITFEKL	T4	border (not used in these studies)
SIIQFEHL	Q4H7	pos.
SIIGFEKL	G4	pos.
EIINFEKL	E1	pos.
RGYVYQGL	VSV	null (non-cognate)

2.2.10 Expression vectors

Name	Retro/Lenti	Selection Marker	Source/Reference
LXSN	Retro	Geneticin (G418)	(33)
LXSP	Retro	Puromycin	(33)
pMFG	Retro	CFP/YFP	(93)
pTRIPΔU3EF1αEGFP	Lenti	GFP	N. Taylor, Montpellier

2.3 cDNA sequences

The OT-I TCR comprises rearranged TCR α (V α 2-J α 26) and TCR β (V β 5-D β 2-J β 2.6) chains and is derived from the K^b-restricted, OVA₂₅₇₋₂₆₄-specific CTL clone, 149.42 (94). The cDNAs encoding the OT-I α and OT-I β wildtype chains were recovered by standard PCR techniques from retroviral vectors described earlier (95). cDNAs encoding the OT-I $\alpha\delta$ chimeras were constructed using the previously described II and IV chimeric cDNAs (33) encoding the 3BBM74 TCR (96). Similarly, the OT-I $\beta\gamma$ chimera III was constructed by replacing the *Xba*I-*Xho*I fragment of the OTI β -chain with the corresponding chimeric β III fragment (33).

2.3.1 OT-I α -chain (wildtype)

5'ATGGACAAGATTCTGACAGCAACGTTTTTACTCCTAGGCCTTCACCTAGCTGGGGTGAATGGCCAGCAGC
 AGGAGAAACGTGACCAGCAGCAGGTGAGACAAAGTCCCCAATCTCTGACAGTCTGGGAAGGAGAGACCGCA
 ATTCTGAACTGCAGTTATGAGGACAGCACTTTTAACTACTTCCCATGGTACCAGCAGTTCCTGGGGAAGG
 CCCTGCACTCCTGATATCCATACGTTTCAGTGTCCGATAAAAAGGAAGATGGACGATTCACAATTTTCTTCA
 AATAAAGGGAGAAAAAGCTCTCCTTGCACATCACAGACTCTCAGCCTGGAGACTCAGCTACCTACTTCTGT
 GCAGCAAGTGACAACACTATCAGTTGATCTGGGGCTCTGGGACCAAGCTAATTATAAAGCCAGACATCCAGAA
 CCCAGAACCTGCTGTGTACCAGTTAAAAGATCCTCGGTCTCAGGACAGCACCTCTGCCTGTTCCACCGACTT
 TGAATCCCAAATCAATGTGCCGAAAACCATGGAATCTGGAACGTTTCATCACTGACAAAACCTGTGCTGGACA
 TGAAAGCTATGGATTCCAAGAGCAATGGGGCCATTGCCTGGAGCAACCAGACTAGTTTCACCTGCCAAGAT
 ATCTTCAAAGAGACCAACGCCACCTACCCAGTTCAGACGTTCCCTGTGATGCCACGTTGACTGAGAAAAG
 CTTTGAAACAGATATGAACCTAAACTTTCAAACCTGTCAGTTATGGGACTCCGAATCCTCCTGCTGAAAG
 TAGCCGGATTTAACCTGCTCATGACGCTGAGGCTGTGGTCCAGTTGA3'

2.3.2 OT-I $\alpha\delta$ -chimera II

(=chimeric α -chain of the α -CPM mutant receptor)

Nucleotides 1-686 identical to OT-I TCR α -chain (wildtype):

5'...CTATGGCCCAAGAGTCACAGTTCACACTGAGAAGGTAAACATGATGTCCCTCACGGTGCTGGGCCTACG
 ACTGCTGTTTGCCAAGACCATTGCCATCAATTTTCTCTTGACTGTAAAGTTATTCTTTTAA3'

2.3.3 OT-I $\alpha\delta$ -chimera IV

(=chimeric α -chain of the TM control receptor)

Nucleotides 1-741 identical to OT-I TCR α -chain (wildtype):

5'...TCCCTCACGGTGCTGGGCCTACGACTGCTGTTTGCCAAGACCATTGCCATCAATTTTCTCTTGACTGTT
 AAGTTATTCTTTTAA3'

2.3.4 OT-I β -chain (wildtype)

5'ATGTCTAACACTGTCCTCGCTGATTCTGCCTGGGGCATCACCTGCTATCTTGGGTTACTGTCTTTCTCT
 TGGGAACAAGTTCAGCAGATTCTGGGGTTGTCCAGTCTCCAAGACACATAATCAAAGAAAAGGGAGGAAG
 GTCCGTTCTGACGTGTATTCCCATCTCTGGACATAGCAATGTGGTCTGGTACCAGCAGACTCTGGGGAAGG
 AATTAAGTTCCCTTATTCAGCATTATGAAAAGGTGGAGAGAGACAAAGGATTCCTACCCAGCAGATTCTCA
 GTCCAACAGTTTGTGACTATCACTCTGAAATGAACATGAGTGCCTTGGAACTGGAGGACTCTGCTATGTA
 CTTCTGTGCCAGCTCTCGGGCCAATTATGAACAGTACTTCGGTCCCGGCACCAGGCTCACGGTTTTAGAGG

ATCTGAGAAATGTGACTCCACCCAAGGTCTCCTTGTTTGAGCCATCAAAAGCAGAGATTGCAAACAAACAA
AAGGCTACCCTCGTGTGCTTGGCCAGGGGCTTCTTCCCTGACCACGTGGAGCTGAGCTGGTGGGTGAATGG
CAAGGAGGTCCACAGTGGGGTCAGCACGGACCCTCAGGCCTACAAGGAGAGCAATTATAGCTACTGCCTGA
GCTCTAGACTGAGGGTCTCTGCTACCTTCTGGCACAATCCTCGCAACCACTTCCGCTGCCAAGTGCAGTTCC
ATGGGCTTTCAGAGGAGGACAAGTGGCCAGAGGGCTCACCCAAACCTGTCACACAGAACATCAGTGCAGAG
GCCTGGGGCCGAGCAGACTGTGGGATTACTAGTGCATCCTATCAACAAGGGGTCTTGTCTGCCACCATCCT
CTATGAGATCCTGCTAGGGAAAGCCACCCTGTATGCTGTGCTTGTGAGTACACTGGTGGTGATGGCTATGG
TCAAAAGAAAAAATCATGA3'

2.3.5 OT-I $\beta\gamma$ -chimera III

(=chimeric β -chain of the α -CPM mutant and the TM control receptor)

Nucleotides 1-855 identical to OT-I TCR β -chain (wildtype):

5'...CTCCTCCTGCTCCTCAAGAGTGTGATCTACTTGGCCATCATCAGCTTCTCTCTGCTTAGAAGAACATCT
GTCTGTGGCAATGAGAAGAAGTCCTAA3'

2.4 DNA constructs

The cDNAs encoding the OT-I α and OT-I β wildtype chains were recovered by standard PCR techniques from retroviral vectors described earlier (95) and ligated into the *Bam*HI and *Xho*I sites of the lentiviral expression vector pTRIP Δ U3EF1 α EGFP, replacing the *Bam*HI-EGFP-*Xho*I fragment. Resulting plasmids were referred to as pTRIP Δ U3EF1 α -OTI α and pTRIP Δ U3EF1 α -OTI β , respectively. The OT-I $\alpha\delta$ chimeric chains were constructed by replacing the *Spe*I-*Xho*I fragment of pTRIP Δ U3EF1 α -OTI α with the corresponding fragment from the α II or α IV chimeric α -chain, respectively. Similarly, the OT-I $\beta\gamma$ chimera III was constructed by replacing the *Xba*I-*Xho*I fragment of pTRIP Δ U3EF1 α -OTI β with the corresponding chimeric β III fragment.

To recover the OT-I α and OT-I β wildtype chains and introduce the *Bam*HI and *Xho*I restriction sites the following primers were used:

OT-I α -chain forward: 5'-CGAACGGATCCATGGACAAGATTCTGACAGCAAC-3'

OT-I α -chain reverse: 5'-CCTTGCTCGAGTCAACTGGACCACAGCCTCAG-3'

OT-I β -chain forward: 5'-GGTTCCGATCCATGTCTAACACTGTCCTCGCTG-3'

OT-I β -chain reverse: 5'-CGAAGCTCGAGTCATGAGTTTTTTCTTTTGACCATA
GCC-3'

2.5 Cell lines

Name	Description	Source/Reference
TSA/293T	Fibroblast derived from HEK293	S. Treves, Basel
Phoenix	Fibroblast derived from 293T	G. Nolan, Stanford
RMA-S-K ^b	RMA-S transfected with H-2K ^b	(37, 97)
P1.32-K ^b	P-815 transfected with H-2K ^b	(95)
3LBM 13.1 (bm12)	Antigen presenting cell, H-2K ^b expressing	
58 hybridoma	TCR- CD4-/CD8- hybridoma	(98)
58 OTI.ZC.8bY	58 hybridoma transfected with OT-I wildtype TCR, ζ -CFP, CD8 α and CD8 β -YFP	(4)
58 sw3.ZC.8bY	58 hybridoma transfected with OT-I α -CPM mutant TCR, ζ -CFP, CD8 α and CD8 β -YFP	(4)
58 sw4.ZC.8bY	58 hybridoma transfected with OT-I TM control TCR, ζ -CFP, CD8 α and CD8 β -YFP	(4)

2.6 Molecular techniques

2.6.1 Transformation of competent bacteria

10ng of plasmid DNA or ligation mix was added to 50ml of XL-1blue competent bacteria and incubated on ice for 30min, followed by incubation at 42°C for 90sec and cooling down on ice. Upon addition of 800 μ l LB medium (no antibiotics!), bacteria were kept at 37°C for 1h before plating on LB agar plates containing 50mg/ml ampicillin. Plates were incubated at 37°C overnight.

2.6.2 Plasmid preparation

2ml of LB broth containing 50mg/ml ampicillin was inoculated with a transformed bacteria clone and incubated on a shaker (280rpm) at 37°C for 6-12h. Depending on the scale of preparation, bacteria cultures were directly used for plasmid preparation (Miniprep) or to inoculate 500ml of LB broth-ampicillin (Maxiprep). For Maxiprep, the 500ml culture was allowed to grow until OD_{600nm} of 0.4-0.5 was reached, representing the transition from exponential into stationary growth phase. Bacteria were harvested by centrifugation at 6000xg for 15min at 4°C. Plasmid preparation was carried out according to the manufacturer's protocol (Qiagen). Concentration of purified plasmids was estimated by measuring OD_{260nm} and adjusted to 1mg/ml with TE buffer.

2.6.3 PCR

1ng of DNA was used as template for PCR. Primers were used at a final concentration of 0.3 μ M. The AccuPrime DNA polymerase was utilized according to the manufacturer's recommendations (Invitrogen). PCRs were carried out in a total volume of 50 μ l in thin-walled 0.5ml reaction tubes, using the T3 thermocycler.

2.6.4 Restriction enzyme digestion of plasmid DNA

Restriction digests were carried out for 1h at 37°C using 1 μ g of plasmid DNA in a total volume of 40 μ l. The appropriate buffer was chosen according to the manufacturer's recommendations (Promega) and BSA was added to 100 μ g/ml if specified. Upon incubation, 10 μ l TAE loading buffer was added and DNA fragments were resolved on a 1.2-2% agarose gels containing ethidium bromide. Appropriate sized DNA fragments were excised from the gel and purified using the gel extraction kit and the manufacturer's protocol (Qiagen).

2.6.5 DNA ligation

DNA ligations were carried out for 30min at 16°C using 100ng of vector DNA and 10ng of insert DNA in a total volume of 20 μ l. The enzyme and the appropriate buffer are provided in the T4 DNA ligase kit (Amersham Biosciences). Upon ligation, 1-10 μ l of the reaction mix was used to transform XL-1blue competent bacteria.

2.6.6 DNA sequencing

DNA constructs were sequenced using the ABI Prism BigDye Terminator v3.0 Ready Reaction Cycle Sequencing kit and the ABI Prism 310 Genetic Analyzer. 600-700ng DNA template was used and 10 μ M specific primers (Microsynth). PCR reaction mix (including DNA polymerase), sequencing controls and thermal cycling was used according to the manufacturer's recommendations (Applied Biosystems).

2.7 Cellular techniques

2.7.1 Production of lentivirus

Lentivirus was produced in a biolevel 2 facility. All the DNA plasmids were at a concentration of 1mg/ml. 2×10^6 TSA fibroblast cells were seeded per 10cm plate in 6.5ml DMEM medium containing 10% FCS. Upon reaching 60-70% confluency, the cotransfection mastermix is prepared, containing

8.6µg gag/pol plasmid, 2.8µg env plasmid (ecotropic vsv-g) and 8.6µg vector plasmid in a total volume of 20µl. 500µl HBS pH 7.00 and 33µl 2M CaCl₂ (both filtered 0.2mm) were added followed by immediate vortexing for 10sec. Subsequently the cotransfection mastermix was dropwise supplied to the plate. 14h after transfection, medium was exchanged with 6.5ml DMEM 2% FBS. Virion production was allowed for 24-30h. Supernatants were filtered with a 0.45µm filter and virions were concentrated by ultracentrifugation for 2h at 25.000rpm at 4°C, using the SW28 Beckman rotor. The virion pellet was resuspended in 100µl RPMI 1% BSA (filtered 0.2mm) and aliquots were frozen at -80°C.

2.7.2 Production of retrovirus

2x10⁶ phoenix fibroblast cells were seeded per 10cm plate in 7ml DMEM medium containing 8% FCS. Upon reaching 70-80% confluency, 10µg vector plasmid and 10µg IPK6 ecotropic helper plasmid (encoding the accessory viral genes) were adjusted to 300µl with DMEM. 80µl PolyFect transfection reagent was added and the transfection mix was vortexed for 10sec and incubated for 5min at room temperature. In the meantime, the phoenix cell medium was exchanged with 5ml fresh DMEM 8% FCS. Then, the transfection mix was combined with 1ml fresh DMEM 8% FCS and dropwise supplied to the plate. Virion production was allowed for 24-30h. Supernatants were filtered with a 0.45µm filter and virions were concentrated by centrifugation for 1h at 14.000rpm at 4°C in 2ml eppendorf tubes. Upon centrifugation, the upper 50% of medium were aspirated and the remaining viral supernatant was immediately used for transduction.

2.7.3 Transduction of 58 hybridomas

58 hybridoma cells were transduced with lentivirus or retrovirus. For lentiviral transductions, 5x10⁵ hybridomas were seeded in 2ml hybridoma medium in 24-well plates with 10µl of concentrated lentivirus. Transduction was allowed for 24h before expression of the transgene was checked by antibody staining and flow cytometry analysis. If antibody staining was not possible (eg. if another transgene was needed for co-expression; like the α-chain and the β-chain of the TCR), subsequent transduction was conducted before flow cytometry analysis. Hybridoma cells showing appropriate expressing the transgene(s) were sorted on a FACS sorter. For retroviral transductions, 5x10⁵ hybridomas were seeded in 1ml hybridoma medium in 24-well plates with 1ml of concentrated retrovirus and 5µg/ml polybrene. Spin infection was carried out twice with fresh retroviral supernatant for 45min at 1.800rpm at room temperature. Transduction was allowed for 24h before expression of the transgene was checked by antibody staining and flow cytometry analysis.

2.7.4 Fluorescence activated cell sorting (FACS)

Staining with fluorescence labeled monoclonal antibodies was performed in FACS buffer for 20min on ice. All antibodies were titrated and used at a concentration that corresponds to saturation of the antibody binding curve. Upon staining, cells were washed twice in FACS buffer and subjected to analysis on a Cyan II flow cytometer using the Summit software. If required, PI staining to exclude dead cells was performed directly before flow cytometry analysis.

2.7.5 RMA-S peptide loading

Tap2 deficient RMA-S cells were loaded with exogenous OVA peptide variants. The loading concentration of each peptide was varied to generate similar peptide-H-2K^b expression (4). Prior to peptide addition, RMA-S cells were incubated at 29°C overnight. If required, the cells were stained with Cy5 mono-reactive dye for 5min at room temperature and washed once. Peptide loading was carried out for 30min at 29°C and 3h at 37°C. pMHC surface expression was assessed by anti-H-2K^b staining and flow cytometry analysis.

2.7.6 Conjugate formation assay

2.5 x10⁵ OT-I hybridomas and 2.5 x10⁵ peptide-loaded, Cy5-labeled RMA-S cells (each in 50μl) were incubated in flat-bottomed wells at 37°C. To stop the stimulation, cells were fixed with 2% formaldehyde at various time points. Upon washing, cells were analyzed by flow cytometry. The percentage of CD8β-YFP (= OT-I hybridomas) and Cy5 (=RMA-S) double positive conjugates was compared to the total number of CD8β-YFP positive cells at each time point.

2.7.7 TCR endocytosis

2.5 x10⁵ OT-I hybridomas and 2.5 x10⁵ peptide-pulsed RMA-S cells (each in 50μl) were incubated in flat-bottomed wells at 37°C. To stop the stimulation, cells were fixed with 2% formaldehyde. Upon washing, staining with monoclonal antibodies for Vβ5 and flow cytometry analysis revealed the percentage of TCRs remaining on the cell surface of CD8β-YFP positive cells (= OT-I hybridomas) at each time point.

2.7.8 IL-2 detection by ELISA

96-well flat-bottomed ELISA plates (Nunc MaxiSorp) were coated with 60 μ l capturing anti-IL-2 at 2 μ g/ml in PBS 0.02% NaN₃ overnight at 4°C. For antigen stimulation, 10⁵ OT-I hybridomas and 10⁵ peptide-pulsed RMA-S cells (each in 100 μ l) were incubated in flat-bottomed wells for 24h at 37°C. 100 μ l of the supernatant was added to the washed and blocked ELISA plates for 1h at room temperature. Detecting anti-IL-2-biotin was applied at 2 μ g/ml for 1h at room temperature. Streptavidin-HRP was applied at 0.3 μ g/ml for 1h at room temperature. Conversion of O-phenylenediamine dihydrochloride was allowed for 5min in the dark followed by stopping the reaction with 50 μ l 10% H₂SO₄ per well. OD_{490nm} was detected and normalized to a standard dilution series by the Softmax Pro software.

2.7.9 Stimulation of T-cell hybridomas for FRET microscopy

2.5 x10⁵ OT-I hybridomas and 2.5 x10⁵ peptide-pulsed, Cy5-labeled RMA-S cells (each in 50 μ l) were incubated in flat-bottomed wells at 37°C. Stimulation was stopped by fixation with 2% formaldehyde. Cells were washed with PBS, 10mM Tris pH 7.5 and finally with buffer C of the Slowfade antifade kit. Cells were mounted on standard glass slides in Slowfade antifade mounting medium and sealed with nail polish.

2.7.10 FRET microscopy

An Olympus IX81 inverted microscope was used to acquire the fluorescence images required for FRET. A triggered F-View II camera was attached to the microscope and the MT20 illumination unit with a 150W Xenon lamp. The system was run by the CellR software. Optical filter cubes on an automated turret were used to change excitation and emission corresponding to the various channels. The filter cubes had the following spectral specifications (center/bandpass): YFP excitation, 500/20nm; YFP emission, 535/30nm; CFP excitation, 436/20nm; CFP emission, 480/40nm. The FRET filter cube was a combination of the CFP excitation filter and the YFP emission filter. Beamsplitting was achieved with a 455nm long pass dichroic mirror in the CFP filter cube and with a 515nm long pass dichroic mirror in the YFP and FRET filter cubes. A 60x, 1.4-numerical aperture oil objective was used for all images.

2.7.11 FRET analysis

For CFP and YFP, the efficiency of energy transfer is greater than 50% within the Förster Radius R₀ of 4.9 - 5.2 nm and approximates zero beyond 2x R₀ (~10nm). Crosstalk coefficients of CFP

fluorescence into the FRET channel (=d) and YFP into the FRET channel (=a) were calibrated using hybridomas transfected with either CD3 ζ -CFP or CD8 β -YFP alone. For the specified filter cubes they were d=36.8% and a=18.1%. For each image, the CFP, YFP and FRET channel was acquired using the 3 specified filter cubes. Background was subtracted as averaged signal from a user-specified, cell-free region of each image. To calculate the FRET efficiency the following formula was used: $E = (\text{FRET} - a \cdot \text{CFP} - d \cdot \text{YFP}) / (\text{FRET} - a \cdot \text{CFP} - d \cdot \text{YFP} + G \cdot \text{CFP})$, which was described earlier (36) (99). G is the independently calibrated ratio of sensitized emission in the FRET channel before photobleaching to donor recovery in the CFP channel after acceptor photobleaching (100). For the imaging system used here, $G = 1.7 \pm 0.1$. FRET efficiencies were calculated from hybridoma:APC interfaces. For illustration, the ImageJ software was used and calculated FRET efficiency images were depicted in pseudo-colors. Statistical analysis of E was performed using Student's two-sample t-test assuming two-tailed distribution and unequal variance. The recruitment of fluorescently tagged proteins to the synapse was calculated as background-corrected ratio of the MFI of the synapse region divided by the MFI of a user-defined membrane region, outside of the synapse.

2.7.12 Isolation of B-cells from spleen

Splenocytes from C57 Bl/6 mice were subjected to red blood cell lysis by incubation in H₂O for 10sec followed by addition of 10x PBS. Upon washing, cells were kept in staining buffer consisting of 50% T-cell medium, 50% PBS and 2mM EDTA. Staining with FITC-labeled anti-CD8 α , anti-CD4 and anti-NK1.1 was allowed for 15min on ice. Upon washing, MACS anti-FITC microbeads were added for 10min on ice. After another washing step, the 'Depletion S' program of the AutoMACS cell isolator (Miltenyi Biotec) was executed and non-FITC-labeled cells were collected. Flow cytometry analysis revealed that the vast majority of the collected cells were positive for CD19 and negative for CD8 α , CD4 or NK1.1.

2.7.13 Stimulation of thymocytes and immunostaining for fluorescence microscopy

B-cells isolated from C57 Bl/6 mice were stained with Cy5 mono-reactive dye for 5min at room temperature and washed once. Peptide loading was carried out with 2 μ M exogenously added specific peptide for 2h at 37°C in T-cell medium. Then, 2.5 x10⁵ thymocytes from OT-I Rag^{-/-} β 2m^{-/-} transgenic mice and 2.5 x10⁵ peptide-loaded B-cells and were pulse spinned at 3.000rpm for 20sec and incubated at 37°C. Stimulation was stopped by putting the tubes on ice. Cells were allowed to adhere on (3-Aminopropyl)triethoxy-silane coated cover slips for 10min on ice before being fixed with 2% formaldehyde for 1h at room temperature. Upon washing, cells were permeabilized with PBS 0.2% Triton X-100 for 2min on ice and blocked with PBS 3% BSA for 1h at room temperature. Staining with primary antibodies was carried out in PBS 1.5% BSA for 1h at room temperature.

Upon washing, fluorescence labeled secondary antibodies were applied in PBS 1.5% BSA for 1h at room temperature. After washing, the cover slips were mounted on microscopy glass slides in FluorSave reagent. Microscopy was performed using the Olympus IX81 fluorescence microscope. The recruitment of fluorescently tagged proteins to the synapse was calculated as background-corrected ratio of the MFI of the synapse region divided by the MFI of a user-defined membrane region, outside of the synapse.

2.7.14 Fetal thymic organ culture (FTOC)

FTOC was performed as described (101). In brief, thymic lobes were excised from OT-I Rag^{-/-} β2m^{-/-} transgenic mice at a gestational age of day 15.5. FTOCs included exogenous β2m (5μg/ml) and peptide (2μM for negative-selecting and 20μM for positive selecting peptides). After 7 days of culture, thymocytes were subjected to flow cytometry analysis.

2.8 Biochemical techniques

2.8.1 Fixation of APCs

Peptide-loaded APCs were kept at 6 x 10⁷ cells/ml in T-cell medium at 37°C. Prewarmed glutaraldehyde was added to 0.1% for 30sec. Fixation was stopped by adding lysine to 0.2% for 10min at room temperature. Cells were washed three times with PBS and adjusted to 6 x 10⁷ cells/ml in T-cell medium.

2.8.2 Immunoprecipitation and Western blot

3 x 10⁷ thymocytes from OT-I Rag^{-/-} β2m^{-/-} transgenic mice and 3 x 10⁷ peptide-loaded, fixed APCs (both in 500ml) were pulse spinned at 3.000rpm for 20sec and incubated at 37°C. Stimulation was stopped by putting the tubes on ice. Cells were lysed in 500μl lysis buffer containing 1% detergent and incubated for 15min on ice. Cell lysates were cleared by centrifugation at 14.000rpm for 10min at 4°C. Immunoprecipitation was performed with 1μg of monoclonal antibody and 20μl of 80% protein G sepharose for a total of 2.5h on a rotator at 4°C. Upon washing, sepharose beads were boiled with 10μl SDS-containing, reducing sample buffer for 5min at 95°C and SDS-PAGE and Western blotting was performed. Protein transfer to nitrocellulose membranes was checked by ponceau red staining before the membranes were treated with blocking buffer. Primary antibodies were applied in TBS-T 5% BSA 0.02% NaN₃ and binding was allowed either over night at 4°C or 1h at room temperature. Upon washing with TBS-T, HRP-conjugated secondary antibodies were applied in TBS-T 3% BSA for 30min at room temperature. After washing, the membranes were

incubated for 1min in 1ml reagent 1 combined with 1ml reagent 2 of the ECL western blotting detection reagents. Chemiluminescence of HRP-mediated conversion of the detection reagent (luminol) was captured by exposing the membranes to ECL hyperfilms for appropriate periods of time and developing the films on a Curix80 developer.

2.8.3 ZAP-70 *in vitro* kinase assay

ZAP-70 was immunoprecipitated from activated TCR complexes like described above, using the α -mouse CD3 ϵ antibody and 1% Brij 58 in the lysis buffer. Upon immunoprecipitation, sepharose beads were 2x equilibrated in kinase assay buffer. 0.5 μ g recombinant LAT was added to each sample and incubation was carried out for 10min at 37°C under constant agitation (1.000rpm). SDS-PAGE and Western blotting was performed as described above. Tyrosine phosphorylation of the recombinant LAT reporter was either shown with anti-phosphotyrosine (4G10) or specific anti-phosphoLAT antisera.

3. Results

3.1 The T-cell receptor's α -chain connecting peptide motif promotes close approximation of the CD8 co-receptor allowing efficient signal initiation

The results of these experiments were published in the Journal of Immunology,
2008 Jun 15;180(12):8211-21

The T Cell Receptor's α -Chain Connecting Peptide Motif Promotes Close Approximation of the CD8 Coreceptor Allowing Efficient Signal Initiation¹

Michel Mallaun,* Dieter Naeher,* Mark A. Daniels,^{2*} Pia P. Yachi,[‡] Barbara Hausmann,* Immanuel F. Luescher,[†] Nicholas R. J. Gascoigne,[‡] and Ed Palmer^{3*}

The CD8 coreceptor contributes to the recognition of peptide-MHC (pMHC) ligands by stabilizing the TCR-pMHC interaction and enabling efficient signaling initiation. It is unclear though, which structural elements of the TCR ensure a productive association of the coreceptor. The α -chain connecting peptide motif (α -CPM) is a highly conserved sequence of eight amino acids in the membrane proximal region of the TCR α -chain. TCRs lacking the α -CPM respond poorly to low-affinity pMHC ligands and are unable to induce positive thymic selection. In this study we show that CD8 participation in ligand binding is compromised in T lineage cells expressing mutant α -CPM TCRs, leading to a slight reduction in apparent affinity; however, this by itself does not explain the thymic selection defect. By fluorescence resonance energy transfer microscopy, we found that TCR-CD8 association was compromised for TCRs lacking the α -CPM. Although high-affinity (negative-selecting) pMHC ligands showed reduced TCR-CD8 interaction, low-affinity (positive-selecting) ligands completely failed to induce molecular approximation of the TCR and its coreceptor. Therefore, the α -CPM of a TCR is an important element in mediating CD8 approximation and signal initiation. *The Journal of Immunology*, 2008, 180: 8211–8221.

Upon binding a peptide-MHC (pMHC)⁴ ligand, the $\alpha\beta$ TCR complex initiates an intracellular signal; when a T cell or thymocyte accumulates a sufficient number of TCR and other signals, a cellular response is induced. An important element in TCR signal initiation is the coreceptor, either CD4 or CD8. These coreceptors bind to MHC class II or class I molecules, respectively (1–4). The coreceptor binding site on an MHC molecule is distinct from its peptide-binding domain and therefore does not interfere with TCR binding (5). By binding to the same MHC molecule as the TCR (6), the coreceptor increases the overall affinity of TCR-pMHC binding (7, 8). Moreover, the CD4 and CD8 coreceptors are important for signal initiation due to their association with the tyrosine kinase Lck (9), which is required for

critical early events in TCR signaling (10–12). Lck phosphorylates the ITAMs of the CD3 molecules within the TCR complex, especially those of CD3 ζ (13). Moreover, Lck phosphorylates tyrosine residues on the Syk family kinase ZAP70 (14), thereby increasing the enzymatic activity of ZAP70 (15). Therefore, the coreceptor has an important function in coupling ligand binding with the initiation of signal transduction.

Although high-affinity TCR-pMHC interactions exhibit some degree of CD8 independence, lower affinity interactions (K_D values $\geq 3 \mu\text{M}$) require CD8 for Ag recognition (16). In the absence of CD8 binding to pMHC, primary CD8 T cells fail to form conjugates with APCs even in the presence of high concentrations of antigenic peptide (17). In this context, the CD8 $\alpha\beta$ heterodimer, but not the CD8 $\alpha\alpha$ homodimer, significantly increases the avidity of TCR-mediated ligand recognition as measured by binding to soluble monomeric pMHC (18). The same study suggests that CD8 β facilitates TCR signal induction, not only by increasing the avidity of TCR-ligand binding but also by docking TCR/CD3 to glycolipid-enriched microdomains.

During thymocyte development, the ability of the TCR to read ligand affinity plays an important role in establishing a self-tolerant T cell repertoire (19, 20). Preselection CD4⁺CD8⁺ double-positive (DP) thymocytes expressing a MHC I-restricted TCR respond to self-Ags by differentiating into mature CD8⁺ single-positive (SP) thymocytes, if the apparent affinity of TCR-CD8/pMHC binding is below a discrete threshold ($K_D > 6 \mu\text{M}$) (21). In contrast, preselection DP thymocytes, whose TCRs bind self-pMHC Ag with an apparent affinity above the selection threshold ($K_D < 6 \mu\text{M}$), initiate apoptosis and fail to develop into mature T lineage cells (21). In this way, overtly self-reactive T cells are removed (negatively selected) from the developing T cell repertoire. The coreceptors play an important role in the selection outcome (22, 23). For example, CD8 β -deficient mice select severely reduced numbers of MHC I-restricted cytotoxic T cells (24, 25).

*Laboratory of Transplantation Immunology and Nephrology, Department of Biomedicine, University Hospital Basel, Basel, Switzerland; [†]Ludwig Institute for Cancer Research, Lausanne Branch, University of Lausanne, Epalinges, Switzerland; and [‡]Department of Immunology, Scripps Research Institute, La Jolla, CA 92037

Received for publication February 19, 2008. Accepted for publication April 14, 2008.

The costs of publication of this article were defrayed in part by the payment of page charges. This article must therefore be hereby marked advertisement in accordance with 18 U.S.C. Section 1734 solely to indicate this fact.

¹This work was supported by grants from the Swiss National Science Foundation, European Association of Plastic Surgeons, Novartis, and Hoffmann La Roche (to E.P.), National Institutes of Health Grant R01AI074074 (to N.R.J.G.), and U.S. Cancer Research Institute (to M.A.D.), and T32HL07195-30 (to P.P.Y.).

²Current address: Department of Molecular Microbiology and Immunology, University of Missouri, One Hospital Drive, Columbia, MO 65212.

³Address correspondence and reprint requests to Dr. Ed Palmer, Laboratory of Transplantation Immunology and Nephrology, Department of Biomedicine, University Hospital Basel, Hebelstrasse 20, 4031 Basel, Switzerland. E-mail address: ed.palmer@unibas.ch

⁴Abbreviations used in this paper: pMHC, peptide-MHC; ABA, azidobenzoic acid; α -CPM, α -chain connecting peptide motif; $\beta_2\text{m}$, β_2 -microglobulin; CFP, cyan fluorescent protein; DP, CD4⁺CD8⁺ double positive; FRET, fluorescence resonance energy transfer; FTOC, fetal thymic organ culture; MFI, mean fluorescence intensity; SP, CD4⁺CD8⁺ single positive; TM, transmembrane; YFP, yellow fluorescent protein; wt, wild type.

Copyright © 2008 by The American Association of Immunologists, Inc. 0022-1767/08/\$2.00

Exactly how the coreceptor and TCR interact to initiate distinct signals with defined cellular consequences is not completely understood. The TCR α -chain contains an evolutionarily conserved motif in its constant region termed the α -chain connecting peptide motif (α -CPM). Mutations in this conserved membrane proximal motif (FET DXNLN) promote unresponsiveness to antigenic stimuli (26) and defects in positive selection; interestingly, negative selection with an agonist ligand was unaffected (27, 28). TCR/CD3 complexes where the α -CPM has been substituted with amino acids from the TCR δ membrane proximal domain exhibit a reduced association with the CD3 δ subunit (27). Interestingly, thymocytes from CD3 δ -deficient mice are defective in undergoing positive selection as well, implying a role for CD3 δ in linking TCR and coreceptor molecules (29). Finally, α -CPM-deficient TCRs bind agonist ligands but cannot cooperate with CD8 to increase ligand binding (30). This further supports the idea that the α -CPM may mediate a molecular interaction between CD8 and the TCR, either directly or via CD3 δ .

To directly measure the role of the α -CPM in the TCR-CD8 interaction, we measured fluorescence resonance energy transfer (FRET) between fluorescently tagged CD3 ζ (of the TCR complex) and CD8 β (31, 32). We used a well-defined set of peptides inducing positive or negative selection of thymocytes expressing the OT-I TCR (33) to assess the role of the α -CPM in mediating an interaction between CD3 ζ and CD8 β . In T cell hybridomas expressing either a wild-type (wt) or α -CPM mutant OT-I TCR, CD3 ζ -CD8 β interactions within the immunological synapse (34) varied in both intensity and time. Although negative-selecting peptides induced fast and sustained FRET signals in hybridomas expressing the wt OT-I TCR, positive-selecting peptides induced markedly delayed and weaker FRET signals. T cell hybridomas expressing α -CPM-deficient TCRs exhibited diminished and delayed CD3 ζ -CD8 β interactions in response to negative-selecting peptides. Strikingly, positive-selecting peptides did not induce detectable CD3 ζ -CD8 β interactions, even though both TCR/CD3 complexes and CD8 molecules were efficiently recruited to the synapse. Because the α -CPM is located in the constant domain of every TCR and does not interfere with TCR specificity (30), we suggest a role for the α -CPM in translating low affinity TCR-MHC binding across the plasma membrane by ensuring a close association of the coreceptor to the TCR.

Materials and Methods

Peptides and Abs

OVA variant peptides were synthesized and purified as described (20, 35) and had the following affinity hierarchy for the OT-I TCR: OVA > Q4 > Q4R7 > T4 > Q4H7 > G4 > E1 \gg VSV (33). Anti-CD8 β (clone 53-5.8), anti-H-2K^b (clone AF6-88.5), anti-TCR β (H57-597), anti-V α 2 (B20.1), capturing anti-mIL-2 (JES6-1A12), and detecting anti-mIL-2-biotin (JES6-5H4) were from BD Biosciences. Rabbit monoclonal anti-GFP was from Eptomics, mouse monoclonal anti-GFP was from Santa Cruz Biotechnology, and anti-phosphotyrosine (4G10) was from Upstate Biotechnology.

DNA constructs

The OT-I TCR comprises rearranged TCR α (V α 2-J α 26) and TCR β (V β 5-D β 2-J β 2.6) chains and is derived from the K^b-restricted, OVA₂₅₇₋₂₆₄-specific CTL clone 149.42 (36). The cDNAs encoding the OT-I α and OT-I β wt chains were recovered by standard PCR techniques from retroviral vectors described earlier (37) and ligated into the *Bam*HI and *Xho*I sites of the lentiviral expression vector pTRIP Δ U3EF1 α EGFP (N. Taylor, Centre National de la Recherche Scientifique Unité Mixte de Recherche 5535, Montpellier, France), replacing the *Bam*HI-EGFP-*Xho*I fragment. Resulting plasmids were referred to as pTRIP Δ U3EF1 α -OTI α and pTRIP Δ U3EF1 α -OTI β , respectively. cDNAs encoding the OT-I TCR $\alpha\delta$ chimeras were constructed using the previously described II and IV chimeric cDNAs (26) encoding the 3BBM74 TCR (38). The *Spe*I-*Xho*I fragment of pTRIP Δ U3EF1 α -OTI α was replaced by the corresponding fragment from

the α II or α IV chimeric α -chain. Similarly, the OT-I β chimera III was constructed by replacing the *Xba*I-*Xho*I fragment of pTRIP Δ U3EF1 α -OTI β with the corresponding chimeric β III fragment (26). The CD8 β -YFP (32) and CD3 ζ -CFP (31) constructs (where YFP is yellow fluorescent protein and CFP is cyan fluorescent protein) have been described.

Fetal thymic organ culture

Fetal thymic organ culture (FTOC) was performed as described (19). In brief, thymic lobes were excised from OT-I Rag^{-/-} β _{2m}^{-/-} transgenic mice (where β _{2m} is β ₂-microglobulin) at a gestational age of day 15.5. FTOCs included exogenous β _{2m} (5 μ g/ml) and peptide (2 μ M for negative-selecting peptides and 20 μ M for positive-selecting ligands). After 7 days of culture, thymocytes were subjected to flow cytometry analysis.

Ligand binding

Tetramer-binding studies were performed as described (33). In brief, DP thymocytes from OT-I Rag^{-/-} β _{2m}^{-/-} mice were stained with fluorescently labeled tetramers and K_D values were determined by nonlinear regression analysis of the mean fluorescence intensities (MFI). Differences related to the replacement of the α -CPM (ΔK_D) were calculated as ratios between the α -CPM and the OT-I wt K_D values. Monomer binding studies were performed as described (21). In brief, the ratio (r) of free TCR was determined by two-step photoaffinity labeling of DP thymocytes from T1 Rag^{-/-} β _{2m}^{-/-} mice. Ligand concentration-dependent binding curves were analyzed by nonlinear regression and K_D values were determined. ΔK_D values were calculated between the α -CPM and the transmembrane (TM) control K_D values.

Cells

Supernatants of Phoenix packaging cells (G. Nolan, Stanford University, Stanford, CA) were used to transduce the TCR/CD8-deficient hybridoma 58 (39) sequentially with constructs for CD8 α , CD8 β -YFP, and CD3 ζ -CFP. Resulting hybridomas were sorted for high CFP and YFP expression. To introduce the wt or chimeric OT-I α -chains and the wt or chimeric OT-I β -chains, CaCl₂-based transfection of 293T cells was used to produce lentiviral supernatants for subsequent transduction.

Transduced hybridomas were FACS sorted for similar TCR expression among wt, mutant α -CPM and TM control hybridomas. All cells were grown in RPMI 1640 supplemented with 4% FCS, 2 mM L-glutamine, 100 U/ml penicillin, 100 μ g/ml streptomycin, and 50 μ M 2-ME.

Microscopy

An Olympus IX81 inverted microscope was used in this study. A triggered F-View II camera was attached to the microscope and the MT20 illuminator with a 150-watt xenon lamp (Olympus). The system was run by CellR software (Olympus). Optical filter cubes on an automated turret were used to change excitation and emission corresponding to the various channels. The filter cubes had the following spectral alignments (center/band-pass): YFP excitation, 500/20 nm; YFP emission, 535/30 nm; CFP excitation, 436/20 nm; CFP emission, 480/40 nm. The FRET filter cube was a combination of the CFP excitation filter and the YFP emission filter. Beam splitting was achieved with a 455-nm-long pass dichroic mirror in the CFP filter cube and a 515-nm-long pass dichroic mirror in the YFP and FRET filter cubes. A 60 \times , 1.4 numerical aperture oil objective was used.

FRET and recruitment analysis

For CFP and YFP, the efficiency of energy transfer is >50% within the Förster radius (R_0) of 4.9–5.2 nm and approximates zero beyond $2 \times R_0$ (~ 10 nm). Cross-talk coefficients of CFP fluorescence into the FRET channel (equal to d) and YFP into the FRET channel (equal to a) were calibrated using hybridomas transduced with either CD3 ζ -CFP or CD8 β -YFP alone. For the specified filter cubes the cross-talk coefficients were $d = 36.8\%$ and $a = 18.1\%$. For each image, the CFP, YFP, and FRET channels were acquired using the three specified filter cubes. Background was subtracted as the averaged signal from a user-specified, cell-free region of each image. To calculate FRET efficiency, the formula $E = [\text{FRET} - (a \times \text{CFP}) - (d \times \text{YFP})] / [\text{FRET} - (a \times \text{CFP}) - (d \times \text{YFP}) + (G \times \text{CFP})]$, which was described earlier (31, 40), was used. G is the independently calibrated ratio of sensitized emission in the FRET channel before photobleaching to donor recovery in the CFP channel after acceptor photobleaching (41). For the imaging system used here, $G = 1.7 \pm 0.1$. FRET efficiencies were calculated from hybridoma:APC interfaces. For illustration, the NIH ImageJ software was used and the calculated FRET efficiency images were illustrated in pseudo-colors. Statistical analysis of E was performed using Student's two-sample t test assuming two-tailed distribution and unequal variance. The recruitment of fluorescently tagged proteins to

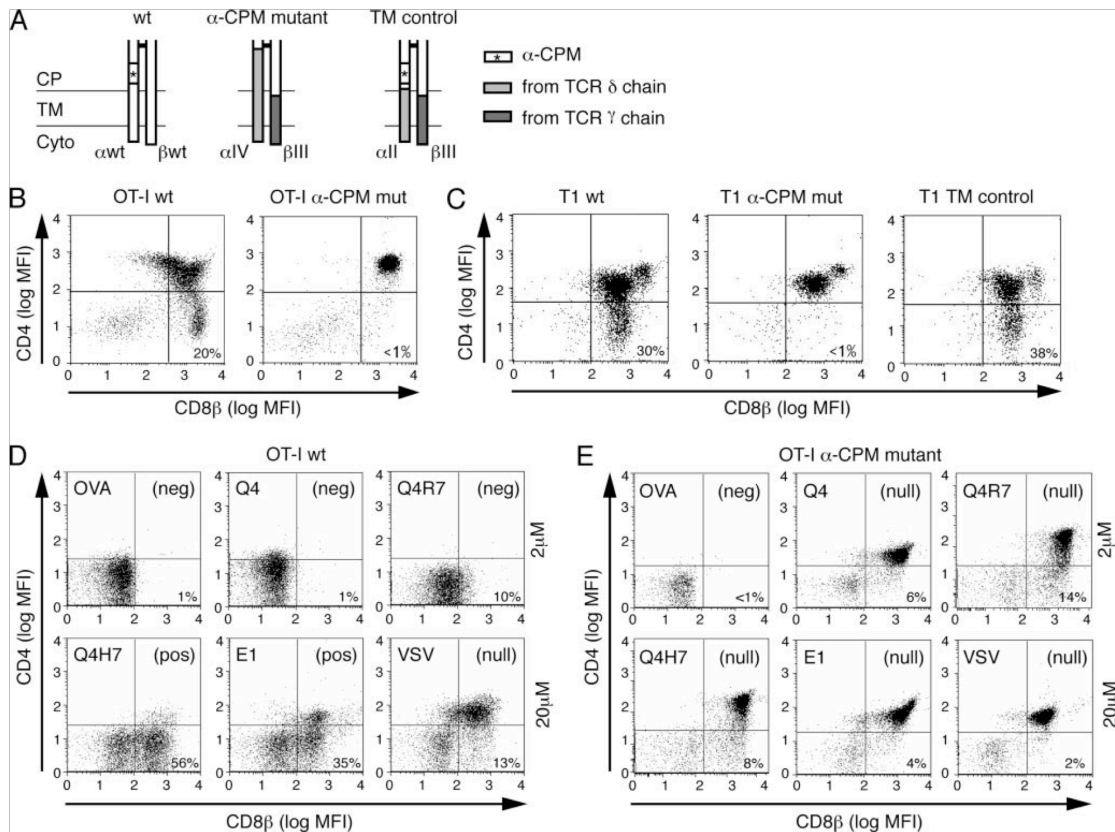


FIGURE 1. Schematic representation of the TCR constant regions used in this study and characterization of the peptide variants. *A*, Schematic representation of the connecting peptide (CP), TM, and cytoplasmic (Cyt) domains of the wt and chimeric TCRs used. The α -CPM sequence is indicated with an asterisk (*). Open bars, TCR α and TCR β sequences; light gray bars, TCR δ sequences; dark gray bars, TCR γ sequences. The α -CPM mutant receptor (α IV/ β III) is similar to the TM control receptor (α II/ β III) except that the α -CPM has been removed and replaced by the corresponding TCR δ sequence in the α IV chain (26). *B*, Flow cytometric analysis of thymocytes expressing wt or α -CPM mutant (mut) OT-I TCR (as previously shown; Ref. 28). Thymocytes from C57BL/6 Rag2^{-/-} mice, transgenic for the wt or α -CPM mutant TCR, were stained with mAbs against CD4 and CD8 β . The numbers in the dot plots indicate the percentage of CD8 $\alpha\beta$ ⁺CD4⁻ SP cells. *C*, Flow cytometric analysis of thymocytes expressing wt, α -CPM mutant, or TM control T1 TCR. Thymocytes from BALB/c Rag2^{-/-} mice, which were transgenic for the wt, α -CPM mutant, or TM control TCR, were stained and analyzed as in *B*. *D*, and *E*, FTOC analysis. Thymi from day 15.5 embryos of either OT-I wt (*D*) or α -CPM mutant (*E*) Rag2^{-/-} β 2m^{-/-} mice were incubated with exogenously added individual peptide and β ₂m. The ability of a peptide to induce the differentiation of CD8 $\alpha\beta$ ⁺CD4⁻ SP cells was analyzed by flow cytometry after 7 days of culture. Cells were electronically gated for TCR β expression and the CD4/CD8 β expression profiles are shown with the percentage of CD8 $\alpha\beta$ ⁺CD4⁻ SP cells indicated. In wt FTOCs the pattern of negative selection (neg) seen with 2 μ M peptide is also seen over a broad concentration range of negative-selecting peptides (data not shown). Positive selection (pos) in FTOC is more efficient using higher peptide concentrations; FTOCs stimulated with 20 μ M peptide are shown in the figure. Lack of positive or negative selection is indicated by "null."

the synapse was calculated as background-corrected ratio of the MFI of the synapse region divided by the MFI of a user-defined membrane region outside of the synapse.

APC peptide loading

Tap2-deficient RMA-S cells (42) were loaded with the exogenous OVA peptide variants described above. We varied the loading concentration of each peptide to generate similar pK^b expressions. RMA-S cells were incubated at 29°C overnight followed by peptide addition for 30 min at 29°C and incubation for 3 h at 37°C. pMHC surface expression was assessed by anti-H-2K^b-PE staining and flow cytometry analysis.

IL-2 release assay

For IL-2 detection, 96-well flat-bottom ELISA plates (Nunc MaxiSorp) were coated with 60 μ l of anti-IL-2 at 2 μ g/ml in PBS with 0.02% NaN₃ overnight at 4°C. For Ag stimulation, 10⁵ OT-I hybridomas and 10⁵ peptide-pulsed RMA-S cells were incubated in flat-bottom wells for 24 h at 37

°C. One hundred microliters of the supernatant was added to the washed and blocked ELISA plates for 1 h at room temperature. Anti-mouse IL-2-biotin secondary Ab was applied at 2 μ g/ml for 1 h at room temperature. Streptavidin-HRP (Zymed Laboratories) was applied at 0.3 μ g/ml for 1 h at room temperature. Conversion of *o*-phenylenediamine dihydrochloride (Sigma-Aldrich) was allowed for 5 min in the dark followed by stopping the reaction with 50 μ l of 10% H₂SO₄ per well. OD_{490 nm} was detected and normalized to a standard dilution series by Softmax Pro software (Molecular Devices).

TCR down-regulation

OT-I hybridomas (10⁵) and peptide-pulsed RMA-S cells (10⁵) were incubated in flat-bottom wells at 37°C. Cells were fixed with 2% formaldehyde, washed, and stained for V β 5 and analyzed by flow cytometry. Data were presented as the percentage of TCRs remaining on the cell surface.

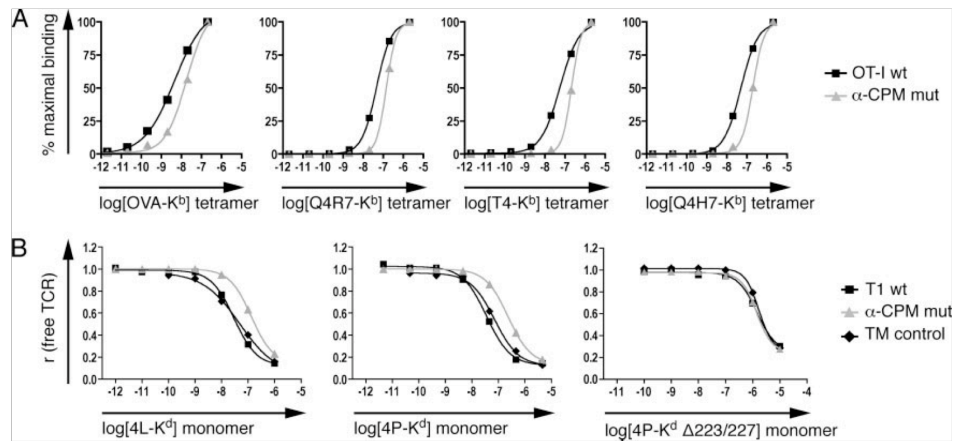


FIGURE 2. Ligand binding of thymocytes with wt or mutant (mut) α -CPM TCRs. *A*, pMHC tetramer binding to thymocytes expressing OT-I wt or α -CPM mutant TCRs. Thymocytes from C57BL/6 Rag^{-/-} $\beta_2m^{-/-}$ mice expressing either the wt or α -CPM mutant OT-I TCR were incubated with various PE-labeled tetramers at indicated concentrations at 37°C. Binding was quantified by flow cytometry and nonlinear regression analysis. A representative experiment of at least three independent experiments is shown. *B*, pMHC monomer binding to thymocytes expressing the T1 wt, α -CPM mutant, or TM control TCR. Thymocytes from BALB/c Rag^{-/-} $\beta_2m^{-/-}$ mice expressing the T1 TCR variants were subjected to two-step labeling experiments as described (21). pMHC Δ 223/227 monomers that significantly reduce CD8 binding were used with the 4P ligand (*right panel*). A representative experiment from a total of two or more independent experiments is shown.

Stimulation of hybridomas for FRET analysis

OT-I hybridomas (2×10^5) and peptide-pulsed RMA-S cells (2×10^5) were incubated in flat-bottom wells at 37°C. Stimulation was stopped by fixation with 2% formaldehyde. Cells were washed with PBS, 10 mM Tris, and finally with buffer C from the SlowFade antifade kit (Invitrogen). Cells were mounted on standard glass slides in SlowFade antifade mounting medium.

Immunoprecipitation and immunoblots

Hybridomas (2×10^7) and peptide-pulsed RMA-S cells (2×10^7) were incubated in round-bottom tubes at 37°C. Cells were lysed in 1% Triton X-100, 50 mM Tris (pH 7.5), 150 mM NaCl, 1 mM EDTA, 20 mM β -glycerophosphate, 1 mM Na₃VO₄, 10 mM NaF, 1 mM PMSF, 2 μ g/ml aprotinin, 5 μ g/ml leupeptin, and 1 mg/ml pepstatin. Lysates were precleared by centrifugation and with protein G-Sepharose beads (GE Healthcare) and were immunoprecipitated overnight with rabbit monoclonal anti-GFP (Epitomics). After washing, samples were separated by electrophoresis with 10% SDS-polyacrylamide gels under reducing conditions, blotted, and probed with anti-phosphotyrosine (clone 4G10; Upstate Biotechnology) followed by anti-mouse-HRP (Cell Signaling) and ECL detection (GE Healthcare). For a loading control, membranes were stripped and probed with mouse monoclonal anti-GFP (Santa Cruz Biotechnology).

Results

Wild-type and α -CPM mutant TCRs

The wt and chimeric TCRs used in this study are schematically represented in Fig. 1A. As point mutations in the α -CPM led to abrogation of surface TCR expression (26), we generated chimeric TCRs that contain corresponding domains from the $\gamma\delta$ TCR, which lacks the α -CPM. Fig. 1A shows the membrane proximal connecting peptide (CP), TM, and cytoplasmic (Cyto) domains of the constant regions of the receptors used in this study. The α -CPM is indicated with an asterisk (*), TCR δ -sequences that replace α -sequences are shown in light gray, and TCR γ -sequences that replace β -sequences are shown in dark gray in Fig. 1A. The α -CPM mutant chain (α IV in Fig. 1A) is a chimera encoding V, J, and parts of the C domain from the TCR α -chain followed by a segment of C δ , which lacks the α -CPM. The β III chain (Fig. 1A) encodes V, D, J, and part of the C domain from the TCR β -chain followed by the C γ TM and cytoplasmic regions. The TM control

receptor is composed of the β III chain and the α II chain, which is identical to the α IV chain except that it contains the α -CPM (Fig. 1A). Therefore, the TM control receptor and the α -CPM mutant receptor are distinguished by the presence or absence of the α -CPM. The V (variable) regions and the bulk of the C (constant) regions among the various receptors were identical and were not affected by the replacements of the domains shown in Fig. 1A.

Defective positive selection in α -CPM mutant mice

Thymocytes from Rag2^{-/-} mice expressing transgenic wt or α -CPM mutant TCRs were analyzed to determine the influence of the α -CPM on thymic selection. As previously shown, wt OT-I transgenic thymocytes generated substantial numbers of CD8 $\alpha\beta^+$ CD4⁻ SP cells (19, 43), whereas only very limited numbers of α -CPM mutant thymocytes were positively selected (Fig. 1B) (28). Similarly, in the T1 TCR transgenic system (21) CD8 $\alpha\beta$ SP cells were generated in the wt and TM control transgenic mice but not in α -CPM mutant mice, clearly indicating a positive selection defect (Fig. 1C).

The ability of different OVA variant peptides to induce positive or negative selection (see *Materials and Methods* for affinity hierarchy) was tested in FTOC (19). As shown here (Fig. 1D) and previously (33), the strong OVA, Q4, and Q4R7 ligands induced negative selection in FTOC as indicated by a low percentage of CD8 $\alpha\beta^+$ CD4⁻ SP thymocytes. In contrast, the weak ligands

Table I. K_D values for pMHC tetramer binding^a

Strain	Tetramer Ligand			
	OVA-K ^b	Q4R7-K ^b	T4-K ^b	Q4H7-K ^b
OT-I wt	4.4×10^{-9}	4.5×10^{-8}	5.5×10^{-8}	5.0×10^{-8}
α -CPM mutant	1.7×10^{-8}	1.4×10^{-7}	2.1×10^{-7}	2.0×10^{-7}
ΔK_D (K_D α -CPM/ K_D wt)	3.9-fold	3.1-fold	3.8-fold	4.0-fold

^a K_D values [M] determined for pMHC tetramer binding to OT-I wt or α -CPM mutant CD4⁺CD8⁺ DP thymocytes. ΔK_D represents K_D α -CPM mutant/ K_D wt.

Table II. K_D values for pMHC monomer binding^a

Strain	Monomer Ligand		
	4L-K ^d	4P-K ^d	4P-K ^d Δ223/227
T1 wt	2.8×10^{-8}	8.8×10^{-8}	1.4×10^{-6}
α-CPM mutant	1.5×10^{-7}	3.9×10^{-7}	1.4×10^{-6}
TM control	3.5×10^{-8}	9.5×10^{-8}	1.7×10^{-6}
ΔK_D (K_D α-CPM/ K_D TM control)	4.3-fold	4.1-fold	0.8-fold

^a K_D values determined for pMHC monomer binding to T1 wt, α-CPM mutant, or TM control CD4⁺CD8⁺ DP thymocytes. Mean values of three experiments are shown.

Q4H7 and E1 generated substantial numbers of CD8αβ⁺CD4⁻ SP cells, which is indicative of positive selection (Fig. 1D and Ref. 33). The noncognate VSV ligand induced neither positive nor negative selection as reflected by high numbers of CD8αβ⁺CD4⁺ DP thymocytes. In contrast with wt OT-I thymocytes, α-CPM mutant thymocytes exhibited a substantially different selection outcome in response to the various peptides (Fig. 1E). Only OVA was identified as negative selector, given the paucity of CD8αβ⁺CD4⁻ SP cells. All other ligands were nonselectors of α-CPM mutant thymocytes; the presence of high numbers of DP thymocytes and relatively few SP thymocytes indicate the lack of positive or negative selection (Fig. 1E).

Ligand binding

The lack of selection in α-CPM mutant FTOC might indicate that the α-CPM mutant receptor cannot bind cognate ligands. To determine the influence of the α-CPM mutation on ligand binding, we performed pMHC tetramer and monomer binding studies. Both binding assays involved concomitant TCR and CD8 coreceptor binding to the MHC and were performed on preselection DP thymocytes at 37°C. α-CPM mutant thymocytes exhibited decreased ligand binding compared with OT-I wt thymocytes when incubated with fluorescently labeled pMHC tetramers (Fig. 2A). Dissociation constants, K_D , were calculated by nonlinear regression analysis of the MFI values of bound tetramers. Relative to wt OT-I thymocytes, α-CPM mutant thymocytes bound all tetramers tested less avidly. The reduction of tetramer avidity (ΔK_D) was 3- to 4-fold (Table I).

Binding studies using monomeric pMHC ligands (21, 44) involve peptides carrying a photoreactive azidobenzoic acid (ABA) that can be photochemically cross-linked to the TCR upon specific ligand binding. The T1 TCR is specific for the pMHC complex SYIPSAEK(ABA)/I/H-2K^d, with the photoreactive ABA attached to the lysine at position 8 of the peptide. The ligand variant 4L was created by replacing proline at position 4 of the agonist peptide (referred to as 4P) (21). Concentration-dependent binding curves were analyzed by nonlinear regression and K_D values were calculated. For low affinity (positive-selecting) ligands, half-maximal TCR saturation was not reached (data not shown) and therefore K_D values could not be determined. Similar to the tetramer-binding experiments, DP thymocytes from α-CPM mutant T1 mice bound pMHC ligands with ~4-fold lower apparent affinity (Table II) compared with wt or TM control thymocytes. The reduced apparent affinity of α-CPM mutant DP thymocytes to bind pMHC is most likely due to defective cooperativity between TCR and CD8, as ligand binding was similar when the interaction between CD8 and MHC was disrupted by point mutations in the MHC (4P-K^d Δ223/227; Fig. 2B and Ref. 21). In both the tetramer and monomer binding experiments, the 3- to 4-fold decrease in ligand binding displayed by α-CPM mutant thymocytes was similar for all ligands (Tables I and II) and was independent of TCR specificity (i.e., similar affinity decreases were observed for OT-I TCR- and T1 TCR-expressing thymocytes). Because the CD8 coreceptor is also

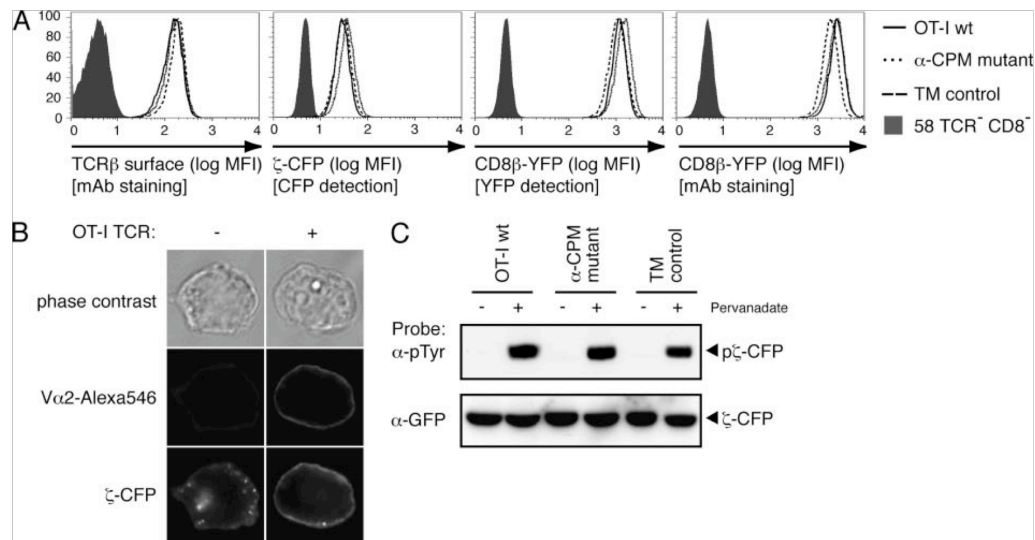


FIGURE 3. Characterization of T cell hybridomas. *A*, OT-I TCR, CD3ζ-CFP (ζ-CFP), and CD8β-YFP expressed on wt, α-CPM mutant, and TM control T cell hybridomas were analyzed by flow cytometry. CD3ζ-CFP expression was measured by CFP detection. CD8β-YFP expression was measured by a fluorescent mAb to CD8β and YFP detection. *B*, Expression and localization of CD3ζ-CFP. When OT-I wt TCR is expressed on the cell surface, CD3ζ-CFP localizes to the plasma membrane. TCR expression is shown upon staining with anti-Vα2 and Alexa Fluor 546. *C*, Phosphorylation of the CD3ζ-CFP (pζ-CFP) construct. OT-I wt or α-CPM mutant hybridomas (20×10^6) were treated with 100 μM pervanadate. Cell lysates were immunoprecipitated with rabbit anti-GFP (Eptomics) and then probed with anti-phosphotyrosine (α-pTy; clone 4G10) mAb. Stripping and reprobing with mouse anti-GFP (α-GFP; Santa Cruz Biotechnology) revealed the presence of CD3ζ-CFP in all samples.

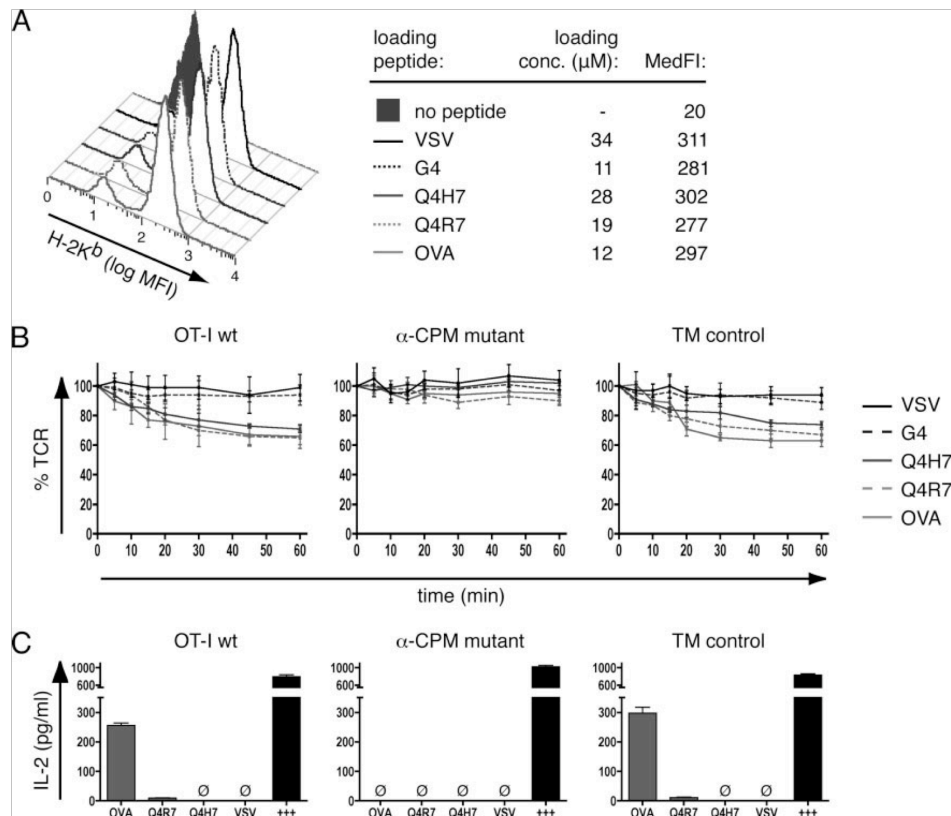


FIGURE 4. Stimulation of T cell hybridomas with peptide-loaded APCs. *A*, Peptide-loading of RMA-S cells. RMA-S cells were loaded with the indicated concentrations (conc.) of peptide as described in *Materials and Methods*. Staining with a fluorescently labeled H2-K^b Ab and flow cytometric analysis revealed similar MFI values (MedFl) and therefore similar peptide-K^b expression with all peptides. *B*, TCR internalization. T cell hybridomas were stimulated with peptide-loaded RMA-S cells (loading concentration as indicated in *A*). At the indicated time points TCR expression was determined by flow cytometry. TCR expression was set as 100% at 0 min and MFI signals were normalized to those values. *C*, IL-2 production. T cell hybridomas were stimulated with peptide-loaded RMA-S cells (loading concentration as indicated in *A*). After 24 h, supernatants were harvested and the amounts of IL-2 determined by ELISA. Calcium ionophore/PHA/PMA stimulation was used as positive control (+++). \emptyset , Not detected.

involved in TCR signaling initiation, we wondered whether the α -CPM mutation might affect signal initiation as well. To test this hypothesis, we set up a system to observe TCR-CD8 interaction directly by FRET microscopy.

Expression of wt and mutant OT-I TCRs and functional expression of chimeric fluorescent constructs in hybridomas

The TCR/CD8-deficient hybridoma 58 was successively transfected with constructs for CD8 α , CD8 β -YFP, CD3 ζ -CFP, and TCR chains for the wt, mutant α -CPM, or TM control receptors. Resulting OT-I wt, α -CPM mutant, and TM control T cell hybridomas were FACS sorted for similar expression of TCR-V α 2, CD8 α (data not shown), CD8 β -YFP, and CD3 ζ -CFP (Fig. 3A). CD3 ζ -CFP surface expression was assessed by fluorescence microscopy of T cell hybridomas before and after transduction of the OT-I wt TCR (Fig. 3B). Plasma membrane expression of CD3 ζ -CFP was only observed in TCR-positive cells. The localization of CD3 ζ -CFP at the plasma membrane was observed for the wt and for both chimeric receptors (data not shown), indicating that CD3 ζ -CFP was assembled in surface TCR/CD3 complexes. Moreover, the CD3 ζ -CFP molecules were tyrosine phosphorylated upon

pervanadate treatment, pointing to its functionality in wt, TM control, and mutant hybridomas (Fig. 3C).

Ag-dependent stimulation of wt and α -CPM mutant OT-I T cell hybridomas

For APCs, we used RMA-S murine lymphoma cells expressing H-2K^b loaded with exogenously added individual peptides (42). RMA-S-H-2K^b cells were pulsed with the indicated peptides at concentrations yielding similar surface expressions of pK^b (Fig. 4A). To assess functional responses, we tested hybridomas for their ability to internalize the TCR and release IL-2 upon stimulation with peptide-loaded APCs. The high-affinity/negative-selecting ligands OVA and Q4R7 induced \sim 35% TCR endocytosis in OT-I wt or TM control hybridomas after 60 min of incubation (Fig. 4B). The positive-selecting ligand Q4H7 showed slightly decreased and delayed kinetics of TCR endocytosis. In contrast, the lower affinity, positive-selecting ligand G4 failed to induce detectable loss of TCR from the cell surface, similarly as the noncognate ligand VSV. In the α -CPM mutant hybridomas, TCR endocytosis was substantially reduced, implicating a role for the α -CPM in the early cellular response to Ag. As readout for a late cellular response, we

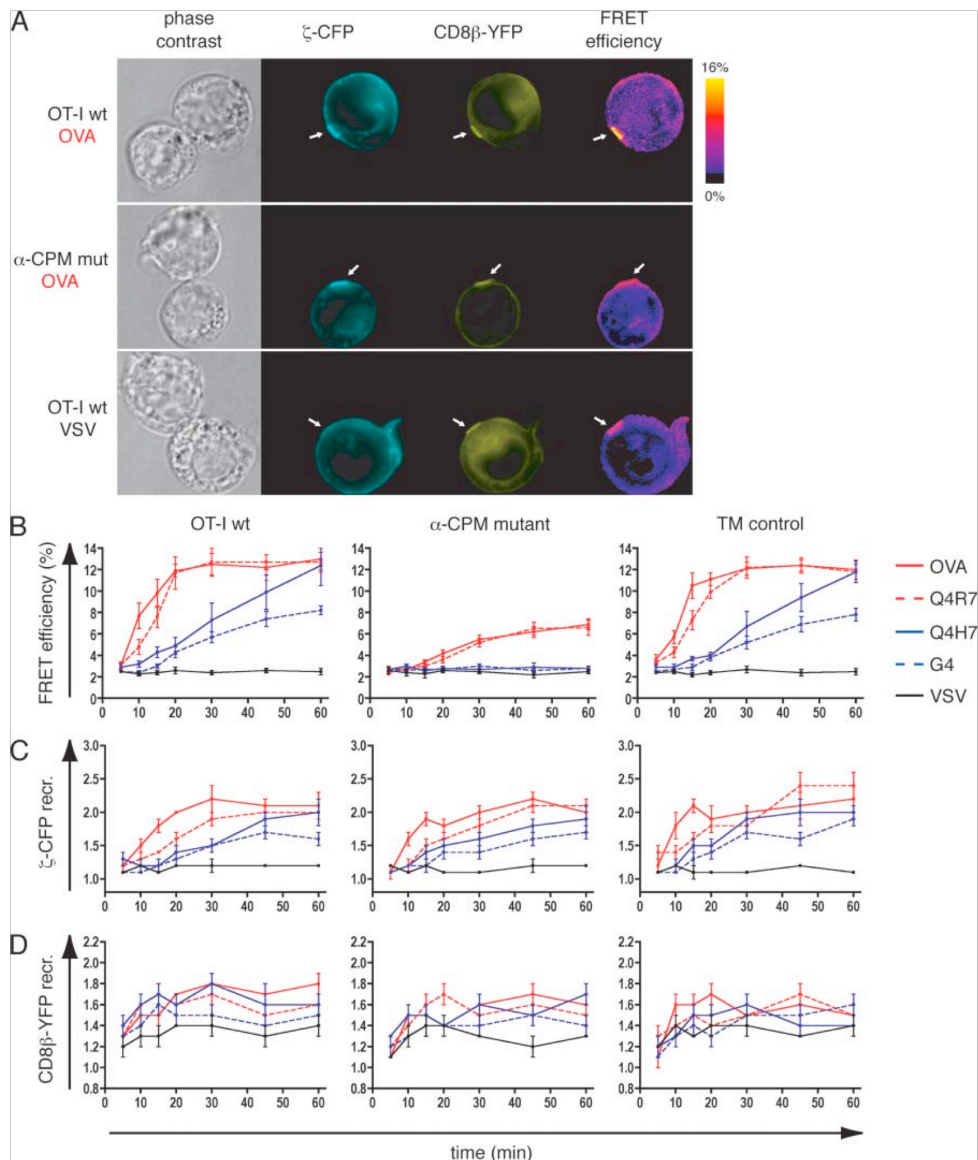


FIGURE 5. Ligand-induced CD3 ζ -CD8 β interaction. **A**, Fluorescence images of conjugates between peptide-loaded APCs and OT-I wt or α -CPM mutant (mut) hybridomas (loading concentration as indicated in Fig. 4A). Conjugates are shown as phase contrast images; CD3 ζ -CFP in cyan, CD8 β -YFP in yellow, and FRET efficiency images as donor-ratioed, compensated color gradients according to the algorithm described in *Materials and Methods*. The color code is depicted in the scale bar. White arrows indicate synapses. **B**, CD3 ζ -CFP and CD8 β -YFP FRET measurements at the interface of T cell hybridoma:APC conjugates. The indicated average values \pm SEM originate from $n \geq 20$ conjugates for OVA, Q4R7, Q4H7, and G4 and $n \geq 10$ for VSV. Negative-selecting ligands (OVA and Q4R7) are depicted in red and positive-selecting ligands (Q4H7 and G4) in blue. The noncognate VSV ligand is shown in black. For OT-I wt and TM control hybridomas, the differences in FRET efficiency induced by the weakest negative selector, Q4R7, or the strongest positive selector, Q4H7, were significant ($p < 0.05$) at 10, 15, 20, and 30 min. For the α -CPM mutant hybridomas, the differences in FRET signals induced by Q4R7 or Q4H7 were significant ($p < 0.05$) at 20, 30, 45, and 60 min. To compare the same ligands between the T cell hybridomas, we compared FRET signals between the α -CPM mutant and the TM control hybridoma. For Q4R7, the FRET signals were significantly different for all time points ($p < 0.05$). For Q4H7, the FRET signals in these two cell lines differed at 10, 15, 20, 30, 45, and 60 min. **C** and **D**, Recruitment (recr.) of CD3 ζ -CFP (**C**) and CD8 β -YFP (**D**) to the synapse. Fold recruitment of CD3 ζ -CFP and CD8 β -YFP to the synapse was calculated as described in *Materials and Methods*. The values are indicated as mean \pm SEM and originate from $n \geq 20$ conjugates for OVA, Q4R7, Q4H7, and G4 and $n \geq 10$ conjugates for VSV.

examined IL-2 release. The negative-selecting ligands OVA and Q4R7 induced IL-2 secretion from wt and TM control hybridomas (Fig. 4C). Neither the positive-selecting Q4H7 ligand nor the non-

cognate VSV ligand produced detectable amounts of IL-2 (Fig. 4C). The α -CPM mutant hybridomas failed to produce IL-2 in response to any of the ligands, excluding the possibility that the

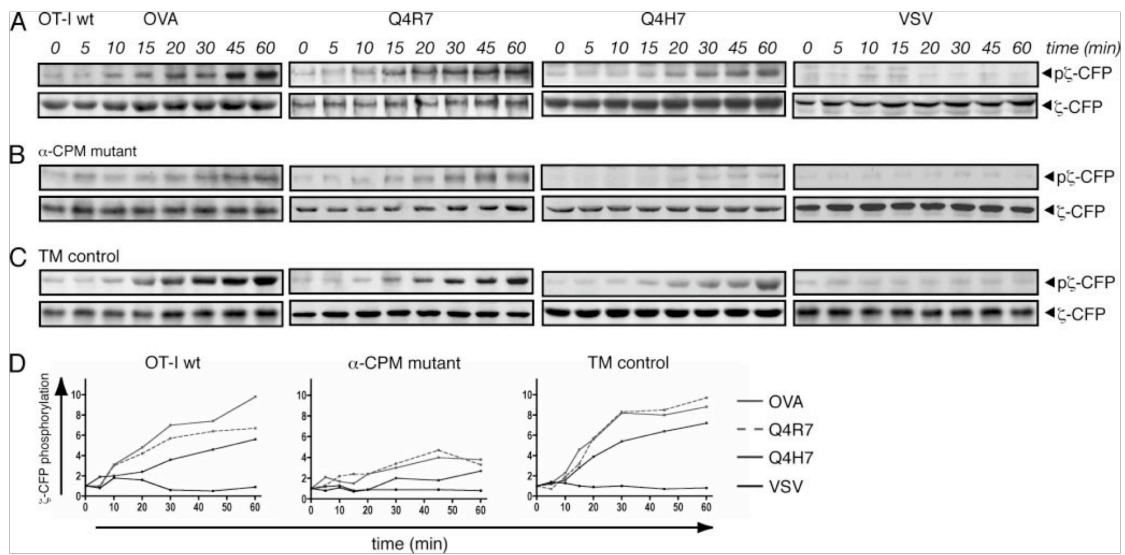


FIGURE 6. Ligand induced CD3 ζ -CFP phosphorylation. *A*, Tyrosine phosphorylation of CD3 ζ -CFP. OT-I wt hybridomas were stimulated with peptide-loaded APCs. CD3 ζ -CFP phosphorylation was assessed by immunoprecipitation and Western blotting. Anti-phosphotyrosine mAb (clone 4G10) indicates phosphorylated CD3 ζ -CFP (p ζ -CFP). Only one species of phosphorylated CD3 ζ -CFP could be observed (\sim 50 kDa) in contrast to endogenous CD3 ζ , which exhibits phosphorylated forms of increased molecular sizes (45). For signal normalization, membranes were stripped and probed with anti-GFP mAb. Representative blots are shown ($n \geq 2$). *B* and *C*, α -CPM mutant (*B*) and TM control (*C*) T cell hybridomas were probed for CD3 ζ -CFP phosphorylation as described in *A*. *D*, Densitometric evaluation of CD3 ζ -CFP phosphorylation. Densitometry of the Western blots from *A–C* was performed using a phosphorimaging device (ChemImager 5500; Alpha Innotech). Mean intensity values were normalized to the values obtained at 0 min and to the anti-GFP signal using the Alpha Ease FC software (Alpha Innotech).

α -CPM mutant cells could accumulate weak signals over time that would not be detected by measuring TCR internalization.

Ag-induced CD3 ζ -CD8 interaction

The approximation of two molecules within 10 nm of each other is an indirect measure of their interaction and can be assessed by FRET imaging (40). For CFP and YFP, the efficiency of energy transfer is $>50\%$ within a radius of ~ 5 nm and approximates zero beyond ~ 10 nm. Because the $\alpha\beta$ TCR has a diameter of ~ 10 nm (7), significant FRET between CFP and YFP strongly suggests physical interaction between the carrier molecules CD3 ζ and CD8 β used in these studies. We compared the FRET signals induced between CD3 ζ -CFP and CD8 β -YFP in the T cell hybridomas upon stimulation with peptide-loaded APCs. Following stimulation of OT-I wt hybridomas with OVA-loaded RMA-S cells, CD3 ζ -CFP and CD8 β -YFP were recruited to the synapse, where FRET efficiency increased significantly (Fig. 5*A*, top panel). Stimulation with the noncognate VSV ligand did not recruit CD3 ζ -CFP to the synapse and consequently no significant FRET was detected (Fig. 5*A*, bottom panel). CD8 β -YFP was recruited to the APC contact area even with the noncognate VSV ligand, as previously observed (32). In contrast, α -CPM mutant hybridomas efficiently recruited both CD3 ζ -CFP and CD8 β -YFP to the synapse but failed to induce substantial FRET (Fig. 5*A*, middle panel). In time course experiments (Fig. 5*B*) the high-affinity, negative-selecting ligands OVA and Q4R7 induced a fast and sustained FRET between CD3 ζ -CFP and CD8 β -YFP in OT-I wt and TM control hybridomas, whereas the low-affinity, positive-selecting ligands Q4H7 and G4 induced a delayed and weaker FRET signal. It is noteworthy that with the positive-selecting Q4H7 ligand, whose affinity for the OT-I receptor is only 2- to 3-fold lower than that of the negative selector Q4R7 (33), the FRET signal developed significantly

more slowly. However, by 60 min the FRET signal induced by Q4H7 reached a similar intensity as that induced by negative-selecting ligands (Fig. 5*B*).

In the mutant α -CPM hybridomas FRET signals were markedly reduced, pointing toward a defect in CD3 ζ -CD8 β approximation (Fig. 5*B*, middle panel). Strikingly, in absence of the α -CPM the low-affinity ligands Q4H7 and G4 caused no detectable CD3 ζ -CD8 β interaction over background (Fig. 5*B*). The reduced FRET signals in the α -CPM mutant hybridomas could not be attributed to reduced TCR or CD8 recruitment to the synapse, because CD3 ζ -CFP and CD8 β -YFP are recruited similarly as in OT-I wt or TM control hybridomas (Fig. 5, *C* and *D*). Therefore, an intact α -CPM is required for cytoplasmic approximation of the CD8 coreceptor and the TCR for low-affinity ligands, explaining the defect in positive selection in α -CPM deficient mice.

Ag induced TCR-CD8 interaction correlates with CD3 ζ phosphorylation

To test whether TCR-CD8 association at the plasma membrane correlates with the initiation of intracellular signaling, we directly examined the phosphorylation of CD3 ζ -CFP, an early event in TCR signal transduction (24, 45). For the Western blot analysis the same time points were chosen as in the microscopy-based FRET experiments. The OT-I wt and TM control hybridomas exhibited similar patterns of CD3 ζ -CFP phosphorylation (Fig. 6, *A* and *C*). The high-affinity/negative-selecting ligands OVA and Q4R7 induced rapid and sustained phosphorylation of CD3 ζ -CFP, whereas the low-affinity/positive-selecting ligand Q4H7 triggered delayed and weaker phosphorylation of CD3 ζ -CFP. In the α -CPM mutant hybridomas only moderate phosphorylation was observed at late time points in response to the high-affinity ligands OVA and Q4R7, whereas markedly reduced phosphorylation was induced by

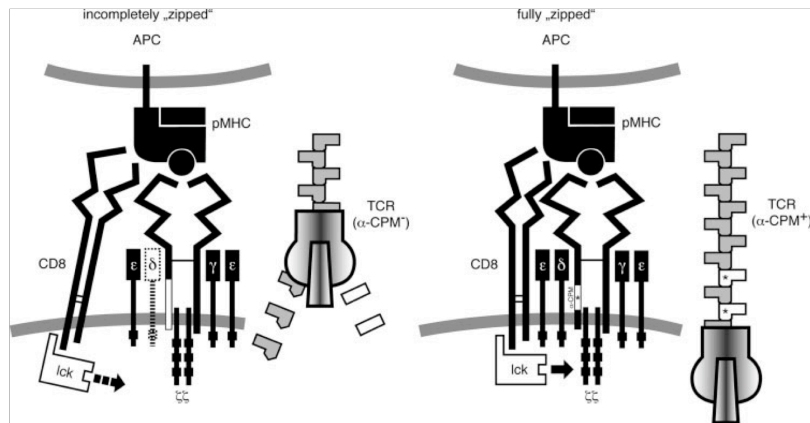


FIGURE 7. The zipper model of TCR-CD8 approximation. In absence of an intact α -CPM, the CD8 coreceptor binds to the pMHC but only inefficiently engages the TCR at the level of the TM and cytoplasmic domains. A candidate for linking the TCR and the CD8 coreceptor is the CD3 δ molecule, which has been previously shown to be poorly associated with the TCR/CD3 complex in α -CPM-deficient cells (26, 29) is indicated in the *left panel*. In analogy to a zipper, the α -CPM receptor is missing a tooth that hinders further zipping in the direction of the T cell plasma membrane (*left image*). As a consequence, the ITAMs of the CD3 complex, especially CD3 ζ , are inadequately phosphorylated. Only high-affinity ligands with a sufficiently long half-life of TCR binding can compensate for the α -CPM mutation. An intact α -CPM therefore allows tight CD8 association and closure of the zipper. In our model, this corresponds to a fully “zipped” approximation (*right panel*) where the coreceptor-associated Lck (lck) can fully access the ITAMs of the CD3 complex.

the positive-selecting ligand Q4H7 (Fig. 6*B*). The noncognate VSV ligand failed to induce phosphorylation in any of the hybridomas. Therefore, the extent and kinetics of TCR-CD8 interaction as measured by FRET correlates with the extent and kinetics of CD3 ζ -CFP phosphorylation (Figs. 5*B* and Fig. 6*D*).

Discussion

TCRs lacking the α -CPM are recruited to the synapse but do not efficiently interact with the CD8 coreceptor. Our FRET experiments indicate that close approximation of the two molecules is delayed and reduced when α -CPM mutant T cell hybridomas encounter a strong ligand and completely absent if they encounter a weak ligand. Therefore, the defective transmission of weak signals in the α -CPM mutant TCR (28) is a consequence of deficient TCR-CD8 interaction and the subsequently decreased CD3 ζ phosphorylation.

We previously showed that thymocytes expressing an α -CPM mutant TCR fail to be positively selected independently of the TCR specificities tested (27, 28). In this study, we showed that positive selectors and weak negative selectors fail to induce any form of thymic selection; only the strong agonist OVA induces negative selection in α -CPM mutant FTOCs. Previous studies performed with hybridoma cells showed a defect of TCR-CD8 cooperation in binding to pMHC (30). To quantify this binding defect, we measured TCR ligand binding on thymocytes of OT-I and T1 TCR transgenic mice expressing wt or mutant α -CPM constant regions. A ~4-fold reduction in TCR binding affinity (Fig. 2 and Tables I and II) could be measured between wt and α -CPM mutant TCRs; this difference in ligand binding was not evident with pMHC ligands that fail to engage CD8 (4P-K d Δ 223/227; Fig. 2*B* and Table II). Therefore, reduced pMHC binding of α -CPM mutant TCRs can plausibly be attributed to defective TCR-CD8 cooperation and not to altered TCR affinity per se. Moreover, this demonstrates that putative structural alterations in the α -CPM mutant TCR do not affect TCR affinity. Nevertheless, the slight reduction in apparent affinity of α -CPM deficient TCRs did not fully explain their thymic selection defects (Fig. 1). For example, the α -CPM mutant TCR binds the Q4H7 ligand with a tetramer K_D of

200 nM (2×10^{-7} M) but is a nonselector for this TCR. Because the positive-selecting complex, G4-Kb binds the wt OT-I receptor with a similar affinity (K_D of 300 nM (3×10^{-7} M); M. A. Daniels and E. Palmer, unpublished results), a K_D of 200 nM is well within the range of positive selection. Therefore, the slight reduction in binding affinity does not completely account for the selection defect.

To more fully understand the mechanism, by which α -CPM mutant receptors fail during thymic selection, we used a T cell hybridoma expressing labeled CD8 β and CD3 ζ molecules (32). Our experiments confirm previous work (32) showing that the CD8 coreceptor is recruited to the synapse similarly for all pMHC ligands (Fig. 5*D*), whereas the extent of TCR/CD3 recruitment correlated with ligand affinity (Fig. 5*C* and Ref. 46). Measuring FRET between CD8 β -YFP and CD3 ζ -CFP in the synapse, which reflects CD8 β -CD3 ζ interaction, we observed different interaction kinetics for negative- and positive-selecting ligands. Negative-selecting ligands induce a rapid and sustained FRET signal, whereas positive-selecting ligands induce slow and delayed FRET (Fig. 5*B*), extending a previous study (46). In the present study we show that the transition between the FRET patterns induced by negative- or positive-selecting ligands (Fig. 5*A*) correlates with the affinity selection threshold previously described (33). These data demonstrate that positive-selecting pMHC ligands exhibit reduced TCR-CD8 interaction in the synapse compared with negative-selecting ligands, which correlates with decreased CD3 ζ phosphorylation during signal initiation in response to positive-selecting ligands (Fig. 6*A* and Ref. 33).

Our data further show that the absence of the α -CPM has no discernible effect on TCR or CD8 recruitment to the immunological synapse (Fig. 5, *C* and *D*). Both CD8 and TCR/CD3 were similarly recruited to the synapse in all cell lines studied (OT-I wt, α -CPM mutant, and TM control; Fig. 5, *C* and *D*). Strikingly, CD8 β -CD3 ζ interaction was significantly reduced in T cell hybridomas expressing α -CPM mutant receptors (Fig. 5*B*). This emphasizes that TCR and coreceptor can be colocalized without any interaction as detected by FRET (31) (32). This reduction of molecular interaction under the plasma membrane had a clear

functional consequence. Phosphorylation of CD3 ζ was markedly reduced in α -CPM mutant hybridomas (Fig. 6D). These data suggest that an important role of the α -CPM is to facilitate the physical approximation of the intracellular domain of CD8 to the TCR/CD3 complex, a requirement for ITAM phosphorylation.

FRET signals observed in α -CPM mutant hybridomas were not always predictive of selection outcome. The high affinity ligands OVA and Q4R7 induced similarly weak FRET signals in α -CPM mutant cells, similar to those observed in wt or TM control cells stimulated by positive-selecting ligands (Fig. 5B). In α -CPM mutant FTOCs OVA is a negative selector, which might be expected because OVA can induce negative selection in wt OT-I FTOCs even in the absence of CD8 expression (47). Thus, negative selection in OVA-stimulated α -CPM mutant FTOCs might occur even without the induction of FRET. In contrast, Q4R7 is a non-selector in α -CPM mutant FTOCs (Fig. 1E), even though this ligand induces a similar FRET signal as does OVA. It is possible that the fluorescent protein labels exaggerate the TCR-CD8 interaction induced by Q4R7, although we consider this less likely because mutant forms of CFP and YFP were used that minimize spurious dimerization (32). Nevertheless, these data clearly show that the α -CPM mutation leads to a diminution in TCR-CD8 interaction as evidenced by a reduction in the contribution of CD8 to pMHC binding, TCR coreceptor approximation, and signal initiation. The corresponding FTOCs show the consequences of this weakened interaction on thymic selection.

We propose a model in which the lateral approximation of CD8 and the TCR is similar to the approximation of two sides of a zipper (Fig. 7). The molecules are first brought together by the pMHC ligand and, while the ligand remains bound to the receptor/coreceptor pair, their close apposition continues downward in the direction of the T cell. The α -CPM functions as a zipper tooth on the TCR side of the CD8/TCR complex, stabilizing the two sides of the zipper. If the membrane proximal domains of CD8 and TCR become "zipped," the CD8-associated Lck can tyrosine phosphorylate the ITAMs of the TCR/CD3 complex. Once the positive-selecting ligand dissociates, CD8 and the TCR disengage and Lck-mediated phosphorylation is terminated. TCRs lacking the α -CPM might not stabilize the TCR-CD8 zipper, compromising ITAM phosphorylation. Signaling by low affinity ligands, which occupy the TCR for a relatively short time, is severely affected by the lack of the α -CPM. Agonist ligands such as OVA could occupy the α -CPM mutant TCR for a sufficiently long time to compensate for the lack of an important tooth in the receptor/coreceptor zipper. Therefore, only the highest affinity ligands are capable of mediating negative selection in mutant α -CPM thymocytes (Fig. 1).

The α -CPM is present in the TCR α -chain throughout vertebrate evolution (26). α -CPM-deficient receptors associate poorly with CD3 δ , and related work has previously shown that the CD3 δ molecule is also required to establish a link between the TCR and the CD8 coreceptor (29). Therefore, the α -CPM and CD3 δ seem to be required for an optimal functional interaction with the CD8 coreceptor and for recognition of low affinity ligands that mediate positive selection and homeostatic expansion of peripheral T cells. The α -CPM may serve an equivalent function for the CD4 coreceptor, because a class II MHC restricted α -CPM mutant TCR also fails to generate positive selection signals (27).

Acknowledgments

We thank Dr. Naomi Taylor (Centre National de la Recherche Scientifique Unité Mixte de Recherche 5535, Montpellier, France) for viral vectors and packaging cell lines, M. Cavallari for help with ELISA experiments, and E. Wagner for animal care. The animal experiments were conducted in accordance with the Federal and Cantonal laws of Switzerland.

Disclosures

The authors have no financial conflict of interest.

References

- Cammarota, G., A. Schierle, B. Takacs, D. Doran, R. Knorr, W. Bannworth, J. Guardiola, and F. Sinigaglia. 1992. Identification of a CD4 binding site on the b2 domain of HLA-DR molecules. *Nature* 356: 799–781.
- Koenig, R., L. Y. Huang, and R. N. Germain. 1992. MHC class II interaction with CD4 mediated by a region analogous to the MHC class I binding site for CD8. *Nature* 356: 796–798.
- Norment, A. M., R. D. Salter, P. Parham, V. H. Engelhard, and V. H. Littman. 1988. Cell-cell adhesion mediated by CD8 and MHC class I molecules. *Nature* 336: 79–81.
- Salter, R. D., H. Benjamin, P. K. Wesley, S. E. Buxton, T. P. J. Garrett, C. Clayberger, A. M. Krensky, A. M. Norment, D. R. Littman, and P. Parham. 1990. A binding site for the T-cell co-receptor CD8 on the α 3 domain of HLA-A2. *Nature* 345: 41–46.
- Huang, J., L. J. Edwards, B. D. Evavold, and Z. Cheng. 2007. Kinetics of MHC-CD8 interaction at the T cell membrane. *J. Immunol.* 179: 7653–7662.
- Gallagher, P. F., F. de St. Groth, and J. F. A. P. Miller. 1989. CD4 and CD8 molecules can physically associate with the same T-cell receptor. *Proc. Natl. Acad. Sci. USA* 86: 10044–10048.
- Garcia, K. C., M. Degano, R. L. Stanfield, A. Brunmark, M. R. Jackson, P. A. Peterson, L. Teyton, and I. A. Wilson. 1996. An α - β T cell receptor structure at 2.5 Å and its orientation in the TCR-MHC complex. *Science* 274: 209–219.
- Wooldridge, L., H. A. van den Berg, M. Glick, E. Gostick, B. Laugel, S. L. Hutchinson, A. Milicic, J. M. Brenchley, D. C. Douek, D. A. Price, and A. K. Sewell. 2005. Interaction between the CD8 coreceptor and MHC class I stabilizes TCR-antigen complexes at the cell surface. *J. Biol. Chem.* 280: 27491–27502.
- Veillette, A., M. A. Bookman, E. M. Horak, and J. B. Bolen. 1988. The CD4 and CD8 T cell surface antigens are associated with the internal membrane tyrosine-protein kinase p56lck. *Cell* 55: 301–308.
- Zamoyska, R. 1998. CD4 and CD8: modulators of T-cell receptor recognition of antigen and of immune responses? *Curr. Opin. Immunol.* 10: 82–87.
- Trobridge, P. A., K. A. Forbush, and S. D. Levin. 2001. Positive and negative selection of thymocytes depends on Lck interaction with the CD4 and CD8 coreceptors. *J. Immunol.* 166: 809–818.
- Molina, T. J., K. Kishihara, D. P. Siderovskid, W. van Ewijk, A. Narendran, E. Timms, A. Wakeham, C. J. Paige, K. U. Hartmann, A. Veillette, et al. 1992. Profound block in thymocyte development in mice lacking p56lck. *Nature* 357: 161–165.
- Lewis, L. A., C. D. Chung, J. Chen, J. R. Parnes, M. Moran, V. P. Patel, and M. C. Miceli. 1997. The Lck SH2 phosphotyrosine binding site is critical for efficient TCR-induced progressive tyrosine phosphorylation of the ζ -chain and IL-2 production. *J. Immunol.* 159: 2292–2300.
- van Oers, N. S. C., N. Killeen, and A. Weiss. 1996. Lck regulates the tyrosine phosphorylation of the T cell receptor subunits and ZAP-70 in murine thymocytes. *J. Exp. Med.* 183: 1053–1062.
- LoGrasso, P. V., J. Hawkins, L. J. Frank, D. Wisniewski, and A. Marcy. 1996. Mechanism of activation for Zap-70 catalytic activity. *Proc. Natl. Acad. Sci. USA* 93: 12165–12170.
- Holler, P. D., and D. M. Kranz. 2003. Quantitative analysis of the contribution of TCR/pepMHC affinity and CD8 to T cell activation. *Immunity* 18: 155–164.
- Potter, T. A., K. Grebe, B. Freiberg, and A. Kupfer. 2001. Formation of supramolecular activation clusters on fresh ex vivo CD8⁺ T cells after engagement of the T cell antigen receptor and CD8 by antigen-presenting cells. *Proc. Natl. Acad. Sci. USA* 98: 12624–12629.
- Arcaero, A., C. Gregoire, T. R. Bakker, L. Baldi, M. Jordan, L. Goffin, N. Boucheron, F. Wurm, P. A. van der Merwe, B. Malissen, and I. F. Luescher. 2001. CD8 β endows CD8 with efficient coreceptor function by coupling T cell receptor/CD3 to raft-associated CD8/p56Lck complexes. *J. Exp. Med.* 194: 1485–1495.
- Hogquist, K. A., S. C. Jameson, W. R. Heath, J. L. Howard, M. J. Bevan, and F. R. Carbone. 1994. T cell receptor antagonist peptides induce positive selection. *Cell* 76: 17–28.
- Alam, S. M., P. J. Travers, J. L. Wung, W. Nasholds, S. Redpath, S. C. Jameson, and N. R. J. Gascoigne. 1996. T-cell-receptor affinity and thymocyte positive selection. *Nature* 381: 616–620.
- Naeher, D., M. A. Daniels, B. Hausmann, P. Guillaume, I. F. Luescher, and E. Palmer. 2007. A constant affinity threshold for T cell tolerance. *J. Exp. Med.* 204: 2553–2559.
- Fung-Leung, W. P., M. W. Schilham, A. Rahemtulla, T. M. Kundig, M. Vollenweider, J. Potter, W. van Ewijk, and T. W. Mak. 1991. CD8 is needed for development of cytotoxic T but not helper T cells. *Cell* 65: 443–450.
- Rahemtulla, A., W. P. Fung-Leung, M. W. Schilham, T. M. Kundig, S. R. Sambhara, A. Narendran, A. Arabian, A. Wakeham, C. J. Paige, R. M. Zinkernagel, et al. 1991. Normal development and function of CD8⁺ cells but markedly decreased helper cell activity in mice lacking CD4. *Nature* 353: 181–184.
- Nakayama, T., A. Singer, E. D. Hsi, and L. E. Samelson. 1989. Intrathymic signalling in immature CD4⁺CD8⁺ thymocytes results in tyrosine phosphorylation of the T-cell receptor ζ -chain. *Nature* 341: 651–655.

25. Fung-Leung, W. P., T. M. Kündig, K. Ngo, J. Panakos, J. De Sousa-Hitzler, E. Wang, P. S. Ohashi, T. W. Mak, and C. Y. Lau. 1994. Reduced thymic maturation but normal effector function of CD8⁺ T cells in CD8 β gene-targeted mice. *J. Exp. Med.* 180: 959–967.
26. Baeckstroem, B. T., E. Milia, A. Peter, B. Jaureguierry, C. T. Bardari, and E. Palmer. 1996. A motif within the T cell receptor α chain constant region connecting peptide domain controls antigen responsiveness. *Immunity* 5: 437–447.
27. Baeckstroem, B. T., U. Mueller, B. Hausmann, and E. Palmer. 1998. Positive selection through a motif in the $\alpha\beta$ T cell receptor. *Science* 281: 835–838.
28. Werlen, G., B. Hausmann, and E. Palmer. 2000. A motif in the $\alpha\beta$ T-cell receptor controls positive selection by modulating ERK activity. *Nature* 406: 422–426.
29. Doucey, M. A., L. Goffin, D. Naeher, O. Michielin, P. Baumgärtner, P. Guillaume, E. Palmer, and I. F. Luescher. 2003. CD3 δ establishes a functional link between the T cell receptor and CD8. *J. Biol. Chem.* 278: 3257–3263.
30. Naeher, D., I. F. Luescher, and E. Palmer. 2002. A role for the α -chain connecting peptide motif in mediating TCR-CD8 cooperation. *J. Immunol.* 169: 2964–2972.
31. Zal, T., A. Zal, and N. R. J. Gascoigne. 2002. Inhibition of T cell receptor-coreceptor interactions by antagonist ligands visualized by live FRET imaging of the T-hybridoma immunological synapse. *Immunity* 16: 521–535.
32. Yachi, P. P., J. Ampudia, N. R. J. Gascoigne, and T. Zal. 2005. Nonstimulatory peptides contribute to antigen-induced CD8-T cell receptor interaction at the immunological synapse. *Nat. Immunol.* 6: 785–792.
33. Daniels, M. A., E. Teixeira, J. Gill, B. Hausmann, D. Roubaty, K. Holmberg, G. Werlen, G. A. Hollaender, N. R. J. Gascoigne, and E. Palmer. 2006. Thymic selection threshold defined by compartmentalization of Ras/MAPK signalling. *Nature* 444: 724–729.
34. Grakoui, A., S. K. Bromley, C. Sumen, M. M. Davis, A. S. Shaw, P. M. Allen, and M. L. Dustin. 1999. The immunological synapse: a molecular machine controlling T cell activation. *Science* 285: 221–227.
35. Santori, F. R., W. C. Kieper, S. M. Brown, Y. Lu, T. A. Neubert, K. L. Johnson, S. Naylor, S. Vukmanovic, K. A. Hogquist, and S. C. Jameson. 2002. Rare, structurally homologous self-peptides promote thymocyte positive selection. *Immunity* 17: 131–140.
36. Kelly, J. M., S. J. Sterry, S. Cose, S. J. Turner, J. Fecondo, S. Rodda, P. J. Fink, and F. R. Carbone. 1993. Identification of conserved T cell receptor CDR3 residues contacting known exposed peptide side chains from a major histocompatibility complex class I-bound determinant. *Eur. J. Immunol.* 23: 3318–3326.
37. Stotz, S. H., L. Bollinger, F. R. Carbone, and E. Palmer. 1999. T cell receptor (TCR) antagonism without a negative signal: evidence from T cell hybridomas expressing two independent TCRs. *J. Exp. Med.* 189: 253–263.
38. DiGiusto, D. L., and E. Palmer. 1994. An analysis of sequence variation in the β -chain framework and complementarity determining regions of an allo-reactive T cell receptor. *Mol. Immunol.* 31: 693–670.
39. Letourneur, F., and B. Malissen. 1989. Derivation of a T cell hybridoma variant deprived of functional T cell receptor $\alpha\beta$ chain transcripts reveals a nonfunctional α -mRNA of BW5147 origin. *Eur. J. Immunol.* 19: 2269–2274.
40. Zal, T., and N. R. J. Gascoigne. 2004. Using live FRET imaging to reveal early protein-protein interactions during T cell activation. *Curr. Opin. Immunol.* 18: 418–427.
41. Zal, T., and N. R. J. Gascoigne. 2004. Photobleaching-corrected FRET efficiency imaging of live cells. *Biophys. J.* 86: 3923–3939.
42. Ljunggren, H. G., N. J. Stam, C. Oehlen, J. J. Neefjes, P. Hoeglund, M. T. Heemels, J. Bastin, T. N. M. Schumacher, A. Townsend, K. Kaerre, and H. L. Ploegh. 1990. Empty MHC class I molecules come out in the cold. *Nature* 346: 476–481.
43. Clarke, S. R., M. Barnden, C. Kurts, F. R. Carbone, J. F. Miller, and W. R. Heath. 2000. Characterization of the ovalbumin-specific TCR transgenic line OT-I: MHC elements for positive and negative selection. *Immunol. Cell Biol.* 78: 110–117.
44. Luescher, I. F., J. C. Cerottini, and P. Romero. 1994. Photoaffinity labeling of the T cell receptor on cloned cytotoxic T lymphocytes by covalent photoreactive ligand. *J. Biol. Chem.* 269: 5574–5582.
45. Love, P. E., and E. W. Shores. 2000. ITAM multiplicity and thymocyte selection: how low can you go? *Immunity* 12: 591–597.
46. Yachi, P. P., J. Ampudia, T. Zal, and N. R. J. Gascoigne. 2006. Altered peptide ligands induce delayed CD8-T cell receptor interaction: a role for CD8 in distinguishing antigen quality. *Immunity* 25: 1046–1054.
47. Goldrath, A. W., K. A. Hogquist, and M. J. Bevan. 1997. CD8 lineage commitment in the absence of CD8. *Immunity* 6: 633–642.

3.2 A discrete affinity driven elevation of ZAP-70 activity distinguishes positive and negative selection

Manuscript in preparation

Michel Mallaun, Gerhard Zenke and Ed Palmer

3.2.1 Summary

By directly binding to the CD3 molecules of the T-cell receptor (TCR) complex, the ζ -chain associated protein of 70 kDa (ZAP-70) plays a central role in proximal TCR signaling. Once the TCR binds antigenic peptide-MHC (p-MHC) ligands, the CD3 molecules are tyrosine phosphorylated allowing ZAP-70 to bind and propagate the signal to downstream signaling molecules. It is unclear to what extent ZAP-70 is recruited to engaged TCRs in response to varying p-MHC-TCR interactions, such as in thymic selection. Using OT-I transgenic double-positive (DP) pre-selection thymocytes, we studied the recruitment of ZAP-70 to the immunological synapse and its phosphorylation at a regulatory and an activating tyrosine residue. The strong recruitment and phosphorylation of ZAP-70 in response to negative selecting ligands correlated with an approximately 2-fold increase in ZAP-70 kinase activity compared to positive selecting ligands. Positive selectors failed to recruit high levels of ZAP-70 into the synapse, although we found that recruited molecules were in fact phosphorylated, which induced moderate ZAP-70 kinase activity. Furthermore, we show that ZAP-70 kinase activity is a determinant of thymic selection outcome. By partial inhibition ZAP-70 kinase activity, negative selection can be converted into positive selection. Using the same ZAP-70 kinase inhibitor, we also show that phosphorylation of tyrosine 493 in the kinase activation loop is mostly mediated by ZAP-70 auto-phosphorylation, whereas phosphorylation of the regulatory tyrosine 319 depends on kinases other than ZAP-70. The 2-fold increase in ZAP-70 recruitment above the negative selection threshold can be explained by a similar increase in TCR recruitment to the synapse and is not due to an increased relative ZAP-70 / TCR ratio. Therefore, we hypothesize that the TCR by binding to ligands of varying affinity, recruits associated ZAP-70 proportionally, thereby determining the amount of ZAP-70 kinase activity. Negative selection is only induced if ZAP-70 kinase activity is elevated 2-fold over positive selection.

3.2.2 Introduction

Following $\alpha\beta$ T-cell receptor (TCR) engagement by pMHC ligands, the Syk family protein tyrosine kinase (PTK) ZAP-70 is activated and phosphorylates several downstream target molecules (63, 102, 103). ZAP-70 initially binds to phosphorylated immunoreceptor tyrosine-based activation motifs (ITAMs) of the ζ and CD3 ϵ subunits of the TCR complex through its tandem Src-homology region 2 (SH2) domain (70, 104). Subsequently, ζ -bound ZAP-70 is tyrosine phosphorylated (78, 81, 105). ZAP-70 is a key signaling component in thymocytes since ZAP-70 deficient mice are blocked in both positive and negative selection (64).

Studies have shown that ZAP-70 dysfunction can lead to autoimmunity. A spontaneous occurring single amino acid substitution in the second SH2-domain (W163C) alters TCR-mediated signaling, the outcome of thymic selection and causes joint inflammation and infiltration of CD4⁺ T-cells, a pathology reminiscent of rheumatoid arthritis in humans (84). Apparently, the efficiency of negative selection is altered in these mutant mice due to the reduction of ZAP-70 activity. In patients with selective T-cell deficiency (STD), who suffer from persistent infections reminiscent of severe combined immunodeficiency, a point mutation leads to alternative splicing of the *zap-70* gene (85). This mutation results in a three amino acid insertion in the kinase domain, abolishing its enzymatic activity. T-cells from patients, homozygous for this point mutation exhibit markedly reduced tyrosine phosphorylation; nevertheless some Ca²⁺ mobilization remains in activated peripheral T-cells. The authors suggest that the Src kinase Fyn takes over some ZAP-70 functions in peripheral T-cells. On the other hand, ZAP-70 deficiency in mice blocks both positive and negative selection of DP thymocytes (64). Another study demonstrates that a spontaneously occurring point mutation in the DLAARN motif (R464C) of ZAP-70's kinase domain results in defective TCR signaling and a complete arrest of thymocyte development at the DP stage (77). These mice express a catalytically inactive form of ZAP-70, again demonstrating the requirement for ZAP-70 activity in thymocyte development.

The number of CD3 ITAMs and by the extension the quantity of ZAP-70 kinase activity seems to play a central role in the establishment of central tolerance. In transgenic mice expressing either class I or class II MHC restricted TCRs, the percentage of positively selected CD8⁺ or CD4⁺ SP cells, respectively, decreases by reducing the number of ζ -chain ITAMs (73). This change of ITAM multiplicity alters the efficiency of thymic selection by reducing ZAP-70 binding and downstream signaling. Another study shows that reducing the number of CD3 and ζ -chain ITAMs, thereby lowering the TCR signal strength, results in autoimmunity due to a failure in deleting self-reactive T-cells, which are instead positively selected in the thymus (106). The authors suggest that the main reason for the TCR/CD3 complex to have a total of 10 ITAMs is rather quantitative than qualitative in order to guarantee scalable signaling and efficient negative selection.

In vitro, binding assays have revealed the parameters for ZAP-70 binding to the CD3 subunits (70). ZAP-70 binding to ζ or CD3 ϵ through its tandem SH2-domain is highly cooperative, which ensures a high affinity for the doubly phosphorylated ζ or CD3 ϵ ITAM. The binding affinities of the ZAP-70 tandem SH2-domains to peptides containing individual phosphorylated ζ or CD3 ϵ ITAMs was measured and the hierarchy described as $\text{ITAM}(\zeta_1) \geq \text{ITAM}(\zeta_2) > \text{ITAM}(\text{CD3}\epsilon) \geq \text{ITAM}(\zeta_3)$ (71). Affinity differences of as much as 30-fold between the individual phospho-ITAMs suggests that ZAP-70 may bind to ITAMs sequentially, provided that they are phosphorylated. Indeed, a study shows that ζ ITAM phosphorylation is sequential and appears to be ordered (72). The authors detected a basal level of partially phosphorylated ζ in resting T-cells whereas fully phosphorylated ζ is induced only upon stimulation with agonist pMHC ligands. On the other hand, antagonist pMHC ligands promote intermediate ζ phosphorylation in mature T-cells, which did not detectably activate ZAP-70. Along the same lines, T-cell clones stimulated with altered peptide ligands (APLs) induce only partial ζ ITAM phosphorylation, which greatly reduces ZAP-70 activation and PLC- γ 1 mediated phospholipid hydrolysis (74).

Fully phosphorylated ζ dimers are sufficient to promote ZAP-70 trans-phosphorylation and kinase activity *in vitro*, whereas monomeric ζ fails to activate ZAP-70 (65). Murine thymocytes exhibit a constitutive association of ZAP-70 with partially phosphorylated ζ , yet ZAP-70 is not activated (66, 67). The discrepancy may originate from negative regulation loops, which do not occur in cell-free assays. Indeed, the phosphatase SHP-1 increases its dephosphorylation activity by directly binding to ZAP-70, which negatively regulates ZAP-70 kinase activity (68, 69).

Substitution of tyrosine 319 with phenylalanine (Y319F) in the interdomain B region of ZAP-70 leads to dominant negative behavior (78). Y319F prevents phosphorylation of further ZAP-70 tyrosine residues such as Y493 in the activation loop. Defective kinase activity ultimately prevents antigen-induced IL-2 expression. Y319 is a substrate for the Src kinase Lck; phosphorylation of Y319 is a critical step in activating ZAP-70 kinase activity (79). Therefore, a ZAP-70 mutant carrying an optimized binding site for Lck (Y³¹⁹EEL instead of wildtype Y³¹⁹SDP) displays a gain-of-function phenotype, encompassing increased tyrosine phosphorylation and catalytic activity. Another study suggests that Y315 and Y319 function as an autoinhibitory switch, thereby regulating ZAP-70's kinase activity (82). By phosphorylating Y319 (and possibly Y315), Lck or other kinases activate ZAP-70, similar to the juxtamembrane region of several RTKs. These findings were supported by the crystallographic structure of ZAP-70 where phosphorylation at Y315 and Y319 in the interdomain B stabilizes a conformational change required to activate the kinase (83). In contrast to the Y319F mutant, a Y315A/Y319A mutant leads to Y493 phosphorylation, presumably via intermolecular *trans*-phosphorylation. The Y315A/Y319A mutant protein may be in an open conformation and therefore is released from autoinhibition, similar to wildtype Y319-phosphorylated ZAP-70 (82).

Tyrosine phosphorylation at residue Y493 is another positive regulatory step (80, 81). Substitution of Y493 with phenylalanine (Y493F) prevents ZAP-70 activation even if Y493F is co-expressed with constitutively active Lck. Along the same lines, Lck is not very efficient in phosphorylating Y493 in a kinase-inactive ZAP-70 mutant (K369A), even when Y319 is phosphorylated and available for Lck-binding. This suggests that Y493 in wildtype ZAP-70 is poorly phosphorylated by Lck, if at all. Interestingly, the K369A kinase-inactive mutant is hyperphosphorylated at both Y319 and Y493 in Cos or 293 cells. Therefore, although not very efficient, Lck can phosphorylate Y493 under certain conditions (79). Hypothetically, Lck may be responsible for the initial but rather inefficient phosphorylation of Y493 on several ZAP-70 molecules that *trans*-autophosphorylate other ZAP-70 molecules with which they are dimerized by paired ITAMs of the CD3 subunits.

The current study shows how the level of ZAP-70 activity controls the outcome of thymic selection. ZAP-70 is differentially recruited and phosphorylated in the immunological synapses (IS) of DP OT-I transgenic thymocytes with antigen presenting cells (APCs) loaded with positive or negative selecting peptides. pMHC ligands with a TCR affinity just over the negative selection threshold induce an abrupt increase in TCR and ZAP-70 recruitment to the IS formed between a DP thymocyte and a peptide-loaded APC. This discrete elevation of TCR and ZAP-70 recruitment occurring at the negative selection threshold is associated with a discontinuous increase in ZAP-70 enzymatic activity. This tightly regulated increase in ZAP-70 activity accounts for the transition from positive to negative selection. This is supported by artificially reducing ZAP-70 enzymatic activity using a ZAP-70 kinase inhibitor. Use of this inhibitor demonstrates that virtually all Y493 phosphorylation is dependent on ZAP-70 kinase activity and results from *trans*-phosphorylation. These data support the idea that the density of TCR/ZAP-70 in the IS determines the extent of Y493 phosphorylation, the amount of ZAP-70 activity and the outcome of thymic selection.

3.2.3 Materials and Methods

Peptides and antibodies

OVA variant peptides were synthesized and purified as described (91, 92) and had the following affinity hierarchy for the OT-I TCR: OVA >> Q4R7 > Q4H7 >> VSV (107, 108). Anti-CD4 (RM4-5), anti-CD8 β (53-5.8), anti-V α 2 (B20.1), anti V β 5 (MR9-4) and capturing anti-ZAP-70 (cl. 29) are from BD Biosciences. Probing antibodies anti-ZAP-70 (99F2), anti-p-Y319 (65E4), anti-p-Y493 (2704) are from Cell Signaling. For flow cytometry, fluorochrome-conjugated anti-ZAP-70 (1E7.2) is from Santa Cruz Biotechnology. Anti-phosphotyrosine (4G10) and anti-LAT (rabbit polyclonal) are from Upstate. Capturing and probing anti-CD3 ϵ (145-2C11) and anti- ζ (H146-968) respectively, were from purified hybridoma supernatants.

Microscopy

CD19⁺ positive B-cells from C57 Bl/6 mice were used as APCs for microscopy. Spleen cell suspensions were subjected to red blood cell lysis and depletion of CD4⁺, CD8 α ⁺ and NK1.1⁺ positive cells by monoclonal antibodies and binding to magnetic beads (AutoMACS system; Miltenyi Biotec). Non-depleted cells (85-90% CD19⁺) were stained with Cy5 mono-reactive dye (GE Healthcare) and loaded with 2 μ M peptide. Thymocytes from OT-I Rag^{-/-} β 2m^{-/-} transgenic mice were stimulated with peptide-loaded APCs (1:1 ratio) by brief centrifugation and incubation at 37°C. Fixation with formaldehyde, permeabilization with Triton X-100 and staining with monoclonal antibodies was carried out on (3-aminopropyl)triethoxysilane (Sigma) coated cover slips. Microscopy was performed on an Olympus IX81 fluorescence microscope. The recruitment or phosphorylation of fluorescently labeled proteins in the synapse was calculated as background-corrected ratio of the mean fluorescence intensity (MFI) in the synapse divided by the MFI of a user-defined membrane region outside the synapse: 'Fold recruitment' = (MFI_{Synapse} - bkgd) / (MFI_{Membrane} - bkgd). Values were plotted using the Prism software (GraphPad Software Inc.).

Stimulation of DP thymocytes and immunoprecipitation

APCs (3LBM 13.1 B-cell hybridomas) expressing H-2K^b were loaded with 2 μ M peptide, followed by fixation with 0.1% glutaraldehyde. DP thymocytes from OT-I Rag^{-/-} β 2m^{-/-} transgenic mice were stimulated with peptide-loaded APCs by brief centrifugation and incubation at 37°C. For immunoprecipitations, cells were lysed with 1% nonionic detergent (Brij58 for TCR-IPs, NP-40 for LAT-IPs and digitonin for ZAP-70 IPs) and isotonic lysis buffer to generate post-nuclear lysates. Immunoprecipitations were performed with 1 μ g of monoclonal antibody and protein G sepharose (GE Healthcare). SDS-PAGE under reducing conditions and Western blotting was performed according to standard techniques. Nitrocellulose membranes were probed with primary antibodies

and subsequently with horseradish peroxidase (HRP)-conjugated secondary antibodies. HRP-mediated conversion of the ECL-reagent (GE Healthcare) was detected on ECL hyperfilms (GE Healthcare). Films were developed on a Curix80 processor (Agfa) and analysed using the Gel Doc 2000 densitometer and the Quantity One software (BioRad). If required, membranes were stripped with Restore Western blot stripping buffer (Thermo Scientific) and reprobed.

In vitro kinase assay

ZAP-70 was co-immunoprecipitated from activated TCR complexes using the monoclonal anti-CD3 ϵ (145-2C11) antibody. Immunoprecipitated complexes were incubated with 0.5 μ g recombinant LAT (Upstate), 5mM MgCl₂ and 10 μ M ATP for 10min at 37°C. Reducing SDS-PAGE, Western blotting and membrane probing was performed as described above.

Fetal thymic organ culture (FTOC)

FTOC was performed as described (109). In brief, thymic lobes were excised from OT-I Rag^{-/-} β 2m^{-/-} transgenic mice at a gestational age of day 15.5. Exogenous β 2m (5 μ g/ml), peptide (2 μ M for negative-selecting and 20 μ M for positive selecting peptides) and varying concentrations of the ZAP-70 kinase inhibitor were added to the FTOCs. After 7 days of culture, thymocytes were analyzed by flow cytometry.

3.2.4 Results

ZAP-70 recruitment and phosphorylation with positive and negative selecting ligands

We used a well-defined set of peptides, inducing positive or negative selection of thymocytes expressing the OT-I TCR (107, 108). Transgenic mice of the OT-I Rag^{-/-} β2m^{-/-} mice are blocked in T-cell development and accumulate large numbers of pre-selection CD8⁺ CD4⁺ double-positive (DP) thymocytes. These DP OT-I thymocytes were stimulated with peptide-loaded APCs and subsequently analyzed by fluorescence microscopy. OVA, Q4R7, Q4H7 or the null ligand, VSV were used in these experiments. OVA is a high affinity negative selector for the OT-I receptor. Q4R7 is the lowest affinity negative selector, whereas Q4H7 has the highest affinity, which still induces positive selection of OT-I thymocytes; both K^b/Q4R7 and K^b/Q4H7 have similar affinities for the OT-I receptor (108). Specific staining for phosphorylated tyrosine at position 319 of ZAP-70 (p-Y319) revealed a synapse-specific increase in response to the negative-selecting peptide Q4R7 compared to the positive-selecting peptide Q4H7 (Fig1A; middle panels). Similar results were obtained for phosphorylation of the tyrosine at position 493 (p-Y493) located in the kinase domain of ZAP-70 (Fig1A; right panels). Increased ZAP-70 tyrosine phosphorylation was accompanied by increased ZAP-70 and ζ recruitment to the synapse (Fig1A; left panels). In time course experiments, microscopy images were analyzed for the recruitment of ZAP-70 and its phosphorylation in the synapse and were quantified at indicated time points (Fig1B). OVA and Q4R7, the strongest and the weakest negative selecting peptides induced increased phosphorylation of Y319 and Y493 in the synapse, as well as increased ZAP-70 recruitment. However, the peak of Q4R7-induced ZAP-70 phosphorylation and recruitment appeared to be only slightly reduced or delayed compared to OVA. In contrast, Q4H7, the positive selector, recruited markedly less ZAP-70 to the synapse in spite of the fact that Q4H7/K^b only has a marginally lower affinity for the OT-I TCR compared to Q4R7/K^b. Non-cognate VSV, a non-selecting peptide for the OT-I TCR fails to induce ZAP-70 recruitment or phosphorylation.

We also investigated ZAP-70 phosphorylation and recruitment to activated TCR complexes by Western analysis in order to confirm the results obtained by microscopy (Fig 1). Immunoprecipitated TCR complexes from OT-I Rag^{-/-} β2m^{-/-} thymocytes stimulated with peptide-loaded APCs were probed for the presence of and tyrosine phosphorylation of ZAP-70 (Fig2A). Similar to what we observed by microscopy, ZAP-70 recruitment to the TCR was enhanced under negative-selecting conditions. TCR associated ZAP-70 demonstrates strong and transient phosphorylation at Y319 and Y493. The positive-selector Q4H7 induces a 2-fold reduced ZAP-70 association to the TCR/CD3 complex and approximately 2-fold reduced Y319 and Y493 phosphorylation. Stimulation with non-cognate VSV shows a background level of ZAP-70 association to the TCR complex but fails to induce any Y319 or Y493 phosphorylation. This is in

accordance with previous observations that ZAP-70 is to some degree associated with the TCR ζ -chain, even in resting cells (63). The amount of TCR captured in these immunoprecipitations was similar as shown by probing for ζ . Densitometric analysis confirmed the patterns of ZAP-70 association to the TCR observed by microscopy (Fig2B). pMHC ligands above the negative selection threshold induce a discrete increase of TCR and ZAP-70 recruitment as well as ZAP-70 phosphorylation in the synapse.

ZAP-70 kinase activity in positive and negative selection

We developed an *in vitro* kinase assay to assess ZAP-70 kinase activity under positive or negative selecting conditions. Following stimulation of OT-I Rag^{-/-} β 2m^{-/-} DP thymocytes with peptide-loaded APCs, TCR/CD3/ZAP-70 complexes were co-immunoprecipitated at various times. ZAP-70 kinase activity was measured using a recombinant LAT substrate in presence of ATP (Fig3). LAT is the main ZAP-70 substrate, which orchestrates TCR downstream signaling (90, 110). The specificity of the assay was confirmed by using the ZAP-70 kinase inhibitor XXX, which abrogated ZAP-70 kinase activity in this *in vitro* assay (Fig3A; lanes 1&2). Control reactions showed that no ZAP-70 kinase activity was detected in unstimulated thymocytes (Fig3A; lane3). Furthermore, endogenous LAT is not co-immunoprecipitated with the TCR under these conditions as shown in the absence of recombinant LAT (Fig3A; lane 4). Isotype control antibodies confirmed the specificity of the immunoprecipitation (Fig3A; lane 5). These controls suggest that LAT phosphorylation in this assay specifically comes from TCR-associated, activated ZAP-70.

OT-I DP thymocytes were stimulated with peptide-loaded APCs and ZAP-70 kinase activity was determined from co-immunoprecipitated TCR/CD3/ZAP-70 complexes using the *in vitro* kinase assay. The negative-selecting peptides OVA and Q4R7 induced increased ZAP-70 activity at early time points compared to the positive-selecting peptide Q4H7 (Fig3B). The decline of ZAP-70 activity at later time points may be due to reduced ZAP-70 association with the TCR complex. ZAP-70 dissociation from activated TCR/CD3 complexes has been previously described (111). The non-cognate peptide, VSV failed to induce any detectable ZAP-70 activity associated with the TCR (Fig3B). Phospho-LAT signals were quantified by densitometry to analyze the kinetics of ZAP-70 activity (Fig3C). To estimate the total ZAP-70 activity over the whole time-course of the experiment or particularly the initiation phase of TCR signaling, we integrated the area under the curves (Fig3D). In both cases, the integrated ZAP-70 activity was at least 2-fold higher for the weakest positive selector Q4R7 compared to the strongest positive selector Q4H7. During the initial phase of stimulation (10min), the strongest negative selector, OVA induced somewhat more ZAP-70 kinase activity than the weak negative selector, Q4R7 (Fig 3D, left panel); however, over the entire time course of the experiment (60 min) both negative selecting peptides induced a similar amount of ZAP-70 activity (Fig 3D, right panel). Therefore, at the selection threshold, negative-selecting

ligands abruptly induce a 2- to 3-fold increase in ZAP-70 recruitment and phosphorylation, which is reflected by the integrated ZAP-70 activity during the initiation phase of TCR signaling.

These results raised the question whether the amount of ZAP-70 activity is a dose-dependent determinant of thymocyte selection outcome. We wondered whether the lowered ZAP-70 activity in presence of the inhibitor could actually convert negative selection of DP thymocytes into positive selection. To assess this question we analyzed selection of OT-I DP thymocytes in fetal thymic organ cultures (FTOC) under negative or positive selecting conditions in either presence or absence of the ZAP-70 inhibitor.

Partial ZAP-70 inhibition converts negative into positive selection

The ability of the ZAP-70 kinase inhibitor to influence thymic selection outcome was tested using FTOC (109). OVA induced negative selection by deleting virtually all DP thymocytes (Fig4A; left panel). In contrast, non-cognate VSV induced neither positive nor negative selection (not shown; (107)). In presence of increasing concentrations of the ZAP-70 kinase inhibitor (XXX), OVA stimulated FTOCs generated increased numbers of positively selected CD8⁺ SP cells (Fig4A; right panels). This demonstrates that positive selection depends on low ZAP-70 kinase activity in a dose-dependent way. A similar phenomenon was observed in Fig4B. In FTOCs stimulated with the weakest negative selector Q4R7, partial inhibition of ZAP-70 kinase activity leads to positive selection of OT-I DP thymocytes (Fig4B, lower panels). Interestingly, partial inhibition of ZAP-70 activity produced only a mild reduction of positive selection induced by Q4H7 (Fig4B, upper panels).

Control of Y493 phosphorylation and ZAP-70 activity

The phosphorylation of Y493 enhances ZAP-70 activity, but it has been controversial whether p-Y493 is generated by a separate kinase or by trans-phosphorylation involving two ZAP-70 molecules. We addressed this using the ZAP-70 kinase inhibitor (XXX). Compound XXX prevented pervanadate-induced phosphorylation of endogenous LAT in DP thymocytes (Fig5A; lanes 3&4). Untreated samples or the inhibitor alone did not have any effect on LAT phosphorylation (Fig5A; lanes 1&2). The inhibitor had no effect on ζ phosphorylation (data not shown).

Using OVA-loaded APCs, we found that increasing concentrations of the ZAP-70 inhibitor abrogated endogenous LAT phosphorylation with an $IC_{50} = 1.63 \pm 0.44 \text{ e}^{-6} \text{ M}$ (Fig5B). We also calculated the IC_{50} of the same inhibitor to prevent Y493 phosphorylation ($IC_{50} = 1.76 \pm 0.64 \text{ e}^{-6} \text{ M}$) (Fig5C). The two IC_{50} values are almost identical ($p = 0.78$) indicating that phosphorylation of Y493 is dependent on ZAP-70 kinase activity. The data are also consistent with the idea that enhanced ZAP-70 kinase activity in DP thymocytes is dependent on Y493 phosphorylation (81). However, even at the highest concentrations of the ZAP-70 kinase inhibitor there is a residual background of Y493 phosphorylation. It has been suggested that other kinases initiate Y493 phosphorylation on a few

molecules and that ZAP-70 trans-phosphorylation propagates and sustains Y493 phosphorylation (79).

As a specificity control we tested whether compound XXX could inhibit Y319 phosphorylation or ZAP-70 recruitment to the TCR (Fig5D and 5E). Even in the presence of high inhibitor concentrations, ZAP-70 was recruited to the TCR and its regulatory Y319 was phosphorylated. These results suggest that ZAP-70 association to activated TCR complexes and its phosphorylation at Y319 does not require ZAP-70 kinase activity. Moreover these data confirm previous results that Y319 phosphorylation is not mediated by ZAP-70 trans-phosphorylation but by another kinase(s), most likely Lck (79).

To investigate the inhibition of Y493 phosphorylation in the synapse, we analyzed Q4R7-stimulated DP thymocytes by microscopy (Fig5F). As described in figure 1, Q4R7 induces strong ZAP-70 recruitment and Y319/Y493 phosphorylation. In the presence of 1 μ M ZAP-70 kinase inhibitor, a concentration slightly less than the IC_{50} of ZAP-70 kinase inhibition ($IC_{50} = 1.63 \pm 0.44 \text{ e-}6 \text{ M}$), Y493 phosphorylation was markedly reduced. $38.3 \pm 8.8 \%$ of all cells stimulated by Q4R7-loaded APCs showed a ≥ 2 -fold reduction of Y493 phosphorylation (3 independent experiments; $n = 47$ cell conjugates analyzed). In contrast, ZAP-70 recruitment to the synapse and its phosphorylation at Y319 remained intact in virtually all thymocyte-APC conjugates examined. These results confirm the co-immunoprecipitation experiments in figures 5B-E.

TCR/ZAP-70 ratio in positive and negative selection

Following TCR engagement, CD3 ϵ and ζ contain various phospho-ITAMs that promote SH2-mediated ZAP-70 binding with different affinities (71). We wondered whether this multiplicity of potential ZAP-70 binding sites is reflected in the ratio of ZAP-70 molecules per TCR complex under different selection conditions. Using microscopy, we examined the recruitment of the TCR and ZAP-70 into the synapse in response to positive and negative selecting ligands (Fig6A). Surprisingly, the relative recruitment of TCR and ZAP-70 into the synapse was similar with both kinds of ligands. This was further confirmed by the integrated (total) recruitment of TCR and ZAP-70 over the whole time-course of the experiment (Fig6B). This result points towards a selection mechanism where the increased number of ZAP-70 molecules in the synapse is the consequence of increased TCR recruitment. However, since microscopy cannot distinguish between a scenario where TCR and ZAP-70 are simply co-localized in the synapse or whether there is a (SH2-mediated) molecular association, we assessed the ratio between the two molecules by co-immunoprecipitation.

Immunoprecipitation of all TCR complexes from OT-I DP thymocytes stimulated with peptide-loaded APCs revealed that the relative amount of TCR associated ZAP-70 correlated with the thymic selection potential of the presented peptide; the strong and weak negative selectors OVA and Q4R7, respectively, induced higher levels of TCR-associated ZAP-70 than the positive selector Q4H7 (Fig6C; left panel). This raised the question whether the increased ZAP-70 association to the TCR

under negative selection conditions is due to an increased ZAP-70 / TCR ratio or due to increased levels of activated TCRs that are each associated with the same number of ZAP-70 molecules. Therefore, we immunoprecipitated ZAP-70 from stimulated OT-I thymocytes and probed for the TCR/CD3 component, ζ . The level of TCR associated to ZAP-70 was clearly higher in response to the negative-selecting ligands OVA and Q4R7 compared to the positive selector Q4H7 (Fig6C; right panel). These data argue against the idea that negative selecting ligands increase the number of ZAP-70 molecules to each triggered TCR; instead these data support the hypothesis that negative selecting ligands actually increase the number of actively signaling TCRs. We also calculated the relative ZAP-70 / TCR ratio in the synapse from the values obtained in figure 6A. Indeed, the ratio remained constant for all peptides at all time points, independent of their selection properties (Fig6D).

Taken together, these experiments suggest, that in the synapses of DP thymocytes with APCs, elevated ZAP-70 levels induced by negative selection are not due to an increased relative ZAP-70 recruitment per triggered TCR, but rather to an increase in the number of TCRs that recruit ZAP-70. For both positive and negative selecting ligands, the relative ZAP-70 / TCR ratio remains constant.

3.2.5 Discussion

ZAP-70 is differentially recruited to synapses in DP thymocytes presented with ligands of varying selection capability. By fluorescence microscopy we observed a strong and transient ZAP-70 recruitment to the synapse in OT-I DP thymocytes responding to negative-selecting peptides. (7) (Fig. 1). In contrast, ZAP-70 recruitment was substantially weaker and delayed in response to a positive-selecting ligand with an affinity only slightly below the selection threshold. Activation of ZAP-70 in the synapse was characterized by phosphorylation of the regulatory tyrosine residue Y319 in the interdomain B (78, 79) and the tyrosine residue Y493 in the activation loop of the kinase domain (81, 83). Phosphorylation at both residues was quickly induced upon stimulation with negative-selecting ligands, whereas it was clearly reduced in response to a positive-selector. No phosphorylation was detected when DP thymocytes were stimulated with a non-cognate ligand for the OT-I receptor. These microscopy results were confirmed by co-immunoprecipitation experiments, examining ZAP-70's association to the CD3 complex and its phosphorylation state (Fig. 2). Moreover, this Western analysis revealed a low amount of TCR-associated ZAP-70 even under non-stimulatory conditions, similar to resting DP cells (data not shown). These results confirm a previous study describing a constitutive association between ZAP-70 and phosphorylated ζ in absence of TCR ligation (66).

The peptide ligands Q4R7 and Q4H7 used in this study represent the weakest negative and the strongest positive selector in the OT-I system, with similar binding affinities as measured by pMHC tetramers (108). However, the increased recruitment and phosphorylation of ZAP-70 by ligands above the selection threshold suggests that efficient ZAP-70 phosphorylation is a hallmark of negative selection whereas weak and delayed ZAP-70 phosphorylation characterizes positive selection.

ZAP-70 kinase activity was determined using in an *in vitro* kinase assay and compared to results obtained by microscopy and Western blot. Phosphorylation of a recombinant substrate (LAT) could be specifically attributed to ZAP-70 enzymatic activity in the assay since a specific ZAP-70 inhibitor abrogated phosphorylation of exogenously added LAT. In response to the negative selecting ligands OVA and Q4R7, ZAP-70 kinase activity was again quickly induced and diminished over the time course of the experiment (Fig. 3). The positive selector Q4H7 induced a ZAP-70 kinase activity that was only slightly above that observed in presence of the non-cognate ligand, VSV. Integrated over the initial phase (10min) or the whole time-course of the experiment (60min), negative selectors (compared to positive selectors) increased ZAP-70 kinase by 2.4- and 2.6-fold, respectively. However, despite the fact that OVA displays a > 10-fold higher affinity for the OT-I TCR than the weak negative selector Q4R7, ZAP-70 kinase activity was not increased in proportion to ligand affinity. Taken together, these results argue that positive selectors, over a wide range of affinities

that are below the selection threshold induce a similar level of ZAP-70 kinase activity. PMHC ligands with affinities just above the selection threshold induce a discretely elevated (2-3 fold) of ZAP-70 kinase activity, which is a hallmark of negative selection signaling.

ZAP-70 mediated phosphorylation of endogenous LAT was investigated using a specific kinase inhibitor (compound XXX). Our experiments confirm that LAT is primarily phosphorylated by ZAP-70 and not by other PTKs (90), since endogenous LAT phosphorylation was almost entirely prevented at high inhibitor concentrations. Additionally, compound XXX substantially inhibits Y493 phosphorylation, implying that phosphorylation of this tyrosine residue is mediated by ZAP-70 itself (i.e. by trans-phosphorylation). The IC₅₀ values for the inhibition of LAT phosphorylation and ZAP-70 Y493 phosphorylation are similar ($p = 0.78$), indicating that ZAP-70 kinase activity mediates both reactions. The importance of tyrosine 493 phosphorylation to induce ZAP-70 kinase activation has been demonstrated previously by point mutations in this residue that abrogate ZAP-70 kinase activity (80, 81). Although these results clearly depend on the specificity of the inhibitor, ZAP-70 is the only known Syk kinase in DP thymocytes.

In contrast, phosphorylation at Y319 in the regulatory domain of ZAP-70 was not affected by inhibiting ZAP-70 kinase activity, which argues that this residue is a phosphorylation target of other PTKs, such as Lck. Indeed, overexpression studies have shown that phosphorylation at Y319 was only achieved upon cotransfection with Lck (82) and Y319 was also identified as binding site for Lck (79). Microscopy studies revealed that inhibition of Y493 phosphorylation was specifically mediated in the synapse. Similar to the biochemical data, the ZAP-70 inhibitor affected neither ZAP-70 recruitment to the synapse nor ZAP-70 phosphorylation at Y319.

In ZAP-70 knockout mice, thymocytes are arrested in their development at the DP stage and fail to become positively selected (64). Negative selection was also impaired since peptide antigens fail to delete these cells. Given that ZAP-70 is a likely branch point for thymic selection signaling, we wondered whether we could influence the selection outcome by modulating ZAP-70 kinase activity. In FTOC, partial inhibition of ZAP-70 kinase activity converted negative selection into positive selection. This supports the idea that negative selection signaling requires a ~ 2 -fold increase in ZAP-70 activity in the immunological synapse.

The increase in ZAP-70 kinase activity in negative selection might be related to a different molecular ratio of ZAP-70 / TCR in the synapse. Previous studies have identified partially phosphorylated ζ -chains in response to antagonist ligands (72), which may provide a mechanism to alter the number of associated ZAP-70 molecules per TCR complex. ZAP-70 binds to doubly phosphorylated ITAMs using both of its SH2-domains (70) and has varying binding affinities for the individual ζ and CD3 ϵ ITAMs (71). It's conceivable that this contributes to an elevated ZAP-70 / TCR ratio during negative selection. However, microscopy experiments indicate that TCR and ZAP-70 are proportionally recruited into the immunological synapse by both positive and negative selecting ligands. Negative selection does not increase the relative ratio of ZAP-70 / TCR (Fig. 6). This finding was further

supported by co-immunoprecipitations of the TCR complex and ZAP-70 from APC-stimulated DP thymocytes. As expected, TCR-associated ZAP-70 was increased in response to the negative-selecting ligands. However, a pulldown of ZAP-70 and subsequent probing for TCR revealed that an increased amount of TCR is associated with ZAP-70 in lysates of DP thymocytes that had been stimulated with negative selecting ligands. Therefore, we postulate a model of negative selection signaling where increased TCR recruitment into the synapse drives a proportional increase in ZAP-70 recruitment. Previous studies have shown that in the synapse, coreceptor-associated Lck phosphorylates ζ ITAMs based on the TCR-coreceptor interaction (107). Negative-selecting ligands quickly induce close coreceptor approximation and exhibit strong ζ phosphorylation whereas positive-selecting ligands promote looser coreceptor association and therefore reduced ζ phosphorylation. We speculate that coreceptor-associated Lck may strongly phosphorylate the regulatory Y319 of TCR-associated ZAP-70 under negative selection conditions. Subsequently, ZAP-70 would be released from autoinhibition and trans-phosphorylate other ZAP-70 molecules at Y493 in the activation loop of the kinase domain. The higher density of ZAP-70 molecules in the synapse facilitates this process. In contrast, with positive selecting ligands the lower ZAP-70 recruitment and kinase activity in the synapse is the consequence of lower TCR recruitment. , Since the concentration of ZAP-70 molecules in the synapse is low, Y319 and subsequent Y493 phosphorylation fails to promote sufficient ZAP-70 kinase activity in the synapse to induce negative selection signaling. Therefore, our data indicate that a 2-fold elevation of ZAP-70 kinase activity, which occurs at the selection affinity threshold is a critical parameter of negative selection signaling.

3.2.6 Figures

Fig1

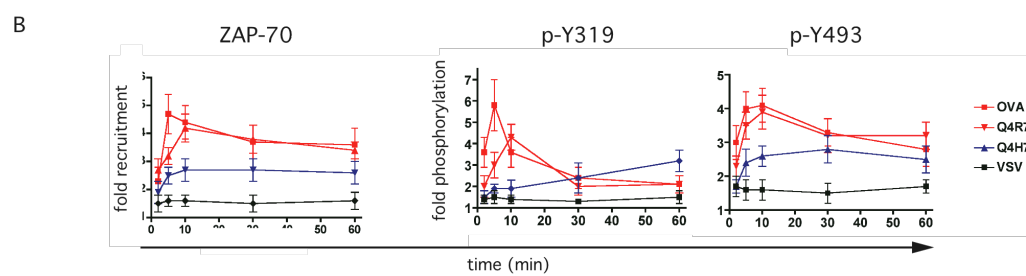
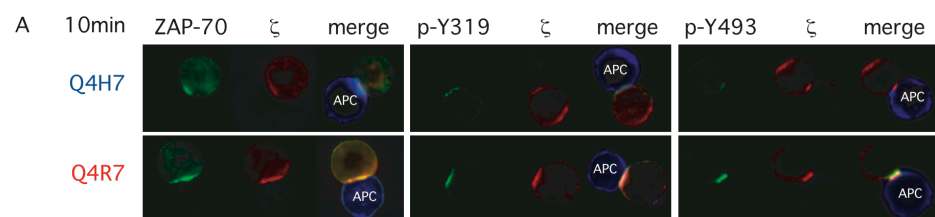


Fig2

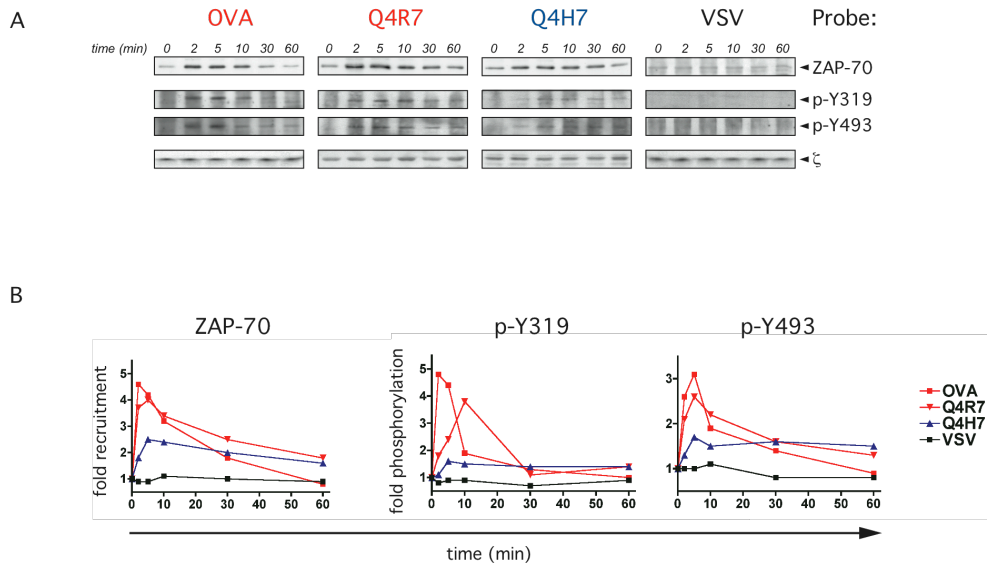


Fig3

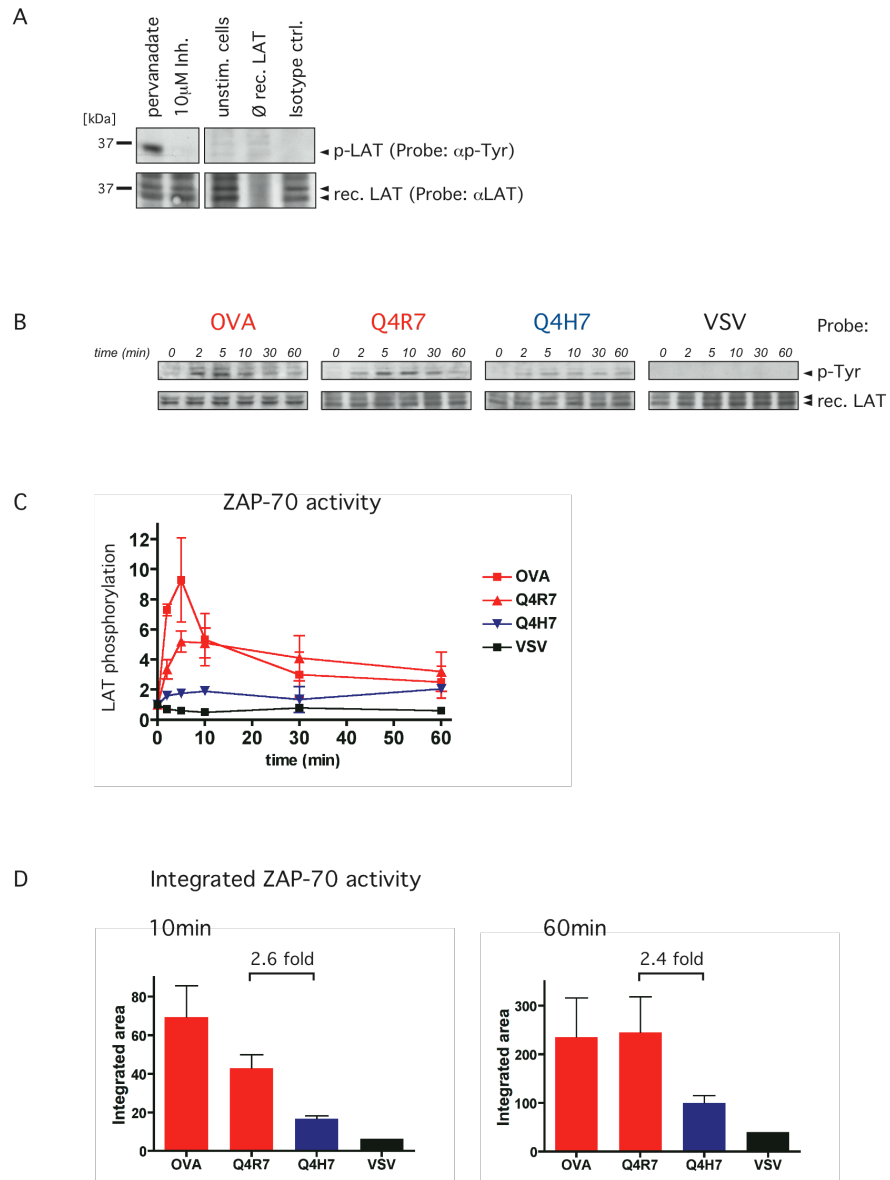


Fig4

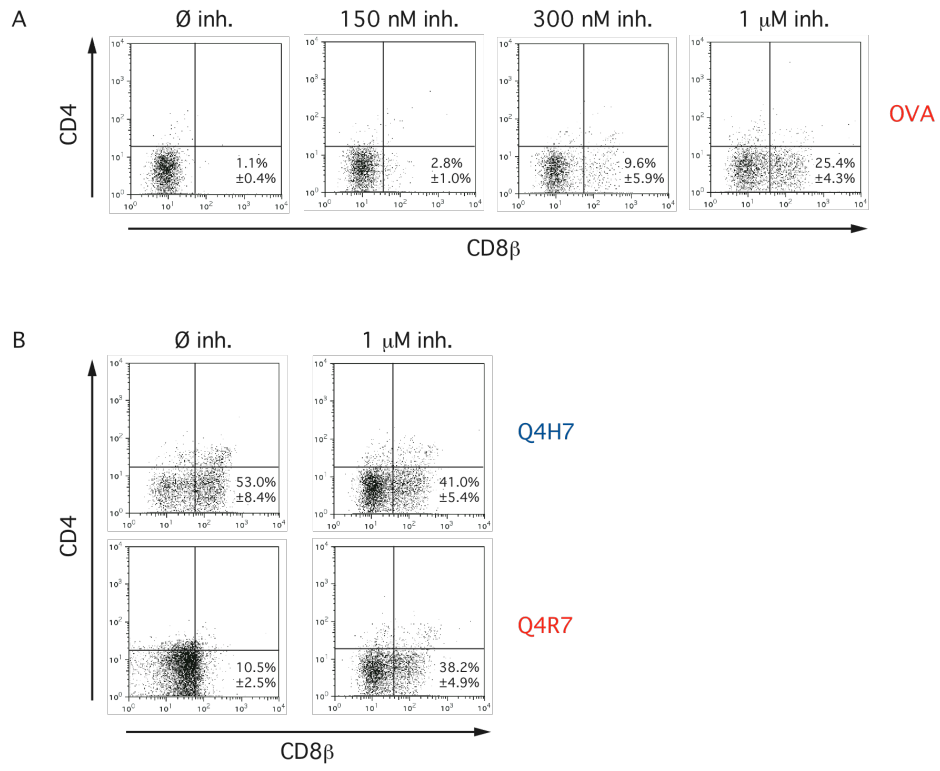


Fig5

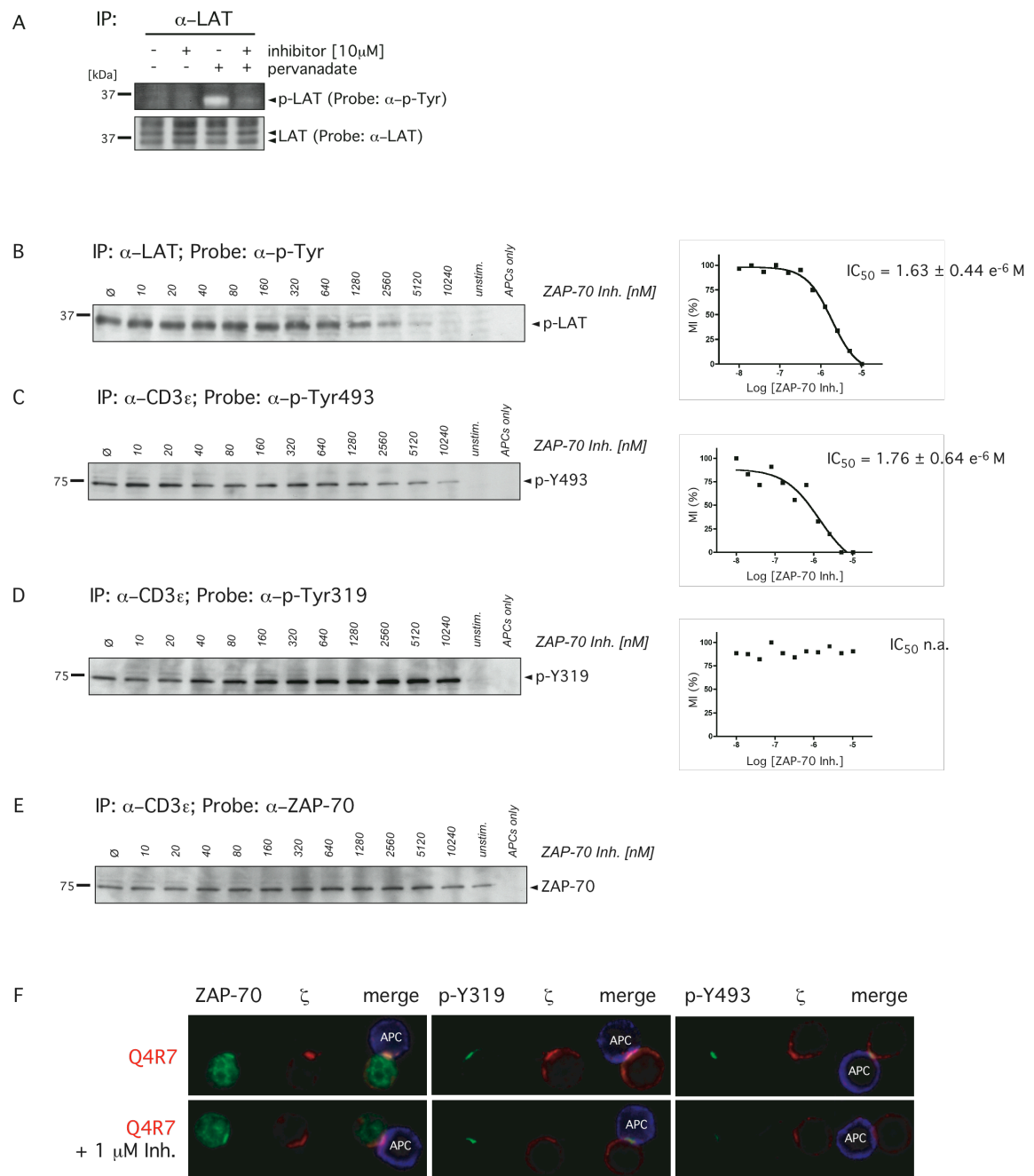
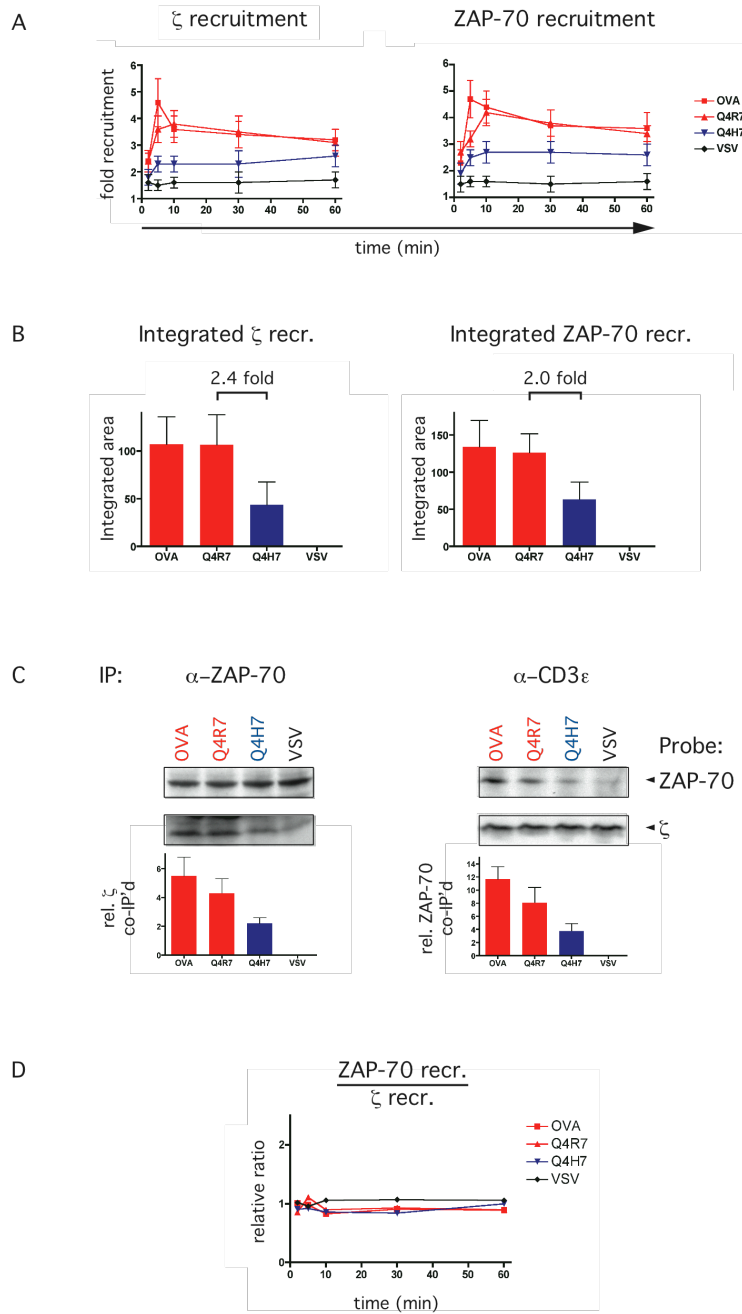


Fig6



3.2.7 Figure Legends

Fig1. ZAP-70 recruitment and phosphorylation at the synapse

A, OT-I Rag^{-/-} β2m^{-/-} DP thymocytes were stimulated with peptide-loaded APCs for 10min. Cells were stained with monoclonal antibodies against ζ (red), ZAP-70 (green) or phosphorylated ZAP-70 species (green) and subjected to fluorescence microscopy analysis. Q4H7 (positive selector) stimulations are shown in the upper panel and Q4R7 (negative selector) stimulations in the lower panel. Enriched B-cells from C57 Bl/6 spleens (blue) were used as APCs.

B, Time-course of ZAP-70 recruitment and phosphorylation at the synapse. APC-stimulated thymocytes were imaged by fluorescence microscopy (as in A) at indicated time points. Calculated ratios (as described in materials and methods) are plotted as 'fold recruitment' (ZAP-70) or 'fold phosphorylation' (p-Y319 or p-Y493). For OVA, Q4R7 and Q4H7, n≥20 cell conjugates were analyzed and for VSV n≥10.

Fig2. Biochemical analysis of ZAP-70 recruitment and phosphorylation

A, Immunoprecipitation of TCR complexes from OT-I Rag^{-/-} β2m^{-/-} DP thymocytes stimulated with peptide-loaded APCs. At indicated time points, TCR complexes were immunoprecipitated and subjected to Western blot analysis. Co-immunoprecipitated ZAP-70 was probed with monoclonal antibodies against ZAP-70 (first row), p-Y319 (second row) or p-Y493 (third row). Membranes were stripped and re-probed for ζ (third row) as loading control. Representative Western blots are shown from several experiments performed for each peptide (n=3 for OVA, Q4R7 and Q4H7; n=2 for VSV).

B, Graphical evaluation of ZAP-70 recruitment and phosphorylation. Western blots as described in A were quantified by densitometry. All values were normalized to 0 min and to ζ.

Fig3. ZAP-70 activity with positive and negative selecting ligands

A, *In vitro* kinase assay to assess ZAP-70 activity. Thymocytes from C57 Bl/6 mice were tested for ZAP-70-mediated phosphorylation of an exogenously added kinase substrate (recombinant LAT). Pervanadate-induced ZAP-70 kinase activity was abolished by 10 μ M specific inhibitor (lanes 1&2). LAT phosphorylation was probed with a monoclonal antibody against phosphotyrosine (upper row) and verified by probing with an anti-LAT mAb (lower row). Unstimulated cells fail to induce detectable LAT phosphorylation (lane 3). Experimental conditions do not co-immunoprecipitate endogenous LAT (lane 4). Immunoprecipitation with isotype control antibody (lane 5).

B, ZAP-70 kinase activity in stimulated DP thymocytes. OT-I Rag^{-/-} β 2m^{-/-} DP thymocytes were stimulated with peptide-loaded APCs for indicated time points and TCR/CD3/ZAP-70 complexes were immunoprecipitated with anti-CD3 ϵ . Following *in vitro* kinase assay and Western blot analysis, phosphorylation of recombinant LAT was probed with anti-phosphotyrosine (upper row) and confirmed with anti-LAT (lower row). Representative Western blots are shown from several experiments performed for each peptide (n=3 for OVA, Q4R7 and Q4H7; n=2 for VSV).

C, Graphical evaluation of ZAP-70 kinase activity. Western blots as described in A were quantified by densitometry. All values were normalized to ZAP-70 kinase activity at 0 min.

D, Integrated ZAP-70 activity. ZAP-70 activity as plotted in C was assessed over the first 10 min of stimulation (left panel) or over the entire time-course (60min, right panel). Areas under the curves were calculated manually.

Fig4. ZAP-70 inhibition converts negative into positive selection

A, Dose dependent effect of ZAP-70 kinase activity in thymic selection. Thymic lobes from OT-I Rag^{-/-}β2m^{-/-} mice at gestational day 15.5 were incubated with 0.2 μM OVA in presence or absence of 100 nM, 300nM or 1 μM ZAP-70 kinase inhibitor. After 7 days of culture, thymocytes were stained with fluorescently labeled antibodies against TCRβ, CD4 and CD8β and subjected to flow cytometry analysis. The percentage of TCRβ-positive, CD8αβ SP cells were determined using the FlowJo software.

B, ZAP-70 kinase inhibition at the negative selection threshold. FTOCs were incubated with 2 μM negative-selecting Q4R7 or 20 μM positive selecting Q4H7 in presence or absence of 1 μM ZAP-70 kinase inhibitor. Thymocytes were processed and analyzed as in A.

Fig5. ZAP-70 activity correlates with Y493 phosphorylation

A, The ZAP-70 kinase inhibitor XXX abrogates endogenous LAT phosphorylation. LAT was immunoprecipitated with an anti-LAT mAb from unstimulated or pervanadate-induced thymocytes from C57 Bl/6 mice and analyzed by Western blot. Pervanadate-induced ZAP-70 activity could be inhibited by 10 μ M XXX. LAT phosphorylation was detected by probing with an anti-phosphotyrosine mAb (upper panel) and verified by probing with an anti-LAT mAb (lower panel).

B, Inhibition of endogenous LAT phosphorylation. OT-I Rag^{-/-} β 2m^{-/-} DP thymocytes were stimulated for 5min with OVA-loaded APCs in presence of titrating ZAP-70 inhibitor concentrations. Immunoprecipitation and Western blot analysis was performed as in A. Phospho-LAT bands were quantified by densitometry, normalized to non-inhibited phospho-LAT and subjected to non-linear regression analysis. The half-maximal inhibition concentration (IC₅₀) was calculated using the Prism software.

C, D, E ZAP-70 phosphorylation in presence of increasing inhibitor concentrations. Cells were stimulated as in B. Co-immunoprecipitation of TCR/CD3/ZAP-70 complexes was performed with anti-CD3 ϵ mAb. Western blots were probed with either anti-p-Y493 mAb (C), anti-p-Y319 mAb (D) or anti-ZAP-70 mAb (E). Determination of IC₅₀ values from corresponding signals was performed as in B. All values were normalized to ZAP-70 recruitment obtained from E.

F, Inhibition of Y493 phosphorylation in the synapse. OT-I Rag^{-/-} β 2m^{-/-} DP thymocytes were stimulated for 10min with Q4R7-loaded APCs either in presence or absence of 1 μ M ZAP-70 kinase inhibitor. Cells were stained and analyzed as in figure 1A. 38.3 ± 8.8 % of the DP thymocytes showed \leq 2-fold reduction of p-Y493 phosphorylation compared to non-inhibited cells (n = 47; 3 independent experiments).

Fig6. Relative ZAP-70 / TCR ratio in positive and negative selection

A, ζ and ZAP-70 recruitment to the synapse. OT-I Rag^{-/-} β 2m^{-/-} DP thymocytes were stimulated, stained and analyzed by microscopy as in figure 1.

B, Integrated ζ and ZAP-70 recruitment to the synapse. ζ and ZAP-70 recruitment as plotted in A was assessed over the entire time-course. Areas under the curves were calculated manually.

C, ZAP-70 to TCR association by co-immunoprecipitation. OT-I Rag^{-/-} β 2m^{-/-} DP thymocytes were stimulated for 10min with APCs loaded with OVA, Q4R7, Q4H7 or VSV. Co-immunoprecipitations performed with either CD3 ϵ (left panel) or ZAP-70 (right panel) were probed with anti-ZAP-70 mAb (upper row) or anti- ζ mAb (lower row). Signals were quantified by densitometry, normalized to the corresponding loading control and VSV. Values are indicated below the blots. One representative experiment is shown of several performed.

D, Relative ZAP-70 / ζ ratio in the synapse. Values obtained from the relative recruitment of ZAP-70 to the synapse (A) were normalized to ζ recruitment.

4. Discussion

4.1 A zipper model for TCR-CD8 interactions

During thymic selection, TCR affinities become restricted to a window of moderate affinities for all self-ligands expressed in the thymus, thus generating a repertoire with potentially high TCR affinities for antigen to be encountered in the periphery. Therefore, the TCR is required to distinguish between different binding affinities for p-MHC ligands using a mechanism that ensures a correct readout of the receptor affinity for self-antigens expressed in the thymus. A known protein to influence TCR-pMHC interaction is the CD4 or CD8 co-receptor. Therefore, we examined the interaction of CD8 with the TCR in response to peptide ligands with defined biological properties. Negative-selecting peptides induced a strong and sustained TCR/CD8 association in the immunological synapse as measured by FRET microscopy (37, 99). At the threshold of thymic selection, the weakest negative selector still generated relatively strong TCR/CD8 association, whereas the strongest positive selector induced substantially weaker and delayed association of CD8 with the TCR. A non-cognate ligand failed to induce any detectable TCR/CD8 association, demonstrating that in absence of specific TCR recruitment there is no detectable steady state interaction between the two molecules. Remarkably, TCR/CD8 interaction was proportionally translated into ζ phosphorylation, which is most likely mediated via the Src kinase Lck associated with the C-terminus of the co-receptor (26, 30, 112). These results indicate that p-MHC ligands of different selection potential substantially differ in their ability to recruit CD8 and thereby, Lck, to the TCR complex.

A conserved stretch of 8 amino acids in the constant region of the TCR α -chain, referred to as the α -CPM is involved in positive selection and cooperation with the CD8 co-receptor (3, 32). We wondered whether the defect in thymic selection displayed by α -CPM mutant thymocytes is based on impaired TCR/CD8 association. FRET microscopy revealed that TCR/CD8 interaction in the synapse was reduced in response to negative selecting ligands. However, positive selecting ligands completely abrogated close approximation of the co-receptor to the TCR complex and therefore, ζ phosphorylation. We suggest that the α -CPM functions to recruit the co-receptor into the TCR complex to allow efficient signal initiation. Interestingly, thymocytes from CD3 δ deficient mice are also defective in positive selection (113). The CD3 $\delta\epsilon$ heterodimer is located on the α -chain side of the TCR (Figure 2), implying a role for CD3 δ in ligand driven association of the TCR and co-receptor molecules. Indeed, such a model has been suggested previously (35).

We hypothesize that the trimeric complex consisting of the TCR, the p-MHC ligand and the CD8 co-receptor may function as a zipper (Figure 6). By binding to the same p-MHC molecule (19), the apposition of the TCR and CD8 continues towards the plasma membrane similar to the

approximation of two sides of a zipper. Complete zipping only occurs in presence of an intact α -CPM, which mediates tight association of the trans-membrane and cytoplasmic regions of the two molecules. In absence of the α -CPM, the ζ and CD3 ITAMs are only inefficiently phosphorylated since coreceptor-associated Lck fails to fully access the TCR complex (Figure 6). Hence, the α -CPM, together with CD3 δ , mediates positive selection by ensuring close approximation of the co-receptor and therefore, efficient signaling initiation. The α -CPM may have an equivalent function for the CD4 co-receptor, because a class II MHC restricted α -CPM mutant TCR also fails to generate positive selection signals (3).

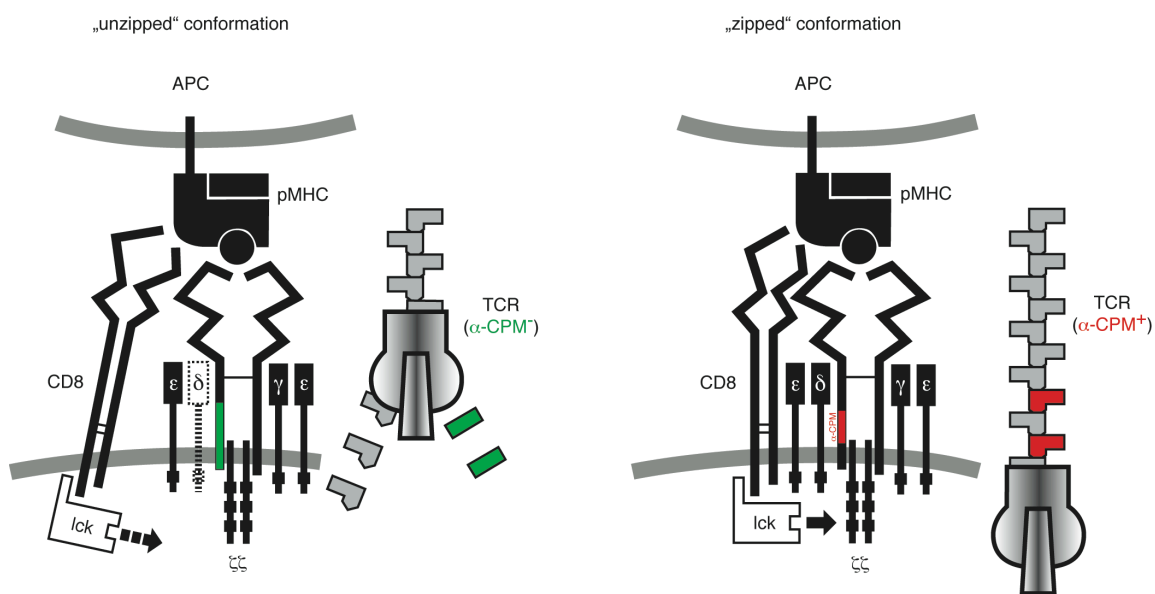


Figure 6. The zipper model of TCR/CD8 approximation (adapted from (4)). In analogy to a zipper, an α -CPM deficient TCR (green) binds to the MHC but fails to engage with the TCR at the level of the trans-membrane and cytoplasmic domains (left panel). Consequently, the ITAMs of the CD3 complex are inadequately phosphorylated by the co-receptor associated tyrosine kinase Lck. Therefore, the α -CPM functions as tooth to ensure efficient zipping in the direction of the plasma membrane. Only an intact α -CPM (red) mediates tight CD8 association to the TCR (most likely via CD3 δ) and closure of the zipper (right panel). The “fully zipped” conformation allows efficient ITAM phosphorylation by Lck.

High-affinity p-MHC ligands exhibit a certain independence of the co-receptor. An agonist peptide (OVA) can induce negative selection in fetal thymic organ cultures in absence of the co-receptor (in OT-I transgenic, CD8-deficient mice; (114)). The binding affinity of agonist ligands for the TCR is characterized by low dissociation constants (K_D) (115, 116). Hence, the time that an agonist engages the TCR is long and may last for several seconds. During this time, stochastic phosphorylation of the ζ and CD3 ITAMs by ‘free’ Lck may compensate for the specific phosphorylation mediated by co-

receptor-associated Lck. On the other hand, antagonist ligands exhibit higher K_D 's, which narrows the time window for ITAM phosphorylation. If the co-receptor is not present to appropriately guide Lck into the TCR/CD3 complex, ζ and CD3 ITAMs will not become phosphorylated. At the same time, 'free' Lck (i.e. not linked to the co-receptor) may not have enough time to diffuse into the CD3 complex when stimulated by low-affinity ligands. Such a mechanism potentially explains why positive selection is highly dependent on the co-receptor.

CD8 binding to class I molecules is characterized by a low affinity ($K_D \sim 100\mu\text{M}$) (117). CD4 has an even lower affinity for class II ($K_D > 100\mu\text{M}$) (118). Nevertheless, CD8 and CD4 have been described to promote cell adhesion (15, 119). In accordance with this, we observe CD8 co-receptor recruitment to the interface with APCs presenting a non-cognate (null) ligand for the TCR, similar to a previous study (37). CD8 is expressed at high levels in a DP thymocyte (much higher than the TCR) and therefore, binding to class I molecules in a cooperative way may partly compensate for its low affinity. Presumably, TCR-independent recruitment of the co-receptor to the synapse is a physiological process, mediated by high levels of class I molecules expressed on thymic epithelial cells. However, to efficiently induce signaling, the TCR is required to tightly and rapidly associate with the co-receptor. Another study suggests that the kinetics of TCR/CD8 interaction induces phospho-ERK in the synapse rapidly in response to high-affinity ligands whereas low-affinity ligands exhibit delayed ERK phosphorylation (120). Thus, CD8 ensures that the TCR can specifically distinguish between structurally very similar peptide ligands through the kinetics of CD8 association to the TCR, thereby translating TCR/p-MHC affinity into a cellular signal.

One apparent discrepancy in the zipper model comes from the fact that Lck associates only with 2% of surface CD8 (and with 25% – 50% of surface CD4) (121, 122), yet we postulate rapid and sustained TCR/CD8 association and ITAM phosphorylation in response to high-affinity ligands (and somewhat delayed kinetics in response to low-affinity ligands), which could turn signaling initiation into a rather inefficient process. However, since the TCR affinity for p-MHC is generally higher (K_D 's in the range nM to μM (115)) than the co-receptor's affinity for MHC, the co-receptor may laterally diffuse from the trimeric complex and be replaced by another co-receptor molecule. This sampling mechanism may allow the ligand engaged TCR to eventually engage an Lck-associated co-receptor, which then phosphorylates the ζ and CD3 ITAMs. The probability of such an encounter is limited by the duration of TCR/p-MHC interaction. Thus, a more dynamic model that accounts for the fact that not all co-receptors carry Lck may modify the zipper model.

4.2 ZAP-70 in positive and negative selection

ZAP-70 kinase activity increases in a discrete (stepwise) manner precisely at the negative selection threshold. Our experiments indicate that the elevation of ZAP-70 activity increases ≥ 2 -fold in DP thymocytes stimulated with negative selecting ligands. When the recruitment of ZAP-70 to the

synapse of APC-stimulated DP OT-I thymocytes was measured by microscopy, the weakest negative-selector exhibited 2x higher levels of ZAP-70 in the synapse compared to the strongest positive selector. Similar results were found for ZAP-70 tyrosine phosphorylation at Y319 in the interdomain B and at Y493 in the kinase activation loop. This 2-fold increase at the negative selection threshold is reflected in the ZAP-70 kinase activity as demonstrated by an *in vitro* kinase assay.

Further evidence for the impact of ZAP-70 kinase activity comes from FTOC experiments, demonstrating that partial inhibition of ZAP-70 activity converts negative into partial positive selection. These results support the idea that selection outcome is controlled by the quantity (within a narrow range) of ZAP-70 kinase activity in the synapse. Therefore, we wondered whether the increased ZAP-70 kinase activity under negative selection conditions is reflected in a higher relative ratio of ZAP-70 molecules per TCR in the synapse. This idea is supported by the fact that multiple ZAP-70 binding sites exist, i.e. a total of 10 potentially phosphorylatable ITAMs among ζ_2 and the CD3 molecules. Indeed, ZAP-70 using its two SH2-domains has a measurable affinity for the doubly phosphorylated ITAMs of ζ and CD3 ϵ , although there are substantial differences in binding affinity for the individual phospho-ITAMs (71). Another study shows that reducing the total number of ITAMs from 10 to below 3 induces a multiorgan autoimmune disease due to a breakdown in central tolerance, suggesting that the multiplicity of ITAMs propagates a quantitative rather than a qualitative signal from the TCR across the plasma membrane (106). Since the TCR signal is read out by ZAP-70, the lack of multiple phospho-ITAMs and therefore, ZAP-70 binding sites, may account for this defect in thymic selection. Therefore, cells that would have been negatively selected become positively selected due to the fact that the relative ZAP-70 / TCR ratio cannot change in these mutant mice.

However, in our experiments we did not observe a change in the ratio of ZAP-70 / TCR in DP thymocytes stimulated with either positive or negative selecting ligands. All peptides of varying selection potential used in these studies exhibited a constant ZAP-70 / TCR. Rather, we found that the number of TCRs recruited to the synapse of thymocyte-APC conjugates determined the amount of associated ZAP-70 molecules in the synapse. Clearly, the recruitment of the TCR into the synapse reflects the apparent binding affinity of the TCR-pMHC-CD8 interaction, as observed in our experiments and as previously described (4). We suggest that pMHC ligands with binding affinities above the negative selection threshold induce a ZAP-70 density in the synapse high enough to induce trans-phosphorylation of tyrosine 493 in the kinase activation loop of ZAP-70. Indeed, our experiments show that ZAP-70 itself is responsible for most of the Y493 phosphorylation, since a specific ZAP-70 kinase inhibitor almost completely abrogated Y493 phosphorylation. This demonstrates that ZAP-70 kinase activity depends on Y493 phosphorylation. On the other hand, positive selecting ligands induce phosphorylation at Y493 as well. Nevertheless, positive selectors are less efficient in recruiting the TCR to the synapse and therefore, co-associated ZAP-70 levels and kinase activity remain low.

Whether tyrosine 493 is a target of auto-phosphorylation or phosphorylated by Src kinases has been an issue of debate in the literature (80, 81, 105). We are the first to use a specific ZAP-70 kinase inhibitor, which clearly showed that Y493 is substantially reduced under inhibitory conditions. However, Y493 was not completely abrogated, suggesting that Src kinases such as Lck maybe responsible for the initial Y493 phosphorylation of a few molecules and subsequently ZAP-70 trans-phosphorylation propagates Y493 phosphorylation among all ZAP-70 molecules in the synapse. In contrast, tyrosine phosphorylation of Y319 in the regulatory interdomain B is not controlled by ZAP-70 auto-phosphorylation since our experiments showed that even at the highest ZAP-70 inhibitor concentration used, Y319 phosphorylation was not affected. Therefore, other kinases must account for Y319 phosphorylation and strong evidence has been provided that Lck has this function (78, 79, 82). Similarly, ZAP-70 recruitment to the synapse does not depend on its kinase activity, since the ZAP-70 kinase inhibitor did not abrogate ZAP-70 TCR association or synapse recruitment. Seemingly, this stands in contrast to a previous report suggesting that ZAP-70 is required for ITAM phosphorylation in DP thymocytes (76). However, the authors show that ITAM phosphorylation in these cells rather depends on the presence of ZAP-70 as adaptor for Lck than on ZAP-70 kinase activity. Therefore, ZAP-70 is most probably recruited to the TCR complex independent of its kinase activity but might have a role in promoting Lck-mediated ITAM phosphorylation. Our zipper model suggests that the critical parameter to recruit Lck to the ITAMs of the CD3 complex is the co-receptor, especially in DP thymocytes where the levels of Lck are limiting. Nevertheless, Lck might bind via its SH2-domain to tyrosine-phosphorylated ZAP-70 (i.e. at p-Y319 (79)) and thereby prolong its association with the CD3 complex to support ITAM phosphorylation. Taken together, we suggest that the precise level of ZAP-70 kinase activity establishes the outcome of thymic selection, which seems to be primarily determined by the amount of TCR recruited into the immunological synapse.

5. References

1. Kreslavsky, T., A. I. Garbe, A. Krueger, and H. von Boehmer. 2008. T cell receptor-instructed alpha-beta versus gamma-delta lineage commitment revealed by single-cell analysis. *J. Exp. Med.* 205:1173-1186.
 2. Kang, J., A. Vokmann, and D. H. Raulet. 2001. Evidence that gamma-delta versus alpha-beta T cell fate determination is initiated independently of T cell receptor signaling. *J. Exp. Med.* 193:689-698.
 3. Baeckstroem, B. T., Mueller, U., Hausmann, B., and Palmer, E. 1998. Positive selection through a motif in the ab T cell receptor. *Science* 281:835-838.
 4. Mallaun, M., Naeher, D., Daniels, M.A., Yachi, P.P., Hausmann, B., Luescher, I.F., Gascoigne, N.R.J., and Palmer, E. 2008. The TCR's alpha-CPM promotes close approximation of the CD8 co-receptor allowing efficient signal initiation. *J. Immunol.*
 5. Liston, A., S. Lesage, J. Wilson, L. Peltonen, and C. C. Goodnow. 2003. Aire regulates negative selection of organ-specific T cells. *Nat Immunol.* 4:350-354.
 6. Anderson, M. S., E. S. Venanzi, Z. Chen, S. P. Berzins, C. Benoist, and D. Mathis. 2005. The cellular mechanism of Aire control of T cell tolerance. *Immunity* 23:227-239.
 7. Naeher, D., Daniels, M.A., Hausmann, B., Guillaume, P., Luescher, I., and Palmer, E. 2007. A constant affinity threshold for T cell tolerance. *J. Exp. Med.* 204:2553-2559.
 8. Daniels, M. A., Teixeira, E., Gill, J., Hausmann, B., Roubaty, D., Holmberg, K., Werlen, G., Hollaender, G.A., Gascoigne, N.R.J., and Palmer, E. 2006. Thymic selection threshold defined by compartmentalization of Ras/MAPK signalling. *Nature* 444:724-729.
 9. Singer, A., S. Adoro, and J. H. Park. 2008. Lineage fate and intense debate: myths, models and mechanisms of CD4- versus CD8 lineage choice. *Nat Rev Immunol.* 8:788-801.
 10. Davis, M. M., Boniface, J.J., Reich, Z., Lyons, D., Hampl, J., Aren, B., and Chien, Y. 1998. Ligand Recognition by alpha beta T Cell Receptors. *Annu. Rev. Immunol.* 16:523-544.
 11. van der Merwe, P. A., and Davis, S.J. 2003. Molecular Interactions Mediating T Cell Antigen Recognition. *Annu. Rev. Immunol.* 21:26.
 12. Kuhns, M. S., M. M. Davis, and K. C. Garcia. 2006. Deconstructing the form and function of the TCR/CD3 complex. *Immunity* 24:133-139.
 13. Marrack, P., J. Scott-Browne, S. Dai, L. Gapin, and J. W. Kappler. 2008. Evolutionarily conserved amino acids that control TCR-MHC interaction. *Annu. Rev. Immunol.* 26:171-203.
 14. Koenig, R., Huang, L.Y., and Germain, R.N. 1992. MHC class II interaction with CD4 mediated by a region analogous to the MHC class I binding site for CD8. *Nature* 356:796-798.
 15. Norment, A. M., Salter, R.D., Parham, P., Engelhard, V.H., and Littman, V.H. 1988. Cell-cell adhesion mediated by CD8 and MHC class I molecules. *Nature* 336:79-81.
-

-
16. Salter, R. D., Benjamin, H., Wesley, P.K., Buxton, S.E., Garrett, T.P.J., Clayberger, C., Krensky, A.M., Norment, A.M., Littman, D.R., and Parham, P. 1990. A binding site for the T-cell co-receptor CD8 on the alpha3 domain of HLA-A2. *Nature* 345:41-46.
 17. Cammarota, G., Schierle, A., Takacs, B., Doran, D., Knorr, R., Bannworth, W., Guardiola, J., and Sinigaglia, F. 1992. Identification of a CD4 binding site on the b2 domain of HLA-DR molecules. *Nature* 356:799-781.
 18. Huang, J., Edwards, L.J., Evavold, B.D., and Cheng, Z. 2007. Kinetics of MHC-CD8 Interaction at the T Cell Membrane. *J. Immunol.* 179:7653-7662.
 19. Gallagher, P. F., de St Groth, F., and Miller, J.F.A.P. 1989. CD4 and CD8 molecules can physically associate with the same T-cell receptor. *PNAS* 86:10044-10048.
 20. Renard, V., P. Romero, E. Vivier, B. Malissen, and I. F. Luescher. 1996. CD8beta Increases CD8 Coreceptor Function and Participation in TCR-Ligand Binding. *J. Exp. Med.* 184:2439-2444.
 21. Garcia, K. C., Degano, M., Stanfield, R.L., Brunmark, A., Jackson, M.R., Peterson, P.A., Teyton, L., and Wilson, I.A. 1996. An alpha-beta T Cell Receptor Structure at 2.5 A and its Orientation in the TCR-MHC Complex. *Science* 274:209-219.
 22. Wooldridge, L., van den Berg, H.A., Glick, M., Gostick, E., Laugel, B., Hutchinson, S.L., Milicic, A., Brenchley, J.M., Douek, D.C., Price, D.A., and Sewell, A.K. 2005. Interaction between the CD8 coreceptor and MHC class I stabilizes TCR-antigen complexes at the cell surface. *J. Biol. Chem.* 280:27491-27502.
 23. Potter, T. A., Grebe, K., Freiberg, B., and Kupfer, A. 2001. Formation of supramolecular activation clusters on fresh ex vivo CD8+ T cells after engagement of the T cell antigen receptor and CD8 by antigen-presenting cells. *PNAS* 98:12624-12629.
 24. Holler, P. D., and Kranz, D.M. 2003. Quantitative Analysis of the Contribution of TCR/pepMHC Affinity and CD8 to T Cell Activation. *Immunity* 18:155-164.
 25. Arcaro, A., Gregoire, C., Bakker, T.R., Baldi, L., Jordan, M., Goffin, L., Boucheron, N., Wurm, F., van der Merwe, P.A., Malissen, B., and Luescher, I.F. 2001. CD8beta Endows CD8 with Efficient Coreceptor Function by Coupling T Cell Receptor/CD3 to Raft-associated CD8/p56Lck Complexes. *J. Exp. Med.* 194:1485-1495.
 26. Kim, P. W., Z. J. Sun, S. C. Blacklow, G. Wagner, and M. J. Eck. 2003. A zinc clasp structure tethers Lck to T cell coreceptors CD4 and CD8. *Science* 301:1725-1728.
 27. Zamoyska, R. 1998. CD4 and CD8: modulators of T-cell receptor recognition of antigen and of immune responses? *Curr. Opin. Immunol.* 10:82-87.
 28. Trobridge, P. A., Forbush, K.A., and Levin, S.D. 2001. Positive and Negative Selection of Thymocytes Depends on Lck Interaction with the CD4 and CD8 Coreceptors. *J. Immunol.* 166:809-818.
-

29. Molina, T. J., Kishihara, K., Siderovskid, D.P., van Ewijk, W., Narendran, A., Timms, E., Wakeham, A., Paige, C.J., Hartmann, K.U., Veillette, A., Davidson, D., and Mak, T.W. 1992. Profound block in thymocyte development in mice lacking p56lck. *Nature* 357:161-165.
 30. Barber, E., J. Dasgupta, S. Schlossman, J. Trevillyan, and C. Rudd. 1989. The CD4 and CD8 antigens are coupled to a protein-tyrosine kinase (p56lck) that phosphorylates the CD3 complex. *PNAS* 86:3277-3281.
 31. Madrenas, J., Chau, L.A., Smith, J., Bluestone, J.A., and Germain, R.N. 1997. The Efficiency of CD4 Recruitment to Ligand-engaged TCR Controls the Agonist/Partial Agonist Properties of Peptide-MHC Molecule Ligands. *J. Exp. Med.* 185:219-230.
 32. Naeher, D., Luescher, I.F., and Palmer, E. 2002. A role for the a-chain connecting peptide motif in mediating TCR-CD8 cooperation. *J. Immunol.* 169:2964-2972.
 33. Baeckstroem, B. T., Milia, E., Peter, A., Jaureguiberry, B., Baldari, C.T., and Palmer, E. 1996. A motif within the T cell receptor a chain constant region connecting peptide domain controls antigen responsiveness. *Immunity* 5:437-447.
 34. Werlen, G., Hausmann, B., and Palmer, E. 2000. A motif in the ab T-cell receptor controls positive selection by modulating ERK activity. *Nature* 406:422-426.
 35. Doucey, M. A., Goffin, L., Naeher, D., Michielin, O., Baumgärtner, P., Guillaume, P., Palmer, E., and Luescher, I.F. 2003. CD3delta Establishes a Functional Link between the T Cell Receptor and CD8. *J. Biol. Chem.* 278:3257-3263.
 36. Zal, T., Zal, A., and Gascoigne, N.R.J. 2002. Inhibition of T cell receptor-coreceptor interactions by antagonist ligands visualized by live FRET imaging of the T-hybridoma immunological synapse. *Immunity* 16:521-535.
 37. Yachi, P. P., Ampudia, J., Gascoigne, N.R.J., and Zal, T. 2005. Nonstimulatory peptides contribute to antigen-induced CD8-T cell receptor interaction at the immunological synapse. *Nature Immunology* 6:785-792.
 38. Kersh, G. J., E. N. Kersh, D. H. Fremont, and P. M. Allen. 1998. High- and low-potency ligands with similar affinities for the TCR: the importance of kinetics in TCR signaling. *Immunity* 9:817-826.
 39. Singer, A., and R. Bosselut. 2004. CD4/CD8 coreceptors in thymocyte development, selection and lineage commitment: analysis of the VD4/CD8 lineage decision. *Adv. Immunol.* 83:91-131.
 40. Stefanova, I., B. Hemmer, M. Vergelli, R. Martin, W. E. Biddison, and R. N. Germain. 2003. TCR ligand discrimination is enforced by competing ERK positive and SHP-I negative feedback pathways. *Nat Immunol.* 4:248-254.
 41. Acuto, O., V. Di Bartolo, and F. Michel. 2008. Tailoring T-cell receptor signals by proximal negative feedback mechanisms. *Nat Rev Immunol.* 8.
-

-
42. van Oers, N. S., N. Killeen, and A. Weiss. 1994. ZAP-70 is constitutively associated with tyrosine-phosphorylated TCR zeta in murine thymocytes and lymph node T cells. *Immunity* 1:675-685.
 43. Zhang, W., R. P. Tribble, M. Zhu, S. K. Liu, C. J. McGlade, and L. E. Samelson. 2000. Association of Grb2, Gads, and Phospholipase C-g1 with Phosphorylated LAT Tyrosine Residues. *The Journal of Biological Chemistry* 275:7.
 44. June, C. H., M. C. Fletcher, J. A. Ledbetter, and L. E. Samelson. 1990. Increases in tyrosine phosphorylation are detectable before phospholipase C activation after T cell receptor stimulation. *J. Immunol.* 144:1591-1599.
 45. Houtman, J. C. D., Y. Higashimoto, N. Dimasi, S. Cho, H. Yamaguchi, B. Bowden, C. Regan, E. L. Malchiodi, R. Mariuzza, P. Schuck, E. Appella, and L. E. Samelson. 2004. Binding specificity of multiprotein signaling complexes is determined by both cooperative interactions and affinity preferences. *Biochemistry* 43:4170-4178.
 46. Love, P. E., and Shores, E.W. 2000. ITAM multiplicity and thymocyte selection: how low can you go? *Immunity* 12:591-597.
 47. Monks, C. R. F., Freiberg, B.A., Kupfer, H., Sciaky, N., and Kupfer, A. 1998. Three-dimensional segregation of supramolecular activation clusters in T cells. *Nature* 395:82-86.
 48. Grakoui, A., Bromley, S.K., Sumen, C., Davis, M.M., Shaw, A.S., Allen. P.M., and Dustin, M.L. 1999. The Immunological Synapse: A Molecular Machine Controlling T Cell Activation. *Science* 285:221-227.
 49. Huppa, J. B., and Davis, M.M. 2003. T-cell-Antigen Recognition and the Immunological Synapse. *Nature Reviews Immunology* 3:973-982.
 50. Yokosuka, T., K. Sakata-Sogawa, W. Kobayashi, M. Hiroshima, A. Hashimoto-Tane, M. Tokunaga, M. L. Dustin, and T. Saito. 2005. Newly generated T cell receptor microclusters initiate and sustain T cell activation by recruitment of Zap70 and SLP-76. *Nat. Immunol.* 6:1253-1262.
 51. Varma, R., G. Campi, T. Yokosuka, T. Saito, and M. L. Dustin. 2006. T cell receptor-proximal signals are sustained in peripheral microclusters and terminated in the central supramolecular activation cluster. *Immunity* 25:117-127.
 52. Douglass, A. D., and R. D. Vale. 2005. Single-molecule microscopy reveals plasma membrane microdomains created by protein-protein networks that exclude or trap signaling molecules in T cells. *Cell* 121:937-950.
 53. Feinerman, O., J. Veiga, J. R. Dorfman, R. N. Germain, and G. Altan-Bonnet. 2008. Variability and robustness in T cell activation from regulated heterogeneity in protein levels. *Science* 321:1081-1084.
 54. Bos, J. L. 1989. Ras oncogenes in human cancer: a review. *Cancer Res.* 49.
-

55. Cantrell, D. A. 2002. Transgenic analysis of thymocyte signal transduction. *Nat Rev Immunol.* 2:20-27.
 56. Swan, K. A., J. Alberola-Ila, J. A. Gross, M. W. Appleby, K. A. Forbush, J. F. Thomas, and R. M. Perlmutter. 1995. Involvement of p21ras distinguishes positive and negative selection in thymocytes. *EMBO J* 14.
 57. Goodwin, J. S., K. R. Drake, V. Rogers, L. Wright, and J. Lippincott-Schwartz. 2005. Depalmitoylated Ras traffics to and from the Golgi complex via a nonvesicular pathway. *J. Cell Biol.* 170:261-272.
 58. Dower, N. A., L. S. Stang, D. A. Bottorff, J. O. Ebinu, P. Dickie, H. L. Ostergaard, and J. C. Stone. 2000. RasGRP is essential for mouse thymocyte differentiation and TCR signaling. *Nat Immunol.* 4:317-321.
 59. de Castro, I., T. Bivona, M. Philips, and A. Pellicer. 2004. Ras activation in Jurkat T cells following low-grade stimulation of the T-cell receptor is specific to N-Ras and occurs only on the Golgi. *Mol. Cell. Biol.* 24.
 60. Parry, R. V., J. M. Chamnitz, K. A. Frauwirth, A. R. Lanfranco, I. Braunstein, S. V. Kobayashi, P. S. Linsley, C. B. Thompson, and J. L. Riley. 2005. CTLA-4 and PD-1 receptors inhibit T-cell activation by distinct mechanisms. *Mol. Cell. Biol.* 25:9543-9553.
 61. Li, Q. J., J. Chau, P. J. R. Ebert, G. Sylvester, H. Min, G. Liu, R. Braich, M. Manoharan, J. Soutschek, P. Skare, L. O. Klein, M. M. Davis, and C. Z. Chen. 2007. miR-181a is an intrinsic modulator of T cell sensitivity and selection. *Cell* 129:147-161.
 62. Werlen, G., B. Hausmann, D. Naeher, and E. Palmer. 2003. Signaling life and death in the thymus: timing is everything. *Science* 299:1859-1863.
 63. Chan, A. C., M. Iwashima, C. W. Turck, and A. Weiss. 1992. ZAP-70: A 70 kd protein-tyrosine kinase that associates with the TCR zeta chain. *Cell* 71:649-662.
 64. Negishi, I., N. Motoyama, K. I. Nakayama, K. Nakayama, S. Senju, S. Hatakenyama, Q. Zhang, A. C. Chan, and D. Y. Loh. 1995. Essential role for ZAP-70 in both positive and negative selection of thymocytes. *Nature* 376:435-438.
 65. LoGrasso, P. V., J. Hawkins, L. J. Frank, D. Wisniewski, and A. Marcy. 1996. Mechanism of Activation for Zap-70 catalytic activity. *PNAS* 93:12165-12170.
 66. van Oers, N. S. C., N. Killeen, and A. Weiss. 1994. ZAP-70 is constitutively associated with tyrosine-phosphorylated TCR zeta in murine thymocytes and lymph node T cells. *Immunity* 1:675-685.
 67. Madrenas, J., R. L. Wange, J. L. Wang, N. Isakov, L. E. Samelson, and R. N. Germain. 1995. Zeta phosphorylation without ZAP-70 activation induced by TCR antagonists or partial agonists. *Science* 267:515-518.
-

-
68. Plas, D. R., R. Johnson, J. T. Pingel, R. J. Matthews, M. Dalton, G. Roy, A. C. Chan, and M. L. Thomas. 1996. Direct regulation of ZAP-70 by SHP-1 in T cell antigen receptor signaling. *Science* 272:1173-1176.
 69. Brockdorff, J., S. Williams, C. Couture, and T. Mustelin. 1999. Dephosphorylation of ZAP-70 and inhibition of T cell activation by activated SHP-1. *Eur. J. Immunol.* 29:2539-2550.
 70. Wange, R. L., S. N. Malek, S. Desiderio, and L. E. Samelson. 1993. Tandem SH2 domains of ZAP-70 bind to T cell antigen receptor zeta and CD3 epsilon from activated Jurkat T cells. *J. Biol. Chem.* 268:19797-19801.
 71. Isakov, N., R. L. Wange, W. H. Burgess, J. D. Watts, R. Aebersold, and L. E. Samelson. 1995. ZAP-70 binding specificity to T cell receptor tyrosine-based activation motifs: the tandem SH2 domains of ZAP-70 bind distinct tyrosine-based activation motifs with varying affinity. *J. Exp. Med.* 181:375-380.
 72. Neumeister Kersh, E., A. S. Shaw, and P. M. Allen. 1998. Fidelity of T cell activation through multistep T cell receptor zeta phosphorylation. *Science* 281:572-575.
 73. Shores, E. W., T. Tran, A. Grinberg, C. L. Sommers, H. Shen, and P. E. Love. 1997. Role of the Multiple T Cell Receptor (TCR)-Zeta Chain Signaling Motifs in Selection of the T Cell Repertoire. *J. Exp. Med.* 185:893-900.
 74. Sloan-Lancaster, J., A. S. Shaw, J. B. Rothbard, and P. M. Allen. 1994. Partial T cell signaling: altered phospho-zeta and lack of Zap70 recruitment in APL-induced T cell anergy. *Cell* 79:913-922.
 75. Wange, R. L., and L. E. Samelson. 1996. Complex complexes: signaling at the TCR. *Immunity* 5:197-205.
 76. Ashe, J. M., D. L. Wiest, R. Abe, and A. Singer. 1999. Zap70 Protein Promotes Tyrosine Phosphorylation of T Cell Receptor Signaling Motifs (ITAMs) in Immature CD4+8+ Thymocytes with Limiting p56lck. *J. Exp. Med.* 189:1163-1167.
 77. Wiest, D. L., J. M. Ashe, T. K. Howcroft, H. M. Lee, D. M. Kemper, I. Negishi, D. S. Singer, A. Singer, and R. Abe. 1997. A Spontaneously Arising Mutation in the DLAARN Motif of Murine ZAP-70 Abrogates Kinase Activity and Arrests Thymocyte Development. *Immunity* 6:663-671.
 78. Di Bartolo, V., D. Mège, V. Germain, M. Pelosi, E. Dufour, F. Michel, G. Magistrelli, A. Isacchi, and O. Acuto. 1999. Tyrosine 319, a Newly Identified Phosphorylation Site of ZAP-70, Plays a Critical Role in T Cell Antigen Receptor Signaling. *J. Biol. Chem.* 274:6285-6294.
 79. Pelosi, M., V. Di Bartolo, V. Mounier, D. Mège, J. M. Pascussi, E. Dufour, A. Blondel, and O. Acuto. 1999. Tyrosine 319 in the Interdomain B of ZAP-70 Is a Binding Site for the Src Homology 2 Domain of Lck. *J. Biol. Chem.* 274:14229-14237.
-

80. Wange, R. L., R. Guitian, N. Isakov, J. D. Watts, R. Aebersold, and L. E. Samelson. 1995. Activating and Inhibitory Mutations in Adjacent Tyrosines in the Kinase Domain of ZAP-70. *J. Biol. Chem.* 270:18730-18733.
 81. Chan, A. C., M. Dalton, R. Johnson, G. Kong, T. Wang, R. Thoma, and T. Kurosaki. 1995. Activation of ZAP-70 kinase activity by phosphorylation of tyrosine 493 is required for lymphocyte antigen receptor function. *EMBO J.* 14:2499-2508.
 82. Brdicka, T., T. A. Kadlecck, J. P. Roose, A. W. Pastuszak, and A. Weiss. 2005. Intramolecular Regulatory Switch in ZAP-70: Analogy with Receptor Tyrosine Kinases. *Mol. Cell. Biol.* 25:4924-4933.
 83. Deindl, S., T. A. Kadlecck, T. Brdicka, X. Cao, A. Weiss, and J. Kuriyan. 2007. Structural Basis for the Inhibition of Tyrosine Kinase Activity of ZAP-70. *Cell* 129:735-746.
 84. Sakaguchi, N., T. Takahashi, H. Hata, T. Nomura, T. Tagami, S. Yamazaki, T. Sakihama, T. Matsutani, I. Negishi, S. Nakatsuru, and S. Sakaguchi. 2003. Altered thymic T-cell selection due to a mutation of the ZAP-70 gene causes autoimmune arthritis in mice. *Nature* 426:454-460.
 85. Arpala, E., M. Shahar, H. Dadi, A. Cohen, and C. M. Roifman. 1994. Defective T Cell Receptor Signaling and CD8+ Thymic Selection in Humans Lacking Zap-70 Kinase. *Cell* 78:947-958.
 86. Orchard, J., R. Ibbotson, G. Best, A. Parker, and D. Oscier. 2005. ZAP-70 in B cell malignancies. *Leukemia and Lymphoma* 46:1689-1698.
 87. Leo, O., Foo, M., Sachs, D.H., and Samelson, L.E. 1987. Identification of a monoclonal antibody specific for a murine T3 polypeptide. *PNAS* 84:1374-1378.
 88. Kubo, R. T., Born, W., Kappler, J.W., Marrack, P., and Pigeon, M. 1989. Characterization of a monoclonal antibody which detects all murine alpha beta T cell receptors. *J. Immunol.* 142:2736-2742.
 89. Mingueneau, M., A. Sansoni, C. Grégoire, R. Roncagalli, E. Aguado, A. Weiss, M. Malissen, and B. Malissen. 2008. The proline-rich sequence of CD3epsilon controls T cell antigen receptor expression and signaling potency in preselection CD4+CD8+ thymocytes. *Nature Immunology* 9:522-532.
 90. Zhang, W., J. Sloan-Lancaster, J. Kitchen, R. P. Tribble, and L. E. Samelson. 1998. LAT: The Zap-70 Tyrosine Kinase Substrate that Links T Cell Receptor to Cellular Activation. *Cell* 92:10.
 91. Alam, S. M., Travers, P.J., Wung, J.L., Nasholds, W., Redpath, S., Jameson, S.C., and Gascoigne N.R.J. 1996. T-cell-receptor affinity and thymocyte positive selection. *Nature* 381:616-620.
 92. Santori, F. R., Kieper, W.C., Brown, S.M., Lu, Y., Neubert, T.A., Johnson, K.L., Naylor, S., Vukmanovic, S., Hogquist, K.A., and Jameson, S.C. 2002. Rare, Structurally Homologous Self-Peptides Promote Thymocyte Positive Selection. *Immunity* 17:131-140.
-

-
93. Köhler, K., A. C. Lellouch, S. Vollmer, O. Stoevesandt, A. Hoff, L. Peters, H. Rogl, B. Malissen, and R. Brock. 2005. Chemical Inhibitors when Timing Is Critical: A PHarmacological Concept for the Maturation of T Cell Contacts. *ChemBioChem* 6:152-161.
 94. Kelly, J. M., Sterry, S.J., Cose, S., Turner, S.J., Fecondo, J., Rodda, S., Fink, P.J., and Carbone, F.R. 1993. Identification of conserved T cell receptor CDR3 residues contacting known exposed peptide side chains from a major histocompatibility complex class I-bound determinant. *Eur. J. Immunol.* 23:3318-3326.
 95. Stotz, S. H., Bollinger, L., Carbone, F.R., and Palmer, E. 1999. T cell receptor (TCR) antagonism without a negative signal: evidence from t cell hybridomas expressing two independent TCRs. *J. Exp. Med.* 189:253-263.
 96. DiGiusto, D. L., and Palmer, E. 1994. An analysis of sequence variation in the beta chain framework and complementarity determining regions of an allo-reactive T cell receptor. *Mol. Immunol.* 31:693-670.
 97. Ljunggren, H. G., Stam, N.J., Oehlen, C., Neefjes, J.J., Hoeglund, P., Heemels, M.T., Bastin, J., Schumacher, T.N.M., Townsend, A., Kaerre, K., and Ploegh, H.L. 1990. Empty MHC class I molecules come out in the cold. *Nature* 346:476-481.
 98. Letourneur, F., and Malissen, B. 1989. Derivation of a T cell hybridoma variant deprived of functional T cell receptor alpha beta chain transcripts reveals a nonfunctional alpha-mRNA of BW5147 origin. *Eur. J. Immunol.* 19:2269-2274.
 99. Zal, T., and Gascoigne, N.R.J. 2004. Using live FRET imaging to reveal early protein-protein interactions during T cell activation. *Curr. Opin. Immunol.* 18:418-427.
 100. Zal, T., and Gascoigne, N.R.J. 2004. Photobleaching-Corrected FRET Efficiency Imaging of Live Cells. *Biophys. J.* 86:3923-3939.
 101. Hogquist, K. A., Jameson, S.C., Heath, W.R., Howard, J.L., Bevan, M.J., and Carbone, F.R. 1994. T cell receptor antagonist peptides induce positive selection. *Cell* 76:17-28.
 102. Hatada, M. H., X. Lu, E. R. Laird, J. Green, J. P. Morgenstern, M. Lou, C. S. Marr, T. B. Phillips, M. K. Ram, K. Theriault, M. J. Zoller, and J. L. Karas. 1995. Molecular basis for interaction of the tyrosine kinase ZAP-70 with the T-cell receptor. *Nature* 377:32-38.
 103. Wange, R. L., A. N. Tony Kong, and L. E. Samelson. 1992. A tyrosine-phosphorylated 70-kDa protein binds a photoaffinity analogue of ATP and associates with both the zeta chain and CD3 components of the activated T cell antigen receptor. *J. Biol. Chem.* 267:11685-11688.
 104. Iwashima, M., B. A. Irving, N. S. C. van Oers, A. C. Chan, and A. Weiss. 1994. Sequential Interaction of the TCR with two distinct cytoplasmic tyrosine kinases. *Science* 263:1136-1139.
 105. Kong, G., M. Dalton, J. Bubeck Wardenburg, D. Straus, T. Kurosaki, and A. C. Chan. 1996. Distinct tyrosine phosphorylation sites in ZAP-70 mediate activation and negative regulation of antigen receptor function. *Mol. Cell. Biol.* 19:5026-5035.
-

106. Holst, J., H. Wang, K. Durik Eder, C. J. Workman, K. L. Boyd, Z. Baquet, H. Singh, K. Forbes, A. Chrusciniski, R. Smeyne, N. S. C. van Oers, P. J. Utz, and D. A. A. Vignali. 2008. Scalable signaling mediated by T cell antigen receptor-CD3 ITAMs ensures effective negative selection and prevents autoimmunity. *Nature Immunol.* 9:658-666.
 107. Mallaun, M., D. Naehrer, M. A. Daniels, P. P. Yachi, B. Hausmann, I. F. Luescher, N. R. J. Gascoigne, and E. Palmer. 2008. The T Cell Receptor's alpha-Chain Connecting Peptide Motif Promotes Close Approximation of the CD8 Coreceptor Allowing Efficient Signal Initiation. *J. Immunol.* 180:8211-8221.
 108. Daniels, M. A., E. Teixeira, J. Gill, B. Hausmann, D. Roubaty, K. Holmberg, G. Werlen, G. A. Hollaender, N. R. J. Gascoigne, and E. Palmer. 2006. Thymic selection threshold defined by compartmentalization of Ras/MAPK signalling. *Nature* 444:724-729.
 109. Hogquist, K. A., S. C. Jameson, W. R. Heath, J. L. Howard, M. J. Bevan, and F. R. Carbone. 1994. T cell receptor antagonist peptides induce positive selection. *Cell* 76:17-28.
 110. Zhang, W., C. L. Sommers, and L. E. Samelson. 1999. Essential role of LAT in T Cell Development. *Immunity* 10:10.
 111. Yokosuka, T., K. Sakata-Sogawa, W. Kobayashi, M. Hiroshima, A. Hashimoto-Tane, M. Tokunaga, M. L. Dustin, and T. Saito. 2005. Newly generated T cell receptor microclusters initiate and sustain T cell activation by recruitment of Zap70 and SLP-76. *Nature Immunol.* 6:1253-1262.
 112. Veillette, A., Bookman, M.A., Horak, E.M., and Bolen, J.B. 1988. The CD4 and CD8 T cell surface antigens are associated with the internal membrane tyrosine-protein kinase p56lck. *Cell* 55:301-308.
 113. Dave, V. P., Z. Cao, C. Browne, B. Alarcon, G. Fernandez-Miguel, J. Lafaille, A. de la Hera, S. Tonegawa, and D. J. Kappes. 1997. CD3 delta deficiency arrests development of the alpha beta but not the gamma delta T cell lineage. *EMBO J* 16:1360-1370.
 114. Goldrath, A. W., Hogquist, K.A., and Bevan, M.J. 1997. CD8 lineage commitment in the absence of CD8. *Immunity* 6:633-642.
 115. Gascoigne, N. R. J., T. Zal, and S. Munir Alam. 2001. T-cell receptor binding kinetics in T-cell development and activation. *Expert Rev. Mol. Med.* 3:1-17.
 116. Alam, S. M., G. M. Davies, C. M. Lin, T. Zal, W. Nasholds, S. C. Jameson, K. A. Hogquist, N. R. J. Gascoigne, and P. J. Travers. 1999. Qualitative and quantitative differences in T cell receptor binding of agonist and antagonist ligands. *Cell* 10:227-237.
 117. Moody, A. M., Y. Xiong, H. C. Chang, and E. L. Reinherz. 2001. The CD8alpha-beta co-receptor on double-positive thymocytes binds with differing affinities to the products of distinct class I MHC loci. *Eur J Immunol.* 31:2791-2799.
 118. Weber, S., and K. Karjalainen. 1993. Mouse CD4 binds MHC class II with extremely low affinity. *Int Immunol.* 5:695-698.
-

-
119. Doyle, C., and J. L. Strominger. 1987. Interaction between CD4 and class II MHC molecules mediates cell adhesion. *Nature* 330:256-259.
 120. Yachi, P. P., Ampudia, J., Zal, T., and Gascoigne, N.R.J. 2006. Altered peptide ligands induce delayed CD8-T cell receptor interaction - a role for CD8 in distinguishing antigen quality. *Immunity* 25:1046-1054.
 121. Wiest, D. L., L. Yuan, J. Jefferson, P. Benveniste, M. Tsokos, R. D. Klausner, L. H. Glimcher, L. E. Samelson, and A. Singer. 1993. Regulation of T cell receptor expression in immature CD4+CD8+ thymocytes by p56lck tyrosine kinase: basis for differential signaling by CD4 and CD8 in immature thymocytes expressing both coreceptor molecules. *J. Exp. Med.* 181:1701-1712.
 122. Bosselut, R., W. Zhang, J. M. Ashe, J. L. Kopacz, L. E. Samelson, and A. Singer. 1999. Association of the adaptor molecule LAT with CD4 and CD8 coreceptors identifies a new coreceptor function in T cell receptor signaling. *J. Exp. Med.* 190:1517-1526.
-

6. Curriculum Vitae

Michel Mallaun

Born November 2, 1979

Swiss Citizen

Education

since 11/04	University Hospital Basel, Department of Biomedicine PhD thesis in Experimental Immunology
04/06 - 07/06	Institute for Start-Up Companies (IFJ), St. Gallen/Basel Entrepreneurship course „Venture Challenge“
10/98 - 09/02	University Basel, Biocenter Graduation as Dipl. Biology II (Molecular Biology) Diploma thesis in Molecular Oncology
08/90 - 06/98	Mathematics and Science Gymnasium (MNG), Basel Graduation with Matura Type C (Mathematics and Natural Sciences)

Work experience

05/04 - 10/04	Research Associate 50%, University Hospital Basel Clinical research project with emphasis on proteomics
06/04 - 09/04	Bicycle Messenger 50%, Veloexpress Basel
11/02 - 07/03	Intern at Werthenstein Chemie AG, Luzern Implementation of a gas chromatography based screening system; Quality management according to GMP standards
07/98 - 09/98	Intern at UBS AG, Basel

Publications

Mallaun M, Hausmann B, Zenke G and Palmer E (2008). A discrete affinity driven elevation of ZAP-70 activity distinguishes positive and negative selection. Manuscript in preparation

Mallaun M, Naeher D, Daniels MA, Yachi PP, Hausmann B, Luescher IF, Gascoigne NRJ and Palmer E (2008). The TCR's α -CPM promotes close approximation of the CD8 co-receptor allowing efficient signal initiation. *Journal of Immunology*, Vol. 180, No. 12: pp. 8211-21

Schmidlin M, Lu M, Leuenberger SA, Stoecklin G, Mallaun M, Gross B, Gherzi R, Hess D, Hemmings BA and Moroni C (2004). The ARE-dependent mRNA-destabilizing activity of BRF1 is regulated by protein kinase B. *The EMBO Journal*, Vol. 8, No. 23(24): pp. 4760-9, December 2004

Stoecklin G, Colombi M, Raineri I, Leuenberger S, Mallaun, M, Schmidlin M, Gross B, Lu M, Kitamura T and Moroni C (2002). Functional cloning of BRF1, a regulator of ARE-dependent mRNA turnover. *The EMBO Journal*, Vol. 2, No. 21(17): pp. 4709-18
